Theoretical Studies on Three membered Rings, Carborynes and Transition Metal Compounds

A Thesis
Submitted for the Degree of
DOCTOR OF PHILOSOPHY

By
Anoop A.

School of Chemistry
University of Hyderabad
Hyderabad 500 046
INDIA

January 2005

Dedicated to

My Parents

Contents

Statement

I hereby declare that the work embodied in this thesis is the result of investigations carried out by me in the School of Chemistry, University of Hyderabad, Hyderabad, India under the supervision of Professor Eluvathingal D. Jemmis.

In keeping with the general practice of reporting scientific observations, due acknowledgments have been made whenever the work described is based on the findings of other investigators.

Anoop A.

31st January 2005

Certificate

Certified that the work contained in this thesis entitled "Theoretical Studies on Three membered Rings, Carborynes and Transition Metal Compounds" has been carried out by Anoop A. under my supervision and same has not been submitted elsewhere for any degree.

Eluvathingal D. Jemmis

Thesis Supervisor

Dean

School of Chemistry

Acknowledgments

With a deep sense of gratitude, I thank my thesis supervisor Prof. E. D. Jemmis for his guidance throughout the course of this thesis work. I am also grateful to him for his kindness, generous help and encouragement. I will cherish the care and concern Prof. Jemmis extended to me, both academically and personally.

I also thank the Dean and all the faculty members of the School, especially Prof. K. D. Sen, Prof. M. Durga Prasad, Prof. T. P. Radhakrishnan and Dr. S. Mahapatra.

I am also thankful to the non-teaching staff of the School, Computer Centre and Centre for Modeling, Simulation and Design (CMSD), a special word of thanks for Mr. Vinodkumar.

I thank CSIR for providing me with financial assistance in the form of JRF/SRF in the course of my research. Besides I also place on record my extreme gratitude to Maui High Performance Computing Center (MHPCC) for enabling me to use their computational facility.

In fact, all of my labmates have been extremely helpful throughout my stay in the lab; working with Kiran helped me in learning the details of carrying out a project; Pankaz was a companion in all aspects; who introduced me to Z-matrices as well as English literature. Ashwini and Bishu extended

Chapter 1

Introduction to Computational Chemistry and Overview of the Thesis

1.1 Introduction to Computational Chemistry

Theoretical basis of computational chemistry, focusing on the methods used in the thesis, is briefly described in this section followed by an overview of the new results discussed in the thesis. Molecular electronic structure theory is the application of the principles of quantum mechanics to calculate the structure and the properties of molecules. Evaluation of structure, energy and properties using 'computer experiments' provides insight into the chemical behavior and supplement experimental efforts in the structural elucidation of short-lived species, in the synthesis and design of materials with desired properties etc. [1]

The emergence of electronic structure theory as a successful field was made possible by the development in methodologies of quantum mechanics and powerful computers and efficient algorithms. Applying the principles of quantum mechanics to molecular problems is a challenging task

because we cannot solve the underlying equations exactly. [2] To solve them approximately, various theoretical models are developed. Understanding the strengths and weaknesses of each method helps to make the right choice of the method for the problem at hand. Some of the factors to be considered in choosing a model are, available computational resources, the size of the molecules, the accuracy needed for a reliable result, number of molecules to be computed. A theoretical model chemistry should ideally be able to give all observable properties of a molecular system. We discuss some of the theoretical models giving importance to the ones that are used in the thesis. The next four chapters detail the application of electronic structure theory to selected problems. A brief summary of these projects is also given in the next section.

The questions that are asked in the thesis are solved by solving the time-independent Schrödinger equation

$$H\Psi = E\Psi \tag{1.1}$$

where H is the Hamiltonian operator and Ψ is the molecular wavefunction for a system of nuclei and electrons. [3] Since nuclei are much heavier than the electrons, they move much slowly. Hence to a good approximation (known as Born-Oppenheimer approximation) one can consider the electrons in a molecule to be moving in the field of fixed nuclei. [4] The resulting molecular electronic Hamiltonian (or total energy operator, sub-

ject to frozen nuclei), in atomic units, is

$$H(r;R) = -\frac{1}{2}\sum_i^n \left(\frac{\partial^2}{\partial x_i^2} + \frac{\partial^2}{\partial y_i^2} + \frac{\partial^2}{\partial z_i^2} \right) - \sum_i^n \sum_\alpha^A \frac{Z_\alpha}{|\mathbf{r_i} - \mathbf{R_\alpha}|} +$$

$$\frac{1}{2}\sum_i^n \sum_j^n \frac{1}{|\mathbf{r_i} - \mathbf{r_j}|} + \frac{1}{2}\sum_\alpha^A \sum_\beta^A \frac{Z_\alpha Z_\beta}{|\mathbf{R_\alpha} - \mathbf{R_\beta}|} \quad (1.2)$$

where first term in the right hand side is the operator for the kinetic energy of the electrons; the second term is the coulomb attraction between electrons and nuclei; the third and fourth term represent the repulsion between electrons and between nuclei, respectively. Partial differential equations in $3n$ unknowns such as we have here are completely intractable to solve exactly, and therefore two important approximations are usually made.

As the first approximation, we reduce the exact function (equation 1.2) of $3n$ variables to n approximate functions of three variables each. That is, the wave function is approximated as a product of one electron wave-functions (Molecular Orbitals) which are in turn, approximated by a Linear Combination of Atomic Orbitals (LCAO). The MO is represented as

$$\psi_i = \sum_{i=1}^n c_{\mu i}\phi_i \quad (1.3)$$

, where ψ_i is the i-th MO, $c_{\mu i}$ are coefficients of linear combination, $\phi_{\mu i}$ is the μ-th atomic orbital and n is the number of atomic orbitals. Once an initial wavefunction is constructed, an electron is selected. The effect of all the other electrons is summed up, and used to generate a potential. (Thus the procedure is sometimes called a mean-field procedure.) This gives a single electron in a defined potential, for which the Schrödinger equation can be solved, giving a slightly different wavefunction for that

electron. This process is then repeated for each of the other electrons, which completes one step of the procedure. The whole procedure is then repeated, until the change from one step to the next is sufficiently small. This is called Hartree-Fock (HF) approximation, which is the foundation of much of modern molecular orbital theory. The procedure for solving the HF equation is often called self-consistent field (SCF) method.

The exact molecular orbital is an infinite set of differential equation. Applying the second approximation we replace the exact MO by a finite set of algebraic functions. These functions are usually called the atomic orbital (AO) basis, because they are atom-centered and resemble solutions to the HF problem for the constituent atoms of a molecule. The earliest compuations were based on the use of Slater Type Orbitals (STO) as approximations to atomic orbitals. STO is represented as

$$\phi_i(\zeta, n, l, m; r, \theta, \phi) = N r^{n-1} e^{-\zeta \tau} Y_{lm}(\theta, \phi) \tag{1.4}$$

where N is a normalization constant, ζ is called exponent. The r, θ and ϕ are spherical coordinates and Y_{lm} is the angular momentum part. The n, l and m are quantum numbers: principal, angular momentum and magnetic respectively. STO's are computationally demanding and hence Gaussian Type Orbitals (GTO) were introduced. GTO's, also called primitives is represented as:

$$g(\alpha, l, m, n; x, y, z) = N e^{-\alpha r^2} x^l y^m z^n \tag{1.5}$$

. where N is a normalization constant, ζ is called exponent. The x, y and z are cartesian coordinates. In practical calculations, the basis function ϕ_μ

are chosen to be contracted Gaussian functions, that is, fixed linear combination of gaussian functions such as

$$g_s(\alpha, r) = (2\alpha/\pi)^{3/4} e^{-\alpha r^2} \tag{1.6}$$

$$g_{px}(\alpha, r) = (128\alpha^5/\pi^3)^{1/4} x e^{-\alpha r^2} \tag{1.7}$$

The smallest possible basis set is called the minimal basis set, and it contains one orbital for every atomic orbital of an atom (including unoccupied orbitals). The STO-3G basis is a well-known minimal basis set which contracts 3 Gaussian functions to approximate the more accurate Slater Type Orbitals. Although a contracted GTO might give a good approximation to an atomic orbital, it lacks any flexibility to expand or shrink in the presence of other atoms in a molecule. Hence, a minimal basis set such as STO-3G is not capable of giving highly accurate results.

The solution is to add extra basis functions beyond the minimum number required to describe each atom. The physical purpose of providing multiple basis functions per atomic orbital is to allow the size of orbitals to increase (for example, along a bond axis) or diminish (for example, perpendicular to a bond axis). Then, the Hartree-Fock procedure can weight each atomic orbital basis function individually to get a better description of the wave function. If we have twice as many basis functions as in a minimum basis, this is called a "double zeta" (DZ) basis set (the zeta, comes from the exponent in the GTO). Split-valance basis sets, which have only a single orbital for the core orbitals and two orbitals for valence orbitals are also widely used. Often additional flexibility is built in by adding higher-angular momentum basis functions. Since the highest angular momentum

orbital for carbon is a p orbital, the "polarization" of the atom can be described by adding a set of d functions on carbon. A set of 3 p functions are used for hydrogen atom as polarization functions. Polarization is added to describe small displacements of the orbitals from their atomic centers in the molecular environment and for the description of electron correlation. A double-zeta plus polarization basis set might be designated DZP. A commonly used example of a split-valence double-zeta plus polarization basis set is Pople's so-called 6-31G* basis. Here the core orbitals are described by a contraction of 6 Gaussian orbitals, while the valence is described by two orbitals, one made of a contraction of 3 Gaussians, and one a single Gaussian function. The star (*) indicates polarization functions on non-hydrogen atoms. If polarization is added to hydrogen atoms also, this basis is labeled as 6-31G**. Finally, for anions and Rydberg excited states, additional diffuse functions are necessary. The 6-31+G basis set has 1 diffuse s-type and p-type gaussians added to the standard 6-31G basis set for heavy atom.

In the *i-jk*G type basis set one ϕ function is used for inner shells and two sets for the valance shells. For a first row atom, there are nine ϕ functions per atom of the form

$$\phi_{1s}(\mathbf{r}) = \sum_{k=1}^{N_1} d_{1s,k} g_s(\alpha 1k, \mathbf{r})$$

$$\phi_{2s'}(\mathbf{r}) = \sum_{k=1}^{N_{2'}} d_{2s,k'} g_s(\alpha 2k', \mathbf{r})$$

$$\phi_{2px'}(\mathbf{r}) = \sum_{k=1}^{N_{2'}} d_{2p,k'} g_{px}(\alpha 2k', \mathbf{r})$$

$$\phi_{2s''}(\mathbf{r}) = \sum_{k=1}^{N_{2''}} d_{2s,k''} g_s(\alpha 2k'', \mathbf{r})$$

$$\phi_{2px''}(\mathbf{r}) = \sum_{k=1}^{N_{2''}} d_{2p,k''} g_{px}(\alpha 2k'', \mathbf{r})$$

and similar expressions for $2py'$, $2py''$, $2pz'$ and $2pz''$. The functions ϕ' and ϕ'' represent inner and outer parts of the valence shell. For hydrogen inner and outer s functions are of the form

$$\phi_{1s'}(\mathbf{r}) = \sum_{k=1}^{N_{1'}} d_{k'} g_s(\alpha k', \mathbf{r})$$

$$\phi_{1s''}(\mathbf{r}) = \sum_{k=1}^{N_{1'}} d_{k''} g_s(\alpha k'', \mathbf{r})$$

For 6-31G: For heavy atoms, $N_1 = 6$, $N_{2'} = 3$, $N_{2''} = 1$. For hydrogen, $N_{1'} = 3$, $N_{1''} = 1$.

Another approach is to consider the core (inner) electrons as an averaged potential, called Effective Core Potential (ECP), because the core orbitals in most cases are not affected by changes in chemical bonding. ECP's reduce the number of electrons to be included in the calculations. This makes very efficient computation and incorporation of relativistic effects can be achieved effectively. LANL2DZ is one such basis set used widely for transition metals. [6]

The general form of ECP is $ECP(r) = \sum_{i=1}^{M} d_i r^{n_i} e^{-\zeta_i r}$ where M is the number of terms in the expansion, d_i is a coefficient for each term, r denotes the distance from the nucleus, n_i is a power of r for the i-th term and ζ_i represents the exponent of the i-th term.

Hartree-Fock theory is an excellent starting point for more accurate

methods. HF energy accounts for the bulk (~99%) of the exact energy and is successful in predicting equilibrium geometries and some properties. Bond making and bond breaking processes are not described well at this level. To a large extend the defects of HF method in estimating electron correlation may be compensated by isodesmic equations, where number of electron pairs are conserved. However, the energy that is left out could still be important in the chemical context. The difference between the Hartree-Fock (HF) energy and the exact nonrelativistic energy is usually termed the electron correlation energy, since it is due to detailed correlations between electrons which are averaged out in the HF approach. The errors in the HF approach are caused by the two major approximations that we make, i) use of approximate functions for exact functions and ii) use of finite set of basis functions for complete set. Electron correlation methods try to tackle this problem. [8] Post-HF electron correlation methods, use a linear combination of many configurations, instead of a single configuration in HF theory. The other configurations are generated by replacing occupied orbitals by virtual orbitals. One of the popular methods is Moller-Plesset (MP) or many-body perturbation theory, [7] where electron correlation is treated as a perturbation to the HF problem. In the MP scheme, wavefunction and energy are expanded in a power series of the perturbation. In Configuration Interaction (CI), a linear combination of configurations (HF determinants) with all determinants formed by single and double orbital substitutions, with coefficients determined variationally. [9] In principle, by increasing the number of configurations included, the CI method is capable of providing arbitrarily accurate solutions to the exact wave function.

If all possible excited configurations are included, the method gives the exact solution within the space spanned by a given basis set and is referred to as full configuration interaction (FCI). Since FCI is computationally highly demanding, limited CI methods are used, and one popular method is CISD, where all single and double excitations are included. [9] Quadratic Configuration Interaction (QCI), [10] have size-consistency added to the CISD method. Coupled Cluster Theory (CC) uses the exponential form of the wave function $\Psi = e^T \Psi_0$, where $T = T_1 + T_2 + \ldots$. [11] The effect of higher excitations are included in the exponential term. The method in which all single and double excitations are included, i.e., $T = T_1 + T_2$, it is called CCSD. [12]

Another approach in electronic structure theory is Density Functional Theory. [13] DFT, unlike the wave function based methods, has electron density as the fundamental property. The exact ground state energy of a molecular system, as stated by first Hohenberg-Kohn theorem, is a functional only of the electron density and the fixed positions of the nuclei. [14] In other words, for a given nuclear coordinates, the electron density uniquely determines the energy and all properties of the ground state. Given the functional, Hohenberg and Kohn proved that the exact electron density function is the one which minimizes the energy (i. e., as a function of density) thereby providing a variational principle to find the density.

The total energy, deriving from the solution of the Schrodinger equation, can be decomposed in terms of kinetic energy, T, electron-nuclear attraction, V_{en}, and electron-electron interaction contributions (plus the nuclear-nuclear repulsion energy, which is constant at a given geometry).

The electron-electron interactions consist of the classical Coulomb repulsion, J, due to the electron density, plus nonclassical terms due to the correlations between electrons and exchange effects of Fermion statistics. Thus, we have

$$E(\rho) = T(\rho) + V_{en}(\rho) + J(\rho) + V_{xc}(\rho) \qquad (1.8)$$

Kohn-Sham formulation of DFT (KS-DFT) uses the kinetic energy of the noninteracting electrons, which can be solved exactly, and the kinetic energy difference between real and noninteracting systems is included in the exchange-correlation (XC) functional. [15] DFT is also an SCF method, in which Kohn-Sham orbitals are solved iteratively.

The major problem with DFT is that the exact functionals for exchange and correlation are not known except for the free electron gas. However, approximations exist which permit the calculation of certain physical quantities quite accurately. The most widely used approximation is the local density approximation (LDA), where the functional depends only on the density at the coordinate where the functional is evaluated. Generalized gradient approximations (GGA) are still local but also take into account the gradient of the density at the same coordinate. [16] Using the latter (GGA) very good results for molecular geometries and ground state energies have been achieved. The combination of gradient-corrected correlation functionals with the Becke exchange functional has been shown to yield significantly more accurate relative energies than the earlier LDA-based forms for KS-DFT.

Accuracy achieved by the DFT calculations are comparable to that of MP2, but the computational requirement of DFT is comparable to HF

methods. As there is no explicit construction of the molecular wave function, the basis set requirements for DFT are far more modest than those needed to obtain reliable results via the MP2 method (or any other correlation method). Perhaps the best DFT results to date have been obtained by mixing a small part of the exact exchange interactions (as modeled in the HF method) with gradient-corrected exchange functionals.

The discussion till now was on the evaluation of energy on fixed nuclear positions, thereby getting a Potential Energy Surface (PES) of the different nuclear coordinates. Geometry Optimization is the technique of arriving at the minimum on the PES. When we are interested in the reaction path, it is necessary to compute the Transition States and higher order Saddle Points along the reaction coordinate. Vibrational frequency analysis helps in characterizing the nature of the stationary points as minima or TS (zero and one imaginary frequency respectively).

There are several state-of-the-art computational chemistry packages available such as, Gaussian 03, GAMESS, ADF, DMol etc. Visualization packages, such as GaussView, Molden, Molekel, helps in the visualization of the structure, orbitals, electron density, laplacian, animation of frequencies or reaction path etc. Calculations in this thesis is carried out using Gaussian 94/03 program packages. The theoretical models used in the thesis are the following. Hybrid Hartree Fock-DFT - B3LYP method which uses a combination of the three-parameter Becke exchange functional with the Lee-Yang-Parr nonlocal correlation functionals is used in all the projects. The basis sets employed in the calculations are: 6-311G(d) (Chapter 2), 6-31G* and 6-311+g* (Chapter 3), LANL2DZ (Chapters 4 and 5). Specific

details of the computational methods are described in the methods section of each chapter.

1.2 Overview of the Thesis

1.2.1 Nonplanarity at Tri-coordinated Aluminum and Gallium: Cyclic Structures for $X_3H_n^m$ (X = B, Al, Ga)

Cyclopentadienyl cation, $C_3H_3^+$, the smallest 2π-aromatic system, and all the three-membered boron ring clusters are studied both theoretically and experimentally. However very little is known about the heavier analogs of boron, the alanes and galanes. In view of the known differences between the hydrocarbons and the heavier analogs, it is interesting to see the differences between boranes, alanes and galanes. Structures and energies of $X_3H_3^{2-}$, $X_3H_4^-$, X_3H_5, and $X_3H_6^+$ (X = B, Al and Ga) were investigated theoretically at B3LYP/6-311G(d) level. The global minimum structures of B are not found to be global minima for Al and Ga. The hydrides of the heavier elements Al and Ga have shown a total of seven, six and eight minima for $X_3H_3^{2-}$, $X_3H_4^-$ and X_3H_5, respectively. However, $X_3H_6^+$ has three and four minima for Al and Ga, respectively. The nonplanar arrangements of hydrogens with respect to X_3 ring is found to be very common for Al and Ga species. Similarly, species with lone pairs on heavy atoms dominate the potential energy surfaces of Al and Ga three-ring systems. The first example of a structure with tri-coordinate pyramidal arrangement at Al and Ga is found in $X_3H_4^-$ (**2g**), contrary to the conventional wisdom of C_3H_4, $B_3H_4^-$, etc. The influence of π-delocalization in stabilizing the

structures decreases from $X_3H_3^{2-}$ to $X_3H_6^+$ for heavier elements Al and Ga. In general, minimum energy structures of $X_3H_4^-$, X_3H_5, and $X_3H_6^+$ may be arrived at by protonating the minimum energy structures sequentially starting from $X_3H_3^{2-}$. The resonance stabilization energy (RSE) for the global minimum structures (or nearest structures to global minimum which contains π-delocalization) is computed using isodesmic equations.

1.2.2 Dehydrogeno closo-Carboranes and closo-Silaboranes: A Theoretical Study of Structure and Reactivity

In this chapter, we compare larger clusters, carborane and silaborane and their dehydrogeno derivatives. 1,2-Carboranes, 1,2-silaboranes ($C_2B_nH_{n+2}$, and $Si_2B_nH_{n+2}$, n = 4,5,8 and 10) and their dehydrogeno derivatives are studied using Density Functional Theory (B3LYP/6-311+G*). 1,2-Dehydrogeno-o-dicarbadodecaborane is comparable in reactivity to benzyne. Several isomers of dehydrogenocarboranes, 1,2-$C_2B_{10}H_{10}$ (**8a**), 2,3- and 2,6-$C_2B_8H_8$ (**10a** and **11a**), and 2,3-$C_2B_5H_5$(**13a**), were found to be more π-stabilized than benzyne, indicating the possibility of their synthesis. The 2,3-$C_2B_5H_5$ (**13a**) is estimated to be more favorable than the experimentally available 1,2-$C_2B_{10}H_{10}$ (**8a**) by 21.5 kcal/mol. This arises from the extra stabilization gained from the better overlap of the $C_2B_3H_3$ rings with the 2 BH caps. These could be ideal dienophiles in pericyclic reactions, according to Frontier Molecular Orbital Analysis. Silaboranes have similar structural features as carboranes with modifications resulting from the larger size of Si. Dehydrogenosilaboranes differ considerably in structure and bonding from the carbon analogs so as to avoid Si-Si multiple

bond. One of the Si atoms moves away from the surface in $Si_2B_{10}H_{10}$ (**15**), $Si_2B_8H_8$ (**16**,**17** and **18**), and 1,2-$Si_2B_5H_5$ (**19**). One Si atom forms a bridge to a trigonal surface in 2,3-$Si_2B_5H_5$ (**20**) and 1,2-$Si_2B_4H_4$ (**21**). Symmetrical structures based on icosahedron and octahedron are found to be more stable compared to the other structures. Three-dimensional aromaticity estimated using NICS calculations follow the trend in stability; symmetrical structures have more negative NICS values.

1.2.3 Theoretical Study on the double Insertion of Acetylene to the Nickel Complexes of Benzyne and Carborynes.

Carborynes, didehydrogenodicarbaboranes, as showed in Chapter 3 has similarity with benzynes in their reactions. In this chapter we explore the possibility of transition metal complexes of carboryne and their reactivity in comparison to that of benzyne. The carborynes, $C_2B_{10}H_{10}$ and $C_2B_5H_5$, which are theoretically estimated to be the best among the carborynes, are chosen for the study. The reactivity of the complexes of these two carborynes along with the benzyne nickel complex are studied for the double insertion reaction of acetylene. The stationary points and transition states involved in the reaction mechanism are optimized under B3LYP/LANL2DZ level of theory. These studies would encourage experimental investigations in the area leading to many functionalization pathways of carboranes.

1.2.4 Transition Metal Catalyzed Activation of β-C-H bond

In the previous chapters we have seen the application of electronic structure theory to the problems ranging from small molecules to the clusters and

transition metal complexes. In this chapter we concentrate on a transition metal catalyzed reaction. The activation of CH bond is central to chemistry since they provide a solution to the industrial preparation of hydrocarbon derivatives from the naturally available saturated hydrocarbons occurring in the petroleum and natural gas. β-hydride elimination reaction which is a crucial intermediate in many useful reactions are studied with the first row transition metal as the catalyst. The free energy of reaction as a function of varying metals is computed. The structure and the stability of the β-agostic complex, the property of which determines the course of the reaction, is studied in detail. The metal-ligand combinations across the whole range of first row transition metals is analyzed to understand factors that control the reaction.

Bibliography

[1] (a) Szabo, A.; Ostlund, N. S. *Modern Quantum Chemistry*; McGraw-Hill Publishing Company, New York, 1982. (b) Foresman, J. B.; Frisch A. *Exploring Chemistry with Electronic Structure Methods*; Gaussian Inc. Pittsburgh, USA. (c) Jensen, F. *Introduction to Computational Chemistry*; John Wiley & Sons, Chichester, 1998. (d) Cramer, C. J. *Essentials of Computational Chemistry*; John Wiley, & Sons, Chichester, 2002. (e) Hinchliffe, A. *Computational Quantum Chemistry*; John Wiley & Sons, Chichester, 1988. (f) Young, D. *Computational Chemistry*; John Wiley, & Sons, Chichester, 2001. (g) Head-Gorder, M. *J. Phys. Chem.* **1996**, *100*, 13213-13225.

[2] (a) Levine, I. N. *Quantum Chemistry*; 2nd Edn. Allyn and Bacon, Boston. (b) Lowe, J. P. *Quantum Chemistry*; Academic Press, New York, 1978. (c) McQuarrie, D. A. *Quantum Chemistry*; Oxford University Press, California, U.S.A., 1983. (d) Pilar, F. L. *Elementary Quantum Chemistry*; Mc-Graw Hill Publishing Company, New York, 1968.

[3] Schrödinger, E. *Ann. Physik.* **1926**, *79*, 361.

[4] Born, M.; Oppenheimer, J. R. *Ann. Physik* **1927**, *84*, 457.

[5] Hehre, W. J.; Ditchfield, R; Pople, J. A. *J. Chem. Phys.* **1971**, *56*, 2257.

[6] Labanowski, J. K. *Simplified Introduction to Ab Initio Basis Sets.* http://www.ccl.net/cca/documents/basis-sets/basis.html

[7] Møller, C.; Plesset, M. S. *Phys. Rev.* **1934**, *46*, 618.

[8] Raghavachari, K.; Anderson, J. B. *J. Phys. Chem.* **1996**, *100*, 12960.

[9] Shavitt, I. In *Modern Theoretical Chemistry*; Schaefer, H. F., Ed.; Plenum Press: New York, 1977; Vol. 3, p 189.

[10] (a) Pople, J. A.; Head-Gordon, M.; Raghavachari, K. *J. Chem. Phys.* **1987**, *87*, 5968. (b) Raghavachari, K.; Pople, J. A.; Head-Gordon, M. In *Many-Body Methods in Quantum Chemistry, Lecture Notes in Chemistry*; Kaldor, U., Ed.; Springer-Verlag: Berlin, 1989; Vol. 52, p 215.

[11] (a) Cizek, J. *J. Chem. Phys.* **1966**, *45*, 4256; *Adv. Chem. Phys.* **1969**, *14*, 35. (b) Bartlett, R. J.; Dykstra, C. E.; Paldus, J. In *Advanced Theories and Computational Approaches to the Electronic Structure of Molecules*; Dykstra, C. E., Ed.; Reidel: Dordrecht, 1984; 127 pp. (c) Bartlett, R. J. *J. Phys. Chem.* **1989**, *93*, 1697. (d) Bartlett, R. J. In *Modern Electronic Structure Theory*; Yarkony, D. R., Ed.; World Scientific: Singapore, 1995; p 1047. (e) Lee, T. J.; Scuseria, G. E. In *Quantum Mechanical Electronic Structure Calculations with Chemical Accuracy*; Langhoff, S. R., Ed.; Kluwer: Dordrecht, 1995; p 47.

[12] Purvis, G. D.; Bartlett, R. J. *J. Chem. Phys.* **1982**, *76*, 1910.

[13] (a) Kohn, W., Becke, A. D., Parr, R. G. *J. Phys. Chem.* **1996**, 100, 12974. (b) Parr, R. G.; Yang, W. *Density Functional Theory of Atoms and Molecules*; Oxford: New York, 1989.

[14] Hohenberg, P.; Kohn, W. *Phys. Rev.* **1964**, *136*, B864.

[15] Kohn, W.; Sham, L. *J. Phys. Rev.* **1965**, *140*, A1133.

[16] (a) Becke, A. D. *Phys. Rev.* **1988**, *38*, A3098. (b) Perdew, J. P.; Chaevary, J. A.; Vosko, S. H.; Jackson, K. A.; Pederson, M. R.; Singh, D. J.; Fiolhais, C. *Phys. Rev.* **1992**, B46, 6671. (c) Becke, A. D. *J. Chem. Phys.* **1992**, *97*, 9173.

Chapter 2

Non-planarity at Tri-coordinated Aluminum and Gallium! Novel Cyclic Structures for $X_3H_n^m$ (X=B, Al, Ga)

2.1 Introduction

Structural properties of the smallest 2π aromatic, cyclopropenyl cation and its boron analogs have been studied in detail. Numerous experimental reports are available on three-membered boron ring clusters. [1–3] The importance of aromaticity in these three-membered boron ring hydrides is well documented. [4–8] Theoretical studies have revealed that the global minimum structures of $X_3H_3^{2-}$ (Scheme 2.1, **1a**), [4,5] $X_3H_4^-$ (Scheme 2.2, **2a**), [4–6] X_3H_5 (Scheme 2.3, **3a**) [4,5,7,8] and $X_3H_6^+$ (Scheme 2.4, **4b**) [4, 8] (X = B, the all boron analogs of $C_3H_3^+$) contain cyclic π-delocalization. Though decreased in aromaticity, these are comparable in many ways to the smallest aromatic species $C_3H_3^+$. Heavier analogs of the cyclopropenyl cation have been studied in detail; especially well established are the differences between carbon and silicon chemistry. However, extremely little is

known for heavier homologues of boron, the alanes and the galanes. Only one example involving a group 13 congener ($Ga_3H_3^{2-}$) has been studied theoretically [9] and a substituted analog has been prepared by utilizing the extraordinary bulky ligand 2,6-$Mes_2C_6H_3$. [9,10] The structural analysis of $Na_2[Ga_3R_3]$ (**5**, R= 2,6-$Mes_2C_6H_3$) and $K_2[Ga_3R_3]$ (**6**) have shown that the Ga_3R_3 ring is also π-delocalized. [9, 10] Stable aromatic four-membered ring structures stabilized by metal ions, have been observed recently as MX_4^- (**7**) [11] and M_2X_4 (**8**), [12] where M=Li, Na, Cu and X=Al, Ga, In. Despite these developments, no systematic study exists for the related three-membered 2π-electron structures composed of Al or Ga. Structures with the molecular formulas $X_3H_3^{2-}$ (**1**), $X_3H_4^-$ (**2**), X_3H_5 (**3**) and $X_3H_6^+$ (**4**); X=B, Al, Ga are discussed in detail in this chapter.

Generally, compounds containing elements from the second or higher row exhibit structural properties that differ from those of the first row elements. [13–29] There are numerous reports highlighting such differences between hydrocarbons and the heavier analogs in group 14. For example, (a) the four substituents of the alkene homologues no longer lie in a plane with the double-bonded atoms (D_{2h} symmetry), but rather show a trans-bent orientation, [14] (b) the stability of H-bridged structures increases in $C_3H_3^+$ homologues, [15] (c) unlike allene, trisilaallene is shown to be non-linear. [16] But very few such comparisons of multiple bonds between more electropositive heavier elements are known in group 13. One example is the nonlinearity of the two substituents in galyne ($Na_2Ga_2R_2$, R=2,4,6-$^iPr_3C_6H_2$) with the Ga-Ga bond. [17, 20] These structural differences of heavier analogs are attributed among others to the decrease in

sp-hybridization caused by different radial extension of s and p valence orbitals and their energy differences in heavier elements starting from the second row. [13, 30] It is of interest to establish how these effects influence the aromatic three-membered ring structures composed of Al and Ga in comparison to those of boron. Of the many differences we found between the B, Al and Ga aromatic systems, the most intriguing structures are those containing pyramidal tricoordinated Al and Ga atoms.

2.2   Computational Methods

The geometries of the structures **1**, **2**, **3**, **4** and all the reference molecules were optimized using the Hartree-Fock (HF) and the hybrid Hartree-Fock/DFT (B3LYP) methods. [31, 32] The B3LYP method uses a combination of the three-parameter Becke exchange functional with the Lee-Yang-Parr non-local correlation functionals. The 6-311G(d) basis set was used for all the calculations. [31] The nature of the stationary points was determined by evaluating the second derivatives of the energy (Hessian matrix). [33] All the computations were done using the Gaussian 98 program package. [34] All total and Zero Point energies of the optimized structures of $X_3H_3^{2-}$, $X_3H_4^-$, X_3H_5 and $X_3H_6^+$ are given in Tables 2.1-2.4. Fragment Molecular Orbital (FMO) and Natural Bond Orbital (NBO) methods were used to analyze the bonding in a given structure. [25, 36]

	1a	1b	1c	1d	1e	1f	1g	1h	1i	1j	1k
B	0.0(0)	--	58.12(0)	88.29(3)	88.25(2)	37.87(1)	--	73.75(3)	--	91.64(2)	57.68(1)
Al	0.0(0)	--	-1.80(0)	11.17(1)	6.13(0)	-1.16(0)	1.82(0)	13.26(2)	3.76(0)	19.82(1)	2.04(0)
Ga	0.0(1)	0.18(0)	-6.82(0)	4.21(1)	0.20(0)	-2.70(0)	-2.14(0)	19.37(1)	-1.55(0)	14.54(1)	0.38(0)

Scheme 2.1

	2a	2b	2c	2d	2e	2f	2g	2h	2i	2j	2k	2l
B	0.0(0)	--	--	--	1.65(0)	47.29(2)	--	44.82(1)	--	81.37(2)	--	26.11(2)
Al	0.0(1)	-1.02(0)	--	4.34(0)	19.29(2)	21.27(2)	7.05(0)	6.48(2)	6.21(0)	8.41(1)	7.63(0)	9.48(0)
Ga	0.0(1)	-2.40(0)	20.26(1)	-4.04(0)	14.14(2)	17.93(3)	-0.97(0)	-1.79(2)	-0.53(0)	4.86(1)	3.90(0)	8.79(0)[a]

[a] C_3 symmetry
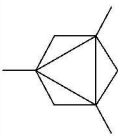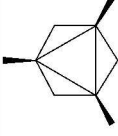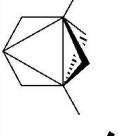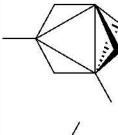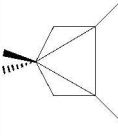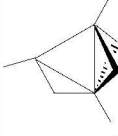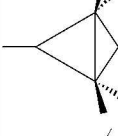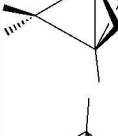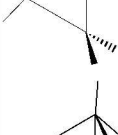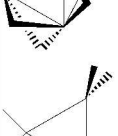
Scheme 2.2

	3a	3b	3c	3d	3e	3f	3g	3h
B	0.0(0)	--	--	--	--	--	--	--
Al	0.0(2)	-18.64(0)	-12.21(1)	-17.14(0)	-16.08(0)	25.20(3)	-14.90(0)	-14.86(0)
Ga	0.0(2)	-23.97(0)	-31.20(1)	-33.88(0)	--	16.15(3)	-26.40(0)	-28.56(0)

	3i	3j	3k	3l	3m	3n	3o	3p
B	--	--	26.33(0)	0.15(0)	56.00(2)	--	56.34(2)	71.78(2)
Al	-15.52(0)	-12.83(0)	-18.49(0)	9.31(3)	-6.98(2)	-9.24(1)	1.02(2)	13.62(2)
Ga	-27.03(0)	-26.46(0)	-21.94(0)	4.90(2)	-19.70(1)	-18.66(0)	-14.66(2)	12.87(3)

Scheme 2.3

2.3   Results and Discussion

The structures considered in this article are obtained in a systematic way starting with the classical D_{3h} geometry with three terminal X-H bonds. Various arrangements are arrived at by considering three terminal X-H bonds, two terminal and one bridging X-H bonds, two bridging and one terminal X-H bonds, three bridging X-H bonds, one XH_2 group and an X-

	4a	4b	4c	4d	4e	4f	4g	4h	4i	4j	4k
B	0.0(1)	-40.68(0)	--	--	-22.09(2)	--	-1.11(2)	-32.50(0)	-23.96(1)	33.96(3)	188.25(4)
Al	0.0(3)	-58.79(0)	-73.69(0)	-59.92(1)	-57.54(1)	-67.99(0)	-46.93(1)	-45.83(1)	-42.51(2)	-18.54(3)	48.69(5)
Ga	0.0(3)	-60.47(0)	-85.79(0)	--	-68.56(0)	-72.58(0)	-63.58(1)	-52.41(2)	-48.81(3)	-38.80(3)	-11.64(3)

Scheme 2.4

Table 2.1: Total energy (in au) and Zero point energy (ZPE, in kcal/mol) of the calculated $X_3H_3^{2-}$ isomers at B3LYP and HF levels using 6-311G(d) basis.

X	Structure	Total Energy B3LYP	Z. P. E.	Total Energy HF	Z. P. E.
B	1a	-76.13605(0)	19.56	-75.49506(0)	20.43
	1b	–	–	–	–
	1c	-76.04298(0)	19.27	-75.39855(0)	20.54
	1d	-75.98810(3)	14.92	-75.31609(3)	16.36
	1e	-75.98920(2)	15.59	-75.33537(0)	19.18
	1f	-76.07366(1)	18.26	-75.42791(0)	19.85
	1g	Collapsed	to 1a	–	
	1h	-76.01688(3)	18.51	-75.36445(3)	19.50
	1i	–		–	
	1j	-75.98452(2)	16.05	-75.34209(2)	17.04
	1k	-76.04195(1)	18.17	-75.39221(1)	19.38
Al	1a	-729.05334(0)	11.05	-727.33170(0)	12.17
	1b	–		–	
	1c	-729.05814(0)	12.29	-727.33364(0)	13.01
	1d	-729.03639(1)	11.60	-727.30656(1)	12.43
	1e	-729.04584(0)	12.50	-727.32263(0)	13.40
	1f	-729.05615(0)	11.66	-727.33140(0)	12.58
	1g	-729.05151(0)	11.74	-727.32938(0)	12.63
	1h	-729.03369(2)	12.00	-727.30792(2)	12.74
	1i	-729.04896(0)	12.08	-727.32481(0)	12.93
	1j	-729.02153(1)	10.91	-727.30195(0)	12.16
	1k	-729.05104(0)	11.66	-727.32215(0)	12.45
Ga	1a	-5776.32355(1)	9.30	-5771.20605(0)	11.02
	1b	-5776.32355(0)	9.48	Collapsed to 1a	
	1c	-5776.33704(0)	10.98	-5771.21505(0)	11.71
	1d	-5776.31874(1)	10.52	-5771.18718(1)	10.78
	1e	-5776.32482(0)	10.32	-5771.19921(0)	10.99
	1f	-5776.32939(0)	10.28	-5771.20745(0)	10.97
	1g	-5776.32891(0)	10.55	Collapsed to	open chain
	1h	-5776.30626(1)	17.99	-5771.19418(1)	9.59
	1i	-5776.32797(0)	10.55	-5771.20433(0)	11.15
	1j	-5776.30054(1)	9.40	-5771.18112(0)	10.02
	1k	-5776.32268(0)	9.13	-5771.19436(1)	9.69

H-X bridge as indicated in Scheme **2.1** for $X_3H_3^{2-}$. Similarly, Schemes **2.2**, **2.3** and **2.4** represent the variety of structures considered for $X_3H_4^-$, X_3H_5 and $X_3H_6^+$ respectively. The structures in the Schemes **2.1-2.4** are arranged so that the similarities between them can be discussed coherently as seen in

Table 2.2: Total energy (in au) and Zero point energy (ZPE, in kcal/mol) of the calculated $X_3H_4^-$ isomers at B3LYP and HF levels using 6-311G(d) basis.

X	Structure	Total Energy B3LYP	ZPE	Total Energy HF	ZPE
B	2a	-76.94825(0)	27.39	-76.30896(0)	28.65
	2b	–		–	
	2c	Collapsed to 2a		–	
	2d	Collapsed to 2a		–	
	2e	-76.94432(0)	26.56	-76.30513(0)	28.03
	2f	-76.86692(2)	23.56	-76.23969(2)	24.82
	2g	–		–	
	2h	-76.87374(1)	25.42	-76.23057(1)	26.88
	2i	–		–	
	2j	-76.81261(2)	23.57	-76.17911(1)	25.46
	2k	–		–	
	2l	-76.90050(2)	23.46	-76.26657(0)	25.08
Al	2a	-729.77469(1)	16.94	-728.05603(1)	17.93
	2b	-729.77635(0)	16.96	-728.05649(0)	18.09
	2c	Collapsed to open chain		–	
	2d	-729.76814(0)	17.17	-728.04423(0)	18.10
	2e	-729.74222(2)	15.83	-728.02138(2)	16.77
	2f	-729.73719(2)	14.63	-727.98262(2)	16.34
	2g	-729.76166(0)	15.79	-728.03867(0)	16.62
	2h	-729.76241(2)	15.69	-728.03667(2)	16.44
	2i	-729.76495(0)	17.04	Collapsed	
	2j	-729.76100(1)	16.76	-727.92559(0)	18.08
	2k	-729.76169(0)	16.40	Collapsed to 2j	
	2l	-729.75594(0)	14.61	-728.03487(0)	15.59
Ga	2a	-5777.03364(1)	15.56	-5771.92189(1)	16.73
	2b	-5777.03703(0)	15.28	-5771.92209(0)	16.78
	2c	-5777.00133(1)	15.55	-5771.86933(1)	16.17
	2d	-5777.03947(0)	15.17	-5771.91661(1)	15.44
	2e	-5777.01165(2)	15.91	-5771.89775(2)	14.41
	2f	-5777.00188(3)	13.52	-5771.89639(2)	14.85
	2g	-5777.03459(0)	15.18	-5771.91562(0)	15.89
	2h	-5777.03620(2)	15.37	-5771.91727(2)	16.01
	2i	-5777.03455(0)	15.60	Collapsed	
	2j	-5777.02480(1)	14.86	-5771.90868(0)	15.99
	2k	-5777.02570(0)	14.46	Collapsed to 2j	
	2la	-5777.01450(0)	12.79	-5771.89682(1)	14.25

Table 2.3: Total energy (in au) and Zero point energy (ZPE, in kcal/mol) of the calculated X_3H_5 isomers at B3LYP and HF levels using 6-311G(d) basis.

X	Structure	Total Energy, B3LYP	ZPE	Total Energy, HF	ZPE
B	3a	-77.51782(0)	34.21	-76.87666(0)	35.68
	3b	–		–	
	3c	Collapsed to 3j		–	
	3d	–		–	
	3e	–		–	
	3f	Collapsed to 3i		–	
	3g	Collapsed to 3i		–	
	3h	–		–	
	3i	–		–	
	3j	–		–	
	3k	-77.47429(0)	33.21	-76.84929(0)	35.08
	3l	-77.51758(0)	34.21	-76.87858(0)	36.03
	3m	-77.42558(2)	32.30	-76.79584(2)	34.22
	3n	–		–	
	3o	-77.42207(2)	30.39	-76.79243(2)	31.69
	3p	-77.39836(2)	30.97	-76.76280(2)	32.79
Al	3a	-730.29625(2)	22.55	-728.57656(2)	23.82
	3b	-730.32620(0)	22.70	-728.61132(0)	23.96
	3c	-730.31360(1)	21.20	-728.60292(1)	22.22
	3d	-730.32333(0)	22.40	-728.60756(0)	23.38
	3e	-730.32147(0)	22.29	-728.60756(0)	23.39
	3f	-730.25477(3)	21.71	-728.52154(3)	22.83
	3g	-730.31962(0)	22.31	-728.60183(0)	23.48
	3h	-730.31914(0)	22.04	Collapsed to	open chain
	3i	-730.32149(0)	22.87	Collapsed to	open chain
	3j	-730.31571(0)	2192	-728.60272(0)	23.00
	3k	-730.32582(0)	22.62	-728.61752(0)	24.05
	3l	-730.27906(3)	21.04	-728.55857(3)	22.28
	3m	-730.30357(2)	20.12	-728.59810(0)	21.83
	3n	-730.30891(1)	21.23	-728.59811(0)	21.84
	3o	-730.28979(2)	19.46	-728.58763(1)	20.93
	3p	-730.27003(2)	19.66	-728.53484(2)	21.17

Schemes **2.7, 2.8** and **2.9**. Relative energies and number of imaginary frequencies are also given in the Schemes **2.1-2.4**. Figures **2.1-2.4** gives the important geometric parameters of the minimum energy structures. While only two of the eleven structures indicated are minima for $B_3H_3^{2-}$, as many

Table 2.3: Continued

X	Structure	Total Energy, B3LYP	ZPE	Total Energy, HF	ZPE
Ga	3a	-5777.53596(2)	21.58	-5772.42651(2)	22.72
	3b	-5777.57175(0)	21.04	-5772.46315(0)	21.94
	3c	-5777.58304(1)	19.89	-5772.47294(1)	20.58
	3d	-5777.58863(0)	20.73	-5772.47482(0)	21.14
	3e	Collapsed to 3d			
	3f	-5777.50939(3)	21.05	-5772.38410(3)	21.90
	3g	-5777.57670(0)	20.73	-5772.46532(0)	21.71
	3h	-5777.57988(0)	20.56	Collapsed to	open chain
	3i	-5777.57856(0)	21.28	Collapsed to	open chain
	3j	-5777.57664(0)	20.63	-5772.46821(1)	21.47
	3k	-5777.56954(0)	20.69	-5772.46645(0)	21.99
	3l	-5777.52681(2)	20.72	-5772.41419(2)	21.71
	3m	-5777.56377(1)	19.29	-5772.46323(1)	20.54
	3n	-5777.56445(0)	20.78	Collapsed	
	3o	-5777.55548(2)	19.12	-5772.46130(1)	20.34
	3p	-5777.50943(3)	17.73	-5772.37900(2)	19.57

as seven are minima for $Al_3H_3^{2-}$ and $Ga_3H_3^{2-}$, justifying the systematic approach. Throughout this chapter various structures in the text are represented by the structure number followed by the atomic symbol. For example the triangular structure **1a** for $B_3H_3^{2-}$ is represented by **1a-B**, $Al_3H_3^{2-}$ by **1a-Al**, $Ga_3H_3^{2-}$ by **1a-Ga** etc. Similarly individual atoms in a structure are identified by the atom number as superscript. For example **2b**-Ga^2 represents the gallium atom which is numbered **2** in **2b-Ga** (Figures **2.1-2.4**).

Several molecules are used as theoretical models for the idealized single, double and H-bridged bonds for comparison. Table 1 gives the X-X bond distances in X_2H_4 (single bond), X_3H_3 (strained single bond), $X_2H_4^{2-}$ (double bond), $X_3H_4^{3-}$ (double bond in 3-membered ring), X_2H_6(doubly bridged structure as in B_2H_6, and doubly bridged X_2H_2. Experimentally known Al and Ga compounds and their bond distances are used for com-

Figure 2.1: Optimized geometries and important bond distances for B, Al (in parentheses) and Ga (in brackets) isomers of $X_3H_3^{2-}$ at B3LYP/6-311G(d) level. Atoms are numbered in italics
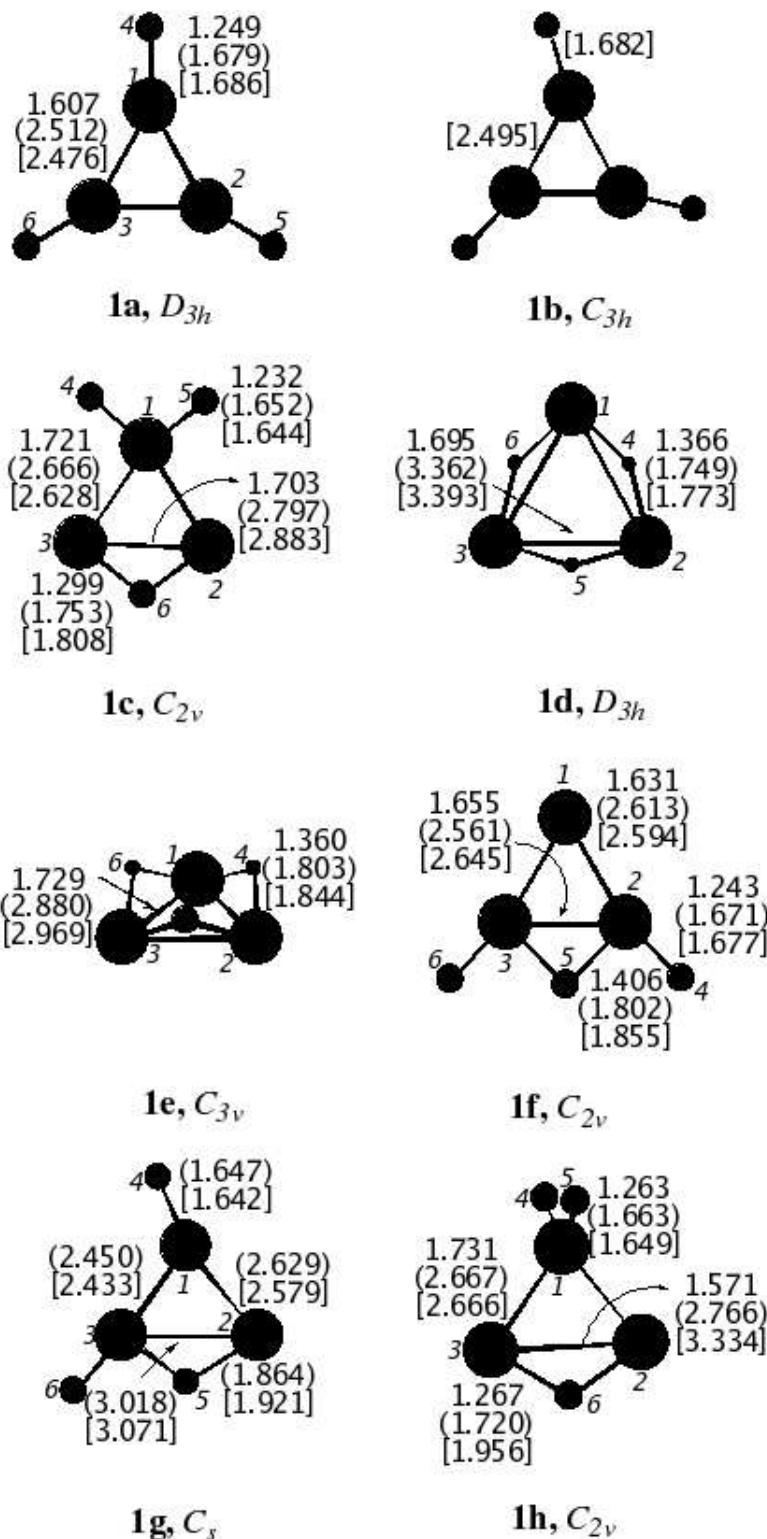
Table 2.4: Total energy (in au) and Zero point energy (ZPE, in kcal/mol) of the calculated $X_3H_6^+$ isomers at B3LYP and HF levels using 6-311G(d) basis.

X	Structure	Total Energy, B3LYP	ZPE	Total Energy, HF	ZPE
B	4a	-77.76101(1)	39.62	-77.10125(1)	42.17
	4b	-77.82878(0)	41.50	-77.20284(0)	43.60
	4c	–		–	
	4d	–		–	
	4e	-77.79360(2)	37.95	-77.17818(1)	40.39
	4f	–		–	
	4g	-77.76097(2)	38.46	-77.14284(2)	40.33
	4h	-77.81388(0)	40.31	-77.19585(0)	42.48
	4i	-77.79924(1)	39.65	-77.18582(1)	41.74
	4j	-77.70196(3)	36.47	-77.10576(3)	38.46
	4k	-77.45232(4)	34.06	-76.76086(4)	36.00
Al	4a	-730.58422(3)	27.28	-728.85937(3)	28.89
	4b	-730.67944(0)	28.26	-728.97089(0)	29.89
	4c	-730.70348(0)	28.45	-729.00131(0)	29.63
	4d	-730.67887(1)	26.74	Collapsed	
	4e	-730.67557(1)	27.06	-728.98151(1)	28.56
	4f	-730.69450(0)	28.51	-728.99437(0)	30.14
	4g	-730.65731(1)	26.19	-728.96047(1)	27.81
	4h	-730.65672(1)	26.94	-728.95226(1)	28.64
	4i	-730.65136(2)	26.89	-728.94775(2)	28.53
	4j	-730.60920(3)	24.36	-728.90687(3)	25.86
	4k	-730.50037(5)	23.28	-728.74077(5)	26.15
Ga	4a	-5777.80544(3)	26.18	-5772.69417(3)	28.03
	4b	-5777.90152(0)	26.00	-5772.80178(0)	27.52
	4c	-5777.94329(0)	26.91	-5772.84951(0)	27.83
	4d	Collapsed	to	open chain	
	4e	-5777.91435(0)	25.96	-5772.82962(0)	27.18
	4f	-5777.92205(0)	26.78	-5772.83036(0)	27.91
	4g	-5777.90595(1)	25.66	-5772.81802(1)	27.03
	4h	-5777.88777(2)	25.42	-5772.79075(2)	26.67
	4i	-5777.88175(3)	25.24	-5772.78556(3)	26.45
	4j	-5777.86430(3)	24.28	-5772.77254(3)	25.52
	4k	-5777.82033(3)	23.84	-5772.66887(5)	26.23

parison where appropriate.

Of all these structures, we will elaborate only the most relevant ones to establish the major bonding features that distinguish the alanes and galanes from the boranes. Bonding principles are highlighted for selected cases.

Figure 2.1: (Continued)

1i, C_1

1j, C_{2v}

1k, C_{2v}
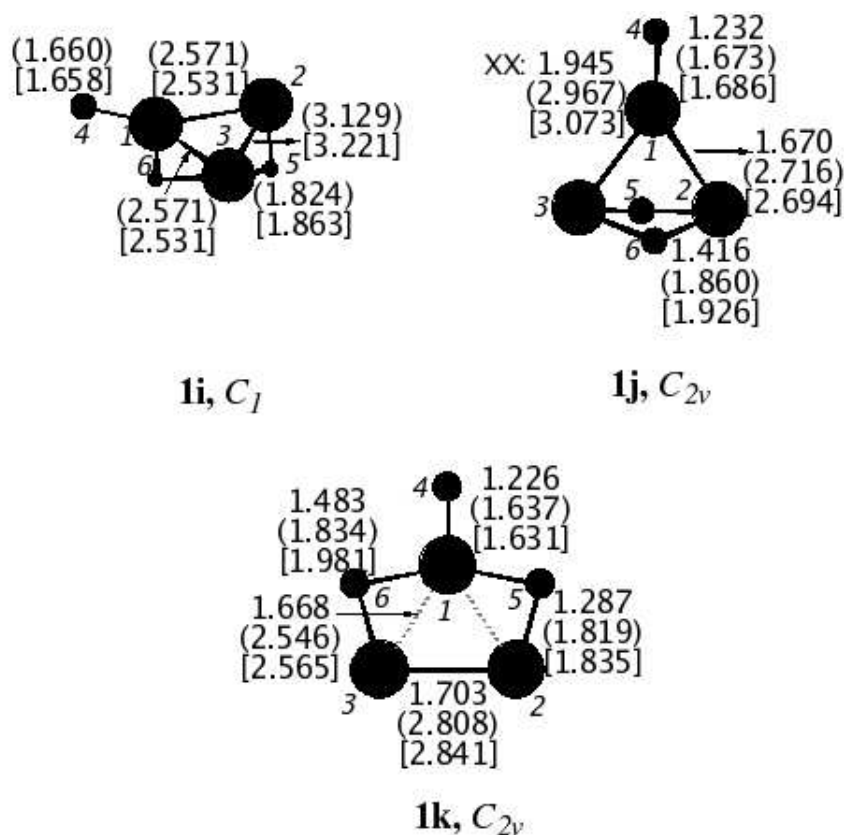
Table 2.5: Calculated X-X bond distances in X_2H_4, X_3H_3, $X_2H_4^{2-}$, $X_3H_4^{3-}$, X_2H_6, X_2H_2 at B3LYP/6-311G(d) level of theory. The reference below involves calculations at different levels.

	$X_2H_4^a$	$X_3H_3^b$	$X_2H_4^{2-c}$	$X_3H_4^{3-c}$	$X_2H_6^d$	$X_2H_2^c$
B-B	1.744	1.727	1.596	1.557	1.767	
Al-Al	2.621	2.664	2.475	2.482	2.623	2.989
Ga-Ga	2.525	2.647	2.371	2.447	2.633	3.069

[a] ref. 22-24,7a, [b] ref. 9,29, [c] ref. 20,25, [d] ref 26-28, [e] ref. 19-21.

Some important geometric parameters are also given in Figures **2.1-2.4**.

$X_3H_3^{2-}$. Total of seven minima were found for $Al_3H_3^{2-}$ and $Ga_3H_3^{2-}$, which contrasts the only two cyclic minima that were reported for $B_3H_3^{2-}$ (Scheme 2.1). [5] Isomer **1a** with all terminal hydrogens, is the global minimum for $B_3H_3^{2-}$. However, H-bridged **1c** with its planar tetra-coordinated heavy atom is the global minima for $Al_3H_3^{2-}$ and $Ga_3H_3^{2-}$. This isomer is

Figure 2.2: Optimized geometries and important bond distances for B, Al (in parentheses) and Ga (in brackets) isomers of $X_3H_4^-$ at B3LYP/6-311G(d) level. Atoms are numbered in italics

2a, C_{2v}

2b, C_s

2c, C_{2v}

2d, C_s

2e, C_{2v}

2f, C_{2v}

2g, C_2

2h, C_{2v}
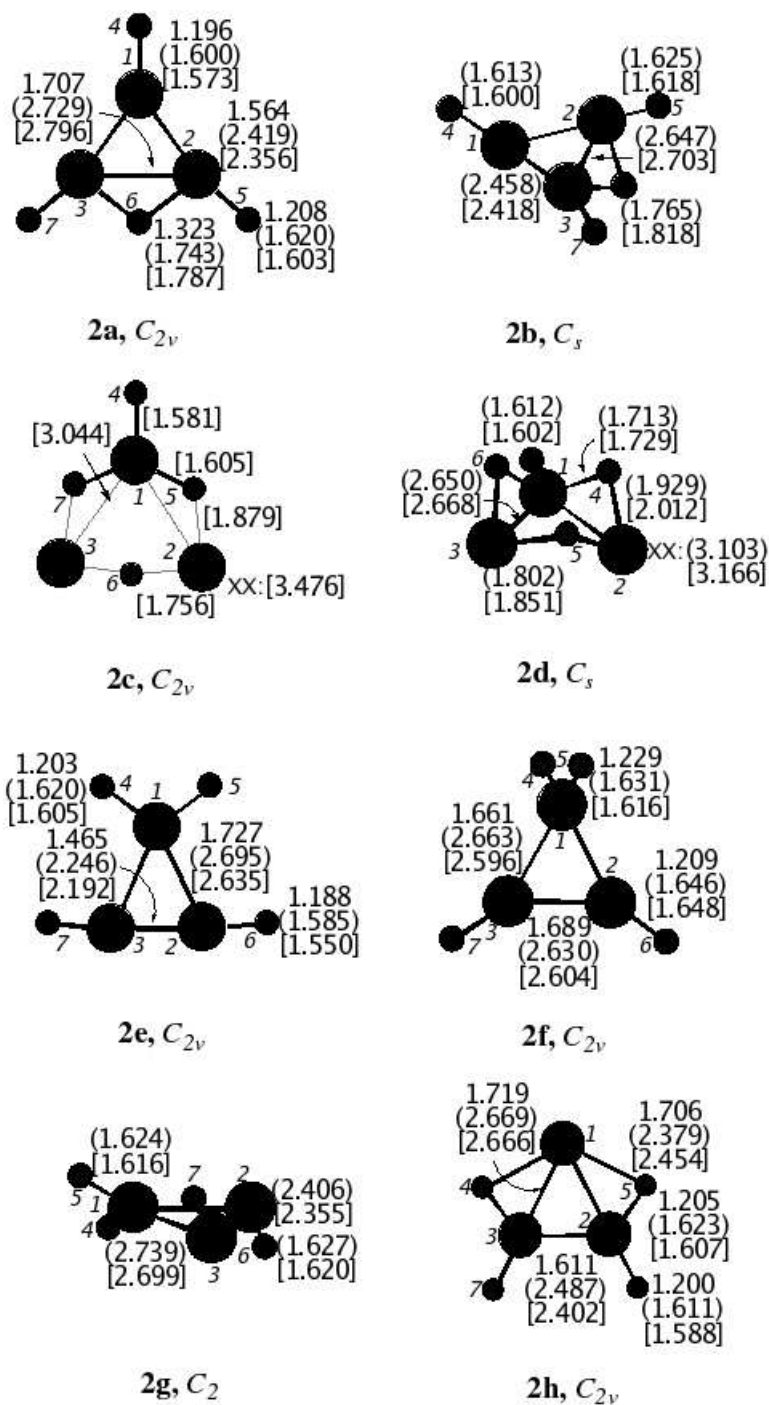
Figure 2.2: (Continued)

2i, C_1

2j, C_{2v}

2k, C_s

2l, C_{3v}

1.8 and 6.8 kcal/mol more stable than **1a** for Al and Ga respectively. Although **1c** is a $B_3H_3^{2-}$ minimum, it is 58 kcal/mol higher in energy than **1a** which highlights the dramatic difference between B and its heavier analogs. It is interesting to note that an isomer similar to **1c** is the global minimum for the isoelectronic Si_2BH_3. [37] **1a-Al** is also a minimum, but **1a-Ga** is a transition structure for the interconversion of C_{3h} structures (**1b-Ga**); the energy difference between **1a** and **1b** is negligible. A similar distortion from D_{3h} to C_{3h} is also seen in Pb_3H_6. [38] The experimentally determined X-ray structures have C_{3h} symmetry. [9, 10] A general bonding picture of **1b-Ga** and **1a-Al,Ga** may be constructed from the X-H fragments in their singlet ground states with a σ lone pair and 2p orbitals in

Figure 2.3: Optimized geometries and important bond distances for B, Al (in parentheses) and Ga (in brackets) isomers of X_3H_5 at B3LYP/6-311G(d) level. Atoms are numbered in italics
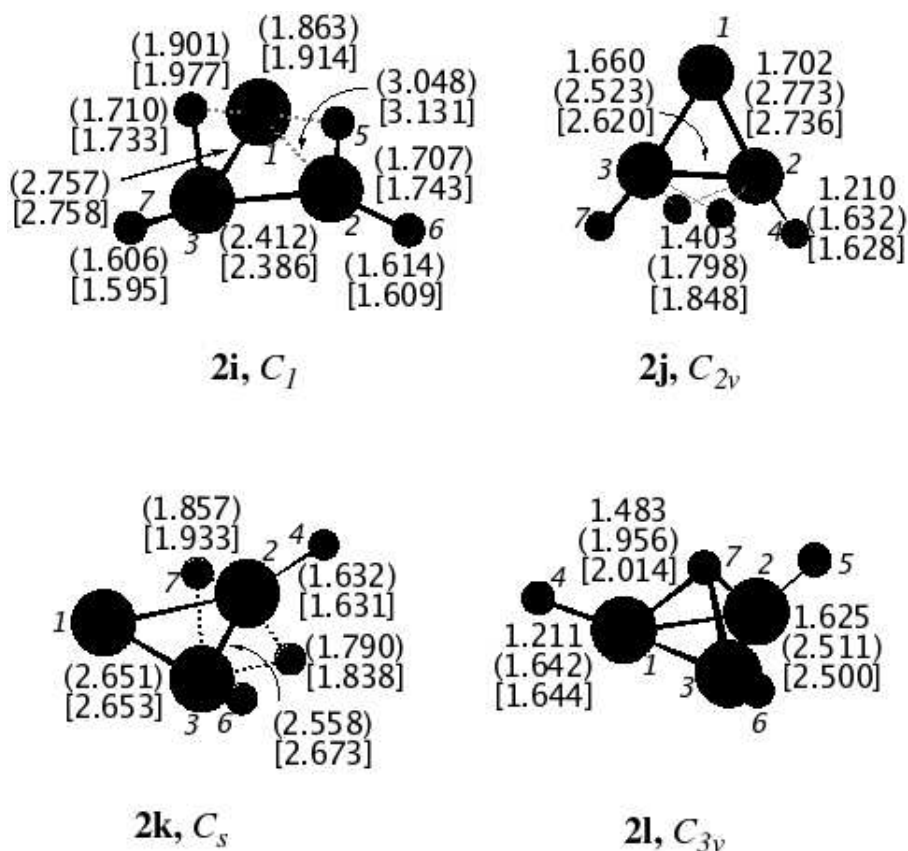

3a, C_{2v}

3b, C_s

3c, C_{2v}

3d, C_s

3e, C_s

3f, C_{2v}

3g, C_s

3h, C_s

Figure 2.3: (Continued)

3i, C_s

3j, C_s

3k, C_{2v}

3l, C_{2v}

3m, C_{2v}

3n, C_2

3o, C_{2v}

3p, D_{3h}

Figure 2.3: (Continued)

3i, C_s

3j, C_s

3k, C_{2v}

3l, C_{2v}

3m, C_{2v}

3n, C_2

3o, C_{2v}

3p, D_{3h}

orthogonal planes. In Ga and to a lower extent in Al, the σ lone pair is found to be mostly of s character and does not prefer to form the traditional sp^2 hybrid orbitals commonly seen in carbon. The bonding then

Figure 2.4: Optimized geometries and important bond distances for B, Al (in parentheses) and Ga (in brackets) isomers of $X_3H_6^+$ at B3LYP/6-311G(d) level. Atoms are numbered in italics
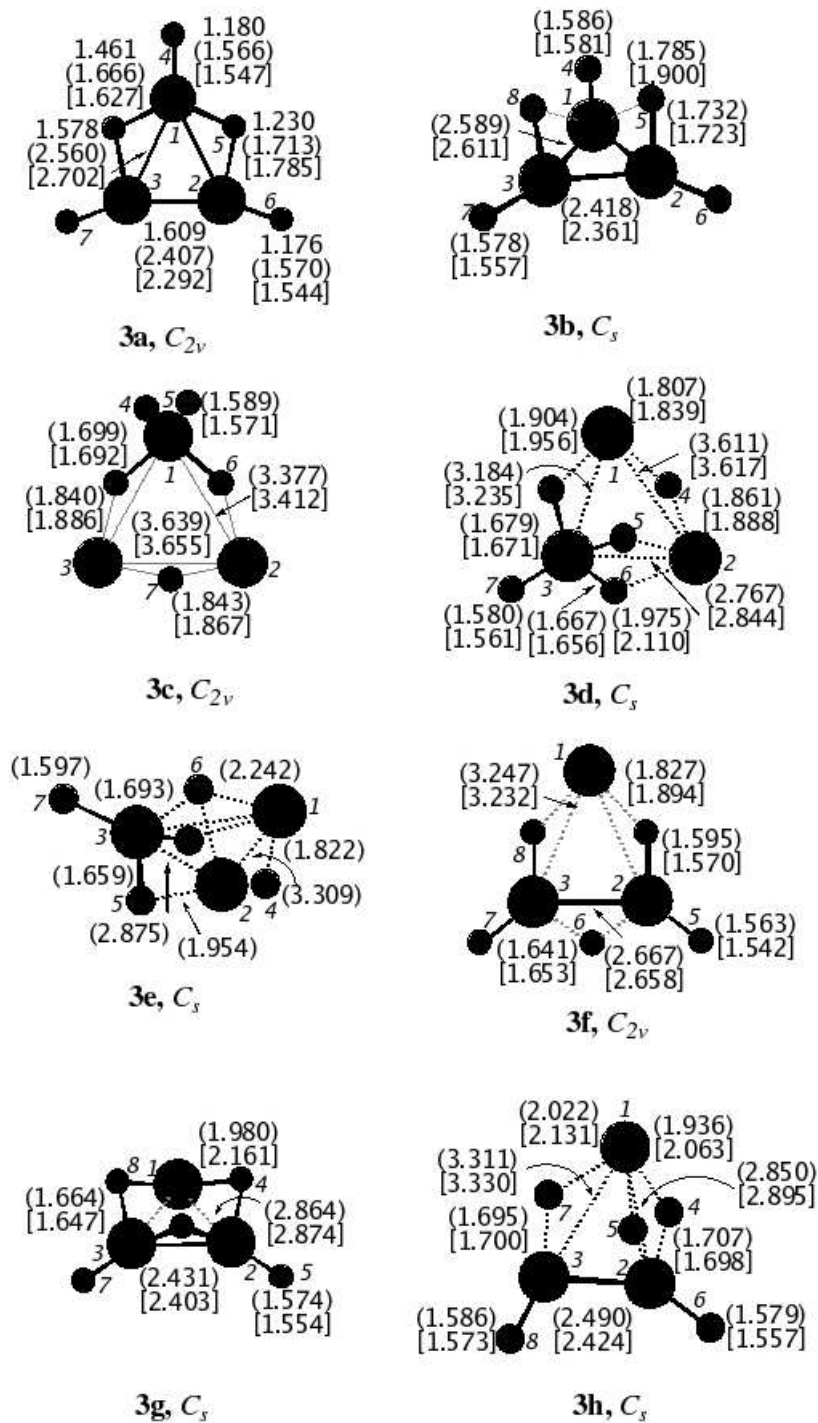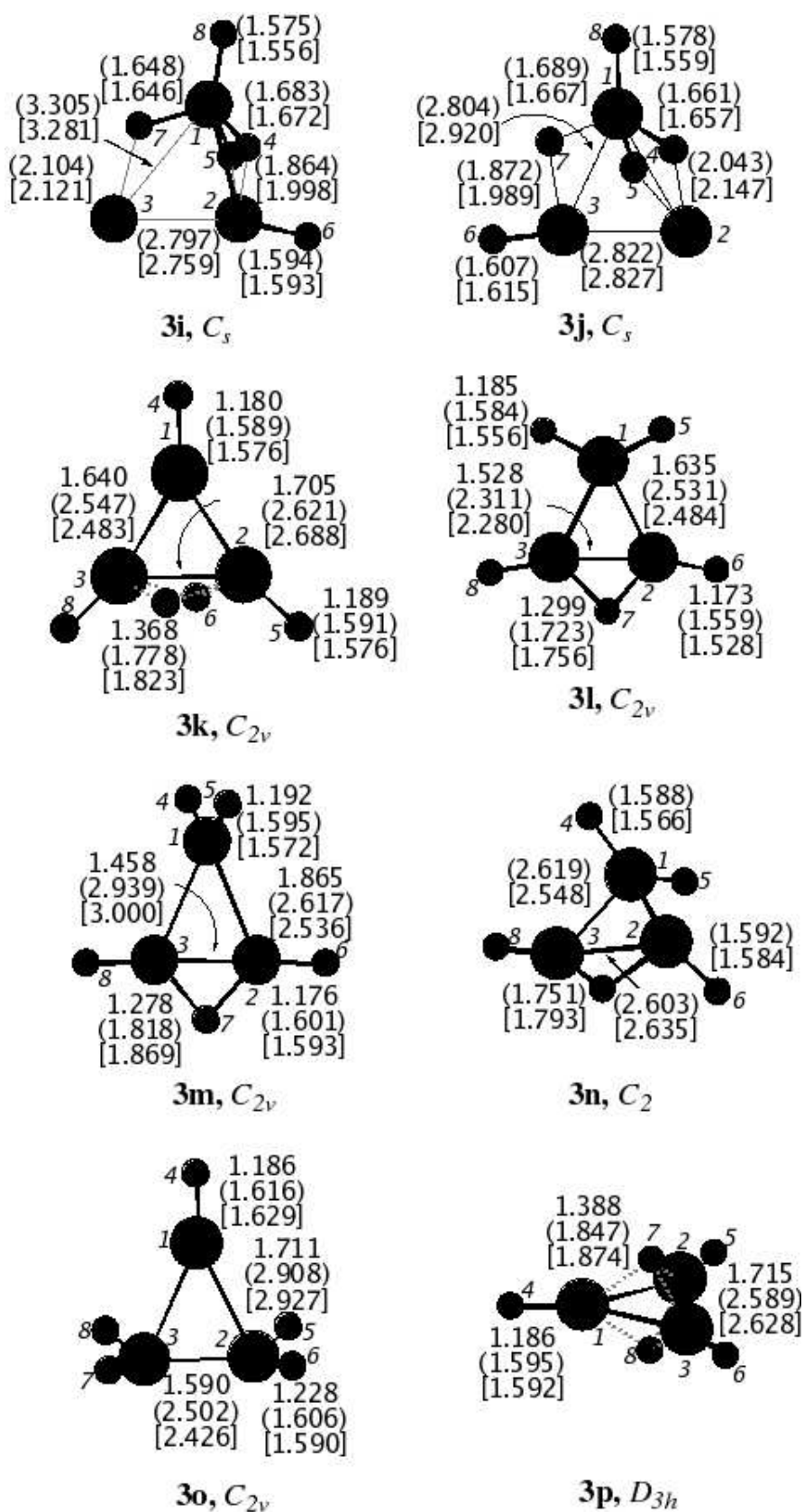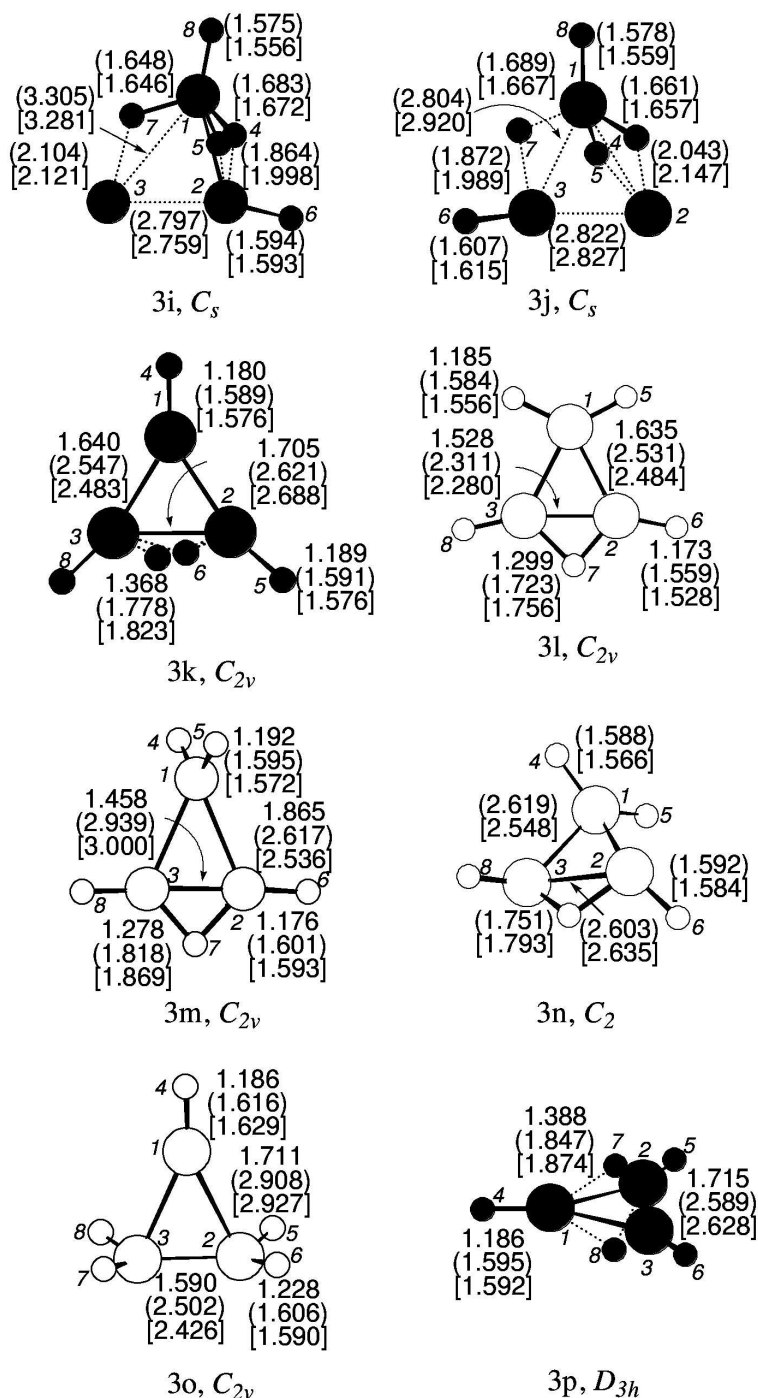

4a, D_{3h}

4b, D_{3h}

4c, C_{2v}

4d, C_s

4e, C_{2v}

4f, C_s

Figure 2.4: (Continued)

1.174
(1.577)
[1.579]
1.723
(2.936)
[2.914]
1.202
(1.567)
[1.546]
1.318
(1.696)
[1.716]
1.746
(2.906)
[2.943]

4g, C_{2v}

1.184
(1.573)
[1.554]
1.514
(2.313)
[2.294]
1.837
(2.863)
[2.794]
1.169
(1.550)
[1.524]
1.339
(1.739)
[1.780]

4h, C_{2v}

1.179
(1.569)
[1.552]
1.475
(2.298)
[2.270]
1.967
(2.950)
[2.914]
1.339
(1.737)
[1.780]
1.173
(1.552)
[1.525]

4i, C_{2v}

1.183
(1.570)
[1.554]
2.008
(2.973)
[2.906]

4j, D_{3h}

XX: 1.547
(4.571)
[4.757]
1.438
(2.321)
[2.412]

4k, D_{3h}
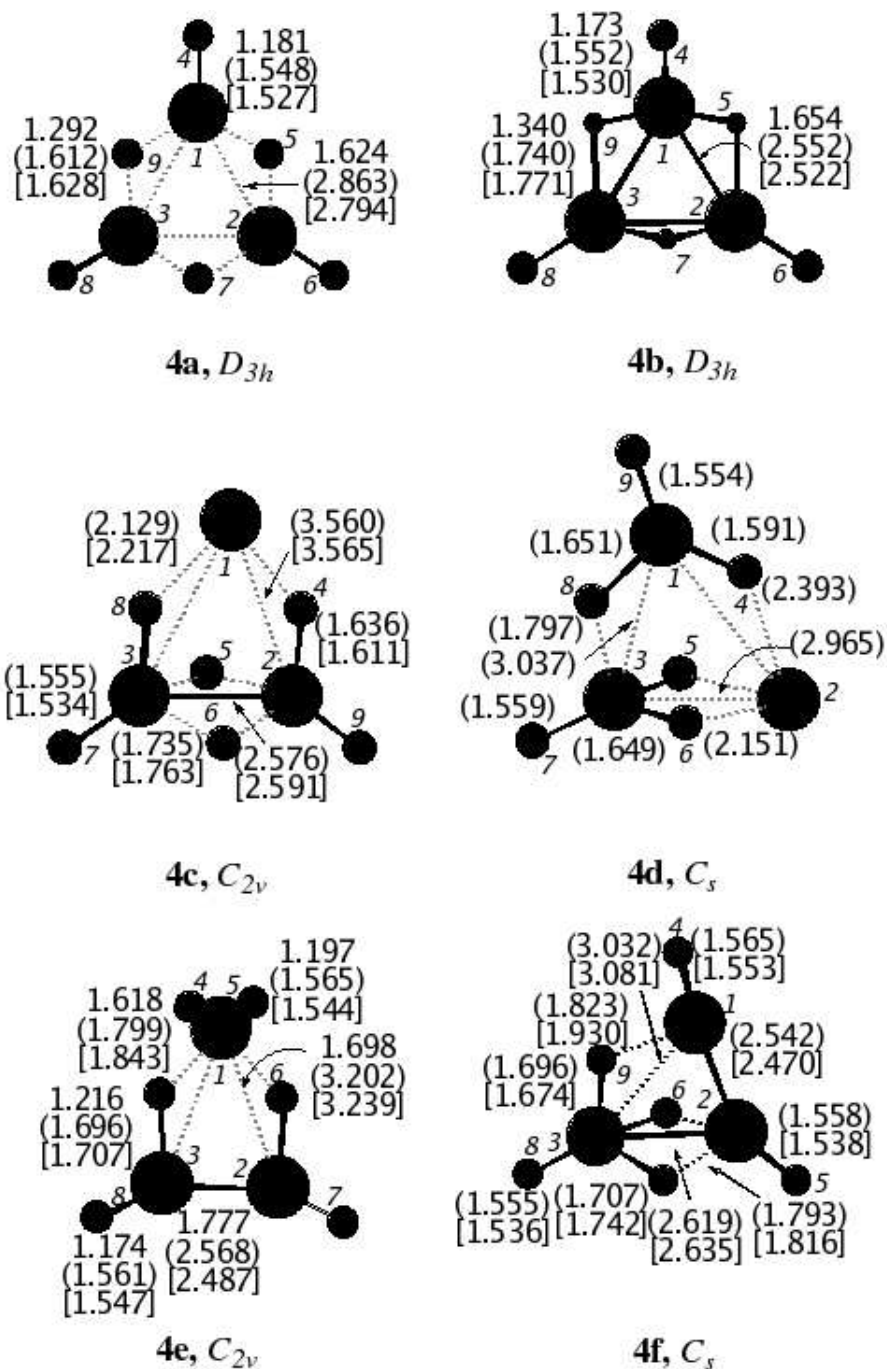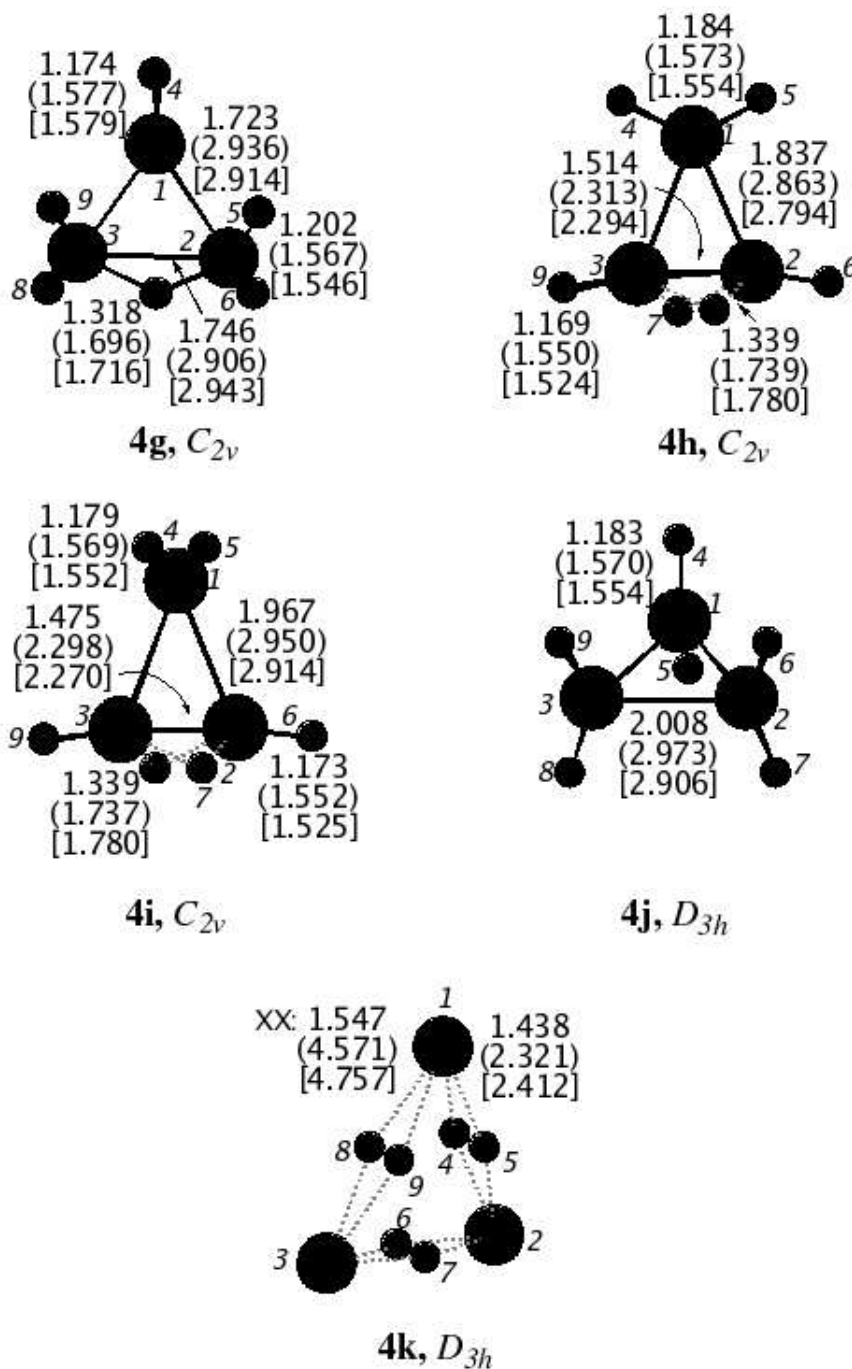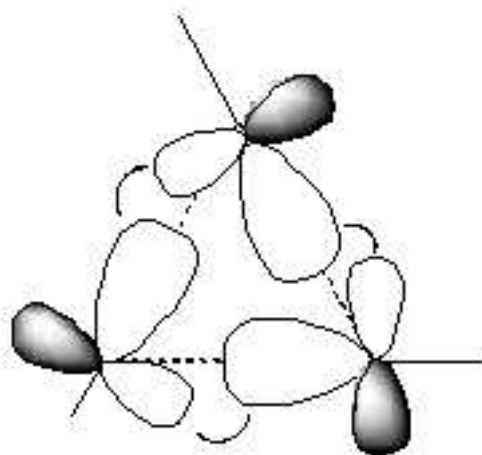
arises from donor acceptor interactions of the type indicated (Scheme 2.5). The extent of distortion depends on the differences in the s and p orbitals, the exact details of sp mixing, and the remaining bonds. Considering the extremely small differences in energy between **1a-Ga** and **1b-Ga**, we do

Scheme 2.5

not attempt to correlate the s and p mixing and relative energies.

The Ga-Ga distance in **1b-Ga** is about 0.07Å longer than those in the experimental structures **5** and **6**. We could not find any experimentally known three-membered Al dianion ring compound to compare to **1a-Al**, but the Al-Al distance in **1a** is in between that of a single bond and a double bond length. A comparison can be made with the experimentally available Al_2R_4 (**9**, R=Si^{t}Bu$_3$, R=CH(SiMe$_3$)$_2$ and R=2,4,6-(^{i}Pr)$_3$C$_6$H$_2$). [39] The Al-Al bond distances here are 2.751Å, 2.660 Å and 2.647 Å respectively. These are indeed longer than the Al-Al distance in **1a-Al** (2.512 Å). A part of this shortening comes from the nature of the bent bonds. For example, the C-C distance in cyclopropane is considerably shorter than in ethane. Another contributor is the 2π electron delocalization. A similar comparison can also be made to the experimental structures of Ga_2R_4 (**10**, 2.541 Å, R=CH(SiMe$_3$)$_2$; 2.515 Å, R=2,4,6-(^{i}Pr)$_3$C$_6$H$_2$) [40] which also show shorter bond distances for **1b-Ga** (2.495 Å).

The Al-Al and Ga-Ga bond distances in **1c** (Figure **2.1**, **1c**-Al^1-Al^3: 2.666 Å, **1c**-Ga^1-Ga^3: 2.628 Å) are similar to those of the single bonds

of X_3H_3 (D_{3h}). This is the result of a weak sigma bond (in fact a 3c-2e bond) and 2π-aromatic delocalization. The H-bridged Al-Al and Ga-Ga distances are longer than those of dialane(**6**) and digalane(**6**) but shorter than in the doubly H-bridged Al_2H_2 and Ga_2H_2. An MO analysis of **1c-Al,Ga** reveals that it has two 3c-2e bonds between X-H-X and X-X(H_2)-X, two 2c-2e X-H bonds, lone pairs on X^2 and X^3, and a delocalized π orbital over the ring. This is a remarkable result. Though minimum energy structures with square planar boron atoms have been found experimentally and theoretically, there were always lower energy alternatives. [41] Here we find that **1c**, the lowest energy that we obtained, has a square planar Al. The unusual stability of the square planar arrangement is also seen with Ga. **1c-Ga** is the lowest energy isomer we considered.

The triply H-bridged planar isomer **1d,** which can display 2π delocalization, is a higher order stationary point for B and a transition structure for both Al and Ga. The imaginary frequency indicates a distortion to a C_{3v} nonplanar structure **1e**. This isomer is about 7-8 kcal/mol less stable than the global minimum **1c** for both Al and Ga. Structure **1b** with only terminal hydrogen and structure **1e** with only bridging hydrogens are nearly isoenergic for Ga, but **1e** is 6 kcal/mol less stable than **1a** for Al. It is interesting to note that a $Si_3H_3^+$ structure similar to **1e** is nearly 42 kcal/mol higher in energy than its **1a**-like global minimum at MP2/6-31G(d) level, [15] whereas, **1e-B** is a higher order stationary point. The observed deformation of **1d** to **1e-Ga** may be understood from its molecular orbital description using a correlation diagram which depicts the interaction of π and σ orbitals on C_{3v} distortion (Figure 2.5). [42] The HOMO in D_{3h} symmetry is the non-

Figure 2.5: Correlation diagram between 1d and 1e showing the dramatic stabilization of the π-orbital.
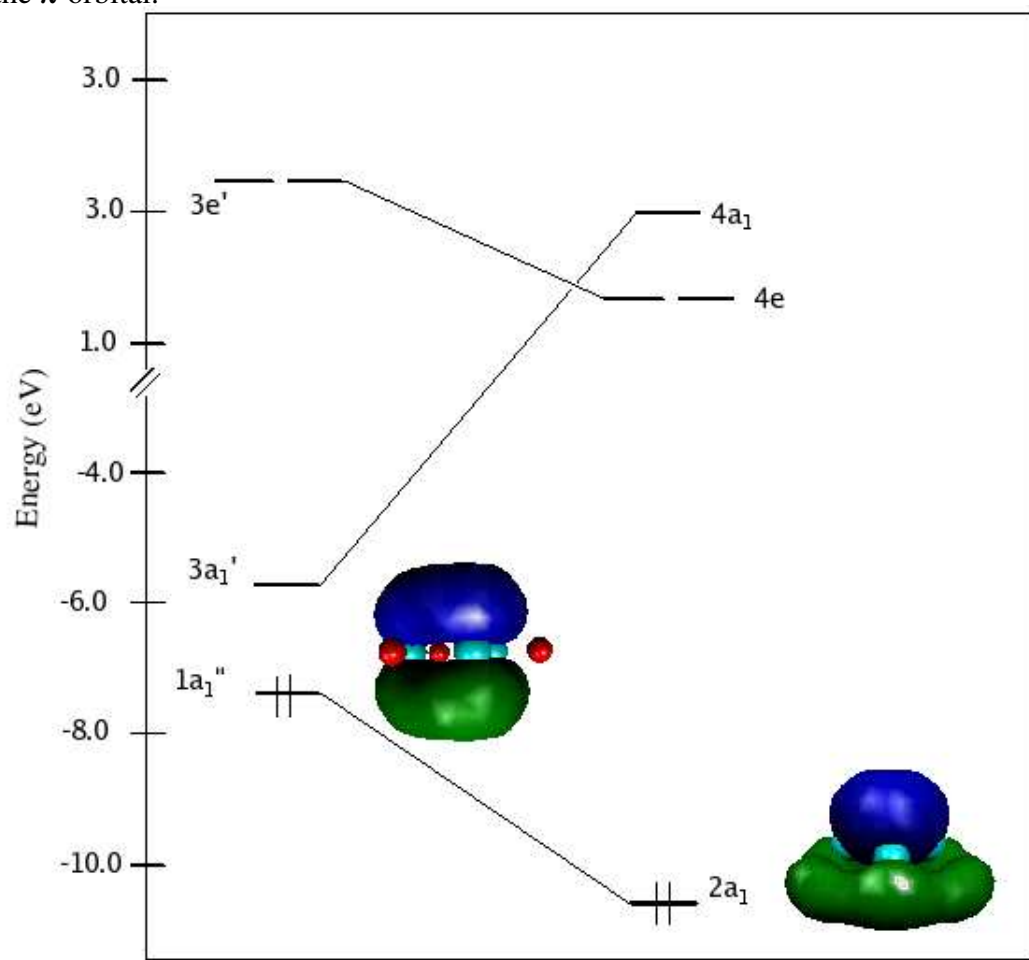
degenerate π-MO. The vacant 3a' orbital which is a bonding combination of the 1s orbitals of the hydrogen atoms, mix with the π MO when the symmetry is lowered to C_{3v}, leading to the stabilization of the π MO. Figure 2.5 shows the dramatic effect of this $\sigma - \pi$ mixing.

Structure **1f** is a minimum for both Al and Ga, and a transition structure for B. Among all ring structures considered, **1f-Al** and **1f-Ga** are the second best structures. The energy differences between **1c** and **1f** increases from Al (0.6 kcal/mol) to Ga (4.1 kcal/mol). Both the X-X and H-bridged X-X bond distances in **1f** are shorter compared to those in **1c**, except for the X-H_b. An analysis of the MO's of **1f** reveals that there are two 2c-2e

X-X bonds, two 2c-2e X-H bonds, one 3c-2e X-H-X bond, a lone pair on X^1, and a delocalized π MO. X^1-X^2 and X^1-X^3 pairs in **1c** are bonded by two 3c-2e bonds (one σ and one π). On the other hand **1f** has a 2c-2e σ-bond and a 3c-2e π-bond to bind X^1-X^2 and X^1-X^3. Therefore the X^1-X^2 and X^1-X^3 bond distances in **1f** are shorter than in **1c** ($\Delta = 0.05$ Å for Al and 0.03 Å for Ga).

An unsymmetrical arrangement of hydrogens around the ring leads to isomer **1g** (C_s), which is also a minimum for both Al and Ga with an energy difference with **1c** of 3.6 and 4.7 kcal/mol, respectively. The H-bridged X-X bond distance is lengthened in **1g** (3.018 Å) compared to **1f** (2.561 Å) and **1c** (2.797 Å). An MO description of **1g-Al,Ga** that account for the long M-M distance is as follows. The structure can be visualized as a combination of H-Al-Al and AlH_2. The sigma lone pair of AlH_2 is donated to the in-plane bonding combination (π-MO) of p orbitals of H-Al-Al (Scheme **2.6a**). The pseudo π (in-plane) AlH_2 MO is involved in weak interaction with the anti-bonding combination of the in-plane p orbitals (Scheme **2.6b**). In addition there is a delocalized 3-center π-MO that forms the HOMO-1. This explains the long Al^2-Al^3 distance as well as long Al^2-H^5 distance. The bonding in the Ga analogs is similar except that the order of HOMO and HOMO-1 are interchanged. A structure similar to **1g** is a minima for Si_2BH_3 and is 6.7 kcal/mol higher in energy than its global minima at QCISD(T)/6-31G(d) level. [37]

Non-planar alternative **1h**, obtained by a twist of the XH_2 group in **1c**, is a higher order saddle point for B and Al, but a transition structure for Ga. The imaginary frequency of **1h-Ga** leads to the nonplanar doubly H-
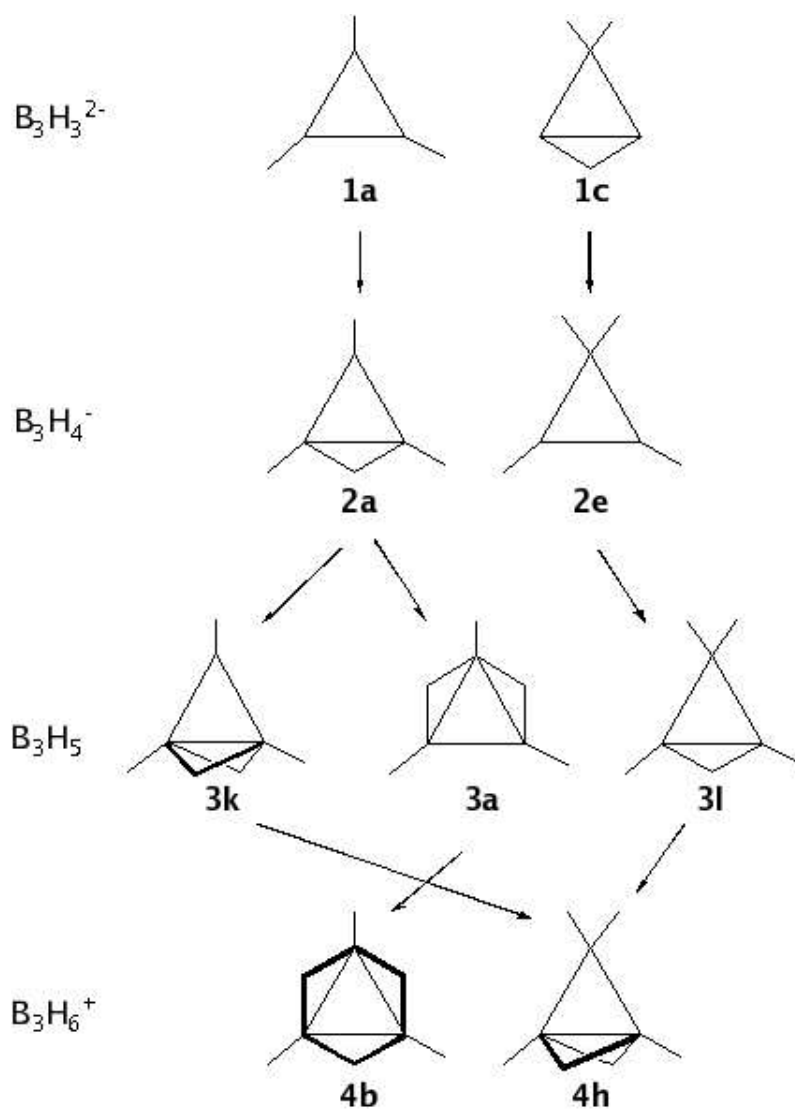
Scheme 2.6

bridged isomer **1i**, which is ∼5 kcal/mol higher in energy than global mini-

mum **1c-Ga**. Isomer **1i** is also a minima for Al and is likewise ∼5 kcal/mol

higher in energy than **1c-Al**. The electronic structure of **1i** consists of 2c-2e

X^1-X^2 and X-H bonds, two 3c-2e X-H-X bonds, and lone pairs on X^2 and

X^3. Its ring-delocalized π-orbital interacts with two bridged H's leading to

a hybrid delocalized orbital similar to that in **1e**.

Isomer **1j**, which has two H-bridging X^2-X^3 bonds, is a transition struc-

ture for both Al and Ga. Optimization in the direction of the imaginary

vector (without any symmetry constrains) leads to planar isomer **1k,** which is a minimum for both Al and Ga with an energy difference of 3.8 and 7.2 kcal/mol, respectively, with **1c**. We note that a similar structure is a minima for the iso-electronic $Si_3H_3^+$ and a transition structure for Si_2BH_3. [15, 37] The electronic structure of **1k** also shows 2π electron delocalization over the ring along with two 3c-2e H-bridged X-X bonds, one 2c-2e X-X bond, and a 2c-2e X-H bond.

$X_3H_4^-$, X_3H_5 and $X_3H_6^+$

Results on the studies of the isomers of $X_3H_4^-$, $X_3H_5$and $X_3H_6^+$ are summarized in Scheme **2.2, 2.3 and 2.4** for X=B, Al and Ga. While each of these structural types may be discussed individually, a better understanding is obtained by considering the evolution of the isomers corresponding to $X_3H_4^-$, X_3H_5 and $X_3H_6^+$ by sequential protonation from $X_3H_3^{2-}$ which is discussed above. These are done for B, Al and Ga separately, starting with the minimum energy structures available for $X_3H_3^{2-}$ (Schemes **2.7, 2.8 and 2.9**). Thus the Scheme **2.7** provides the minimum energy structures available starting from **1a** and **1c**, the only two minima on the $B_3H_3^{2-}$ PES with triangular B_3 arrangement. Arrows indicate the direct relationships that exist between structures via protonation. A comparison of Scheme **2.7** with the general Schemes **2.1-2.4** indicates that this formal protonation strategy includes all minimum energy structures. The basic structural preferences appear to be decided already in the isomers of $X_3H_3^{2-}$. The large number of transition states and other higher order stationary points calculated for $B_3H_3^{2-}$ do not lead to any minimum energy structures. There are two interesting points to be noted here. First is the preference for the planar tetraco-
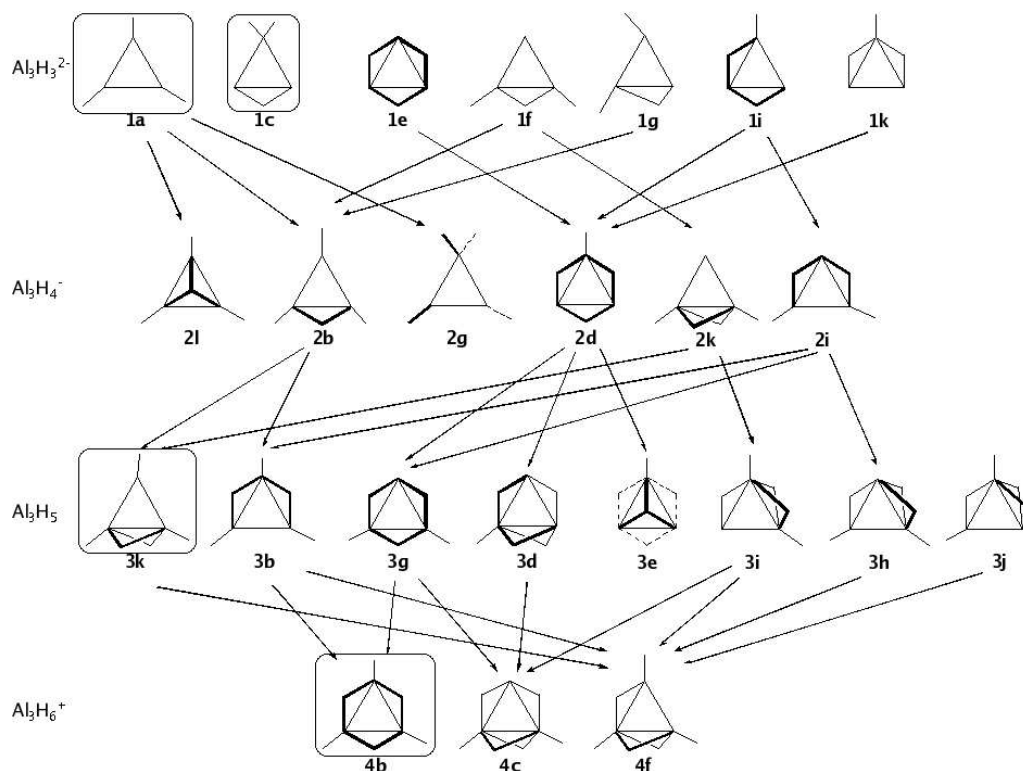
Scheme 2.7

ordinate arrangement at boron seen in **1c-B**, **2e-B**, **3l-B** and **4h-B**. By contrast stabilization of planar tetracoordinate carbon is more difficult. [43] Differences in relative energies of 2c-2e and 3c-2e bonds involving carbon and boron atoms contribute to this trend. Carbon-carbon single bonds are considerably stronger than boron-boron single bonds. Still **1c-B** is higher in energy than **1a-B** by 58.12 kcal/mol. A second important aspect of the minimum energy structures is the non-planar $B_3H_6^+$ structure. The interplay of mixing mentioned earlier control the energetics here. However, the balance is delicate, as structures **2a-B**, **3a-B** and **3l-B** prefer planar arrangements (see Figure **2.5** for analogous MO's). This is in contrast to the behavior of Al and Ga structures seen below.

The number of triangular structures calculated to be minimum in energy

for Al_3H_n is considerably larger. Scheme **2.8** attempts to relate all struc-
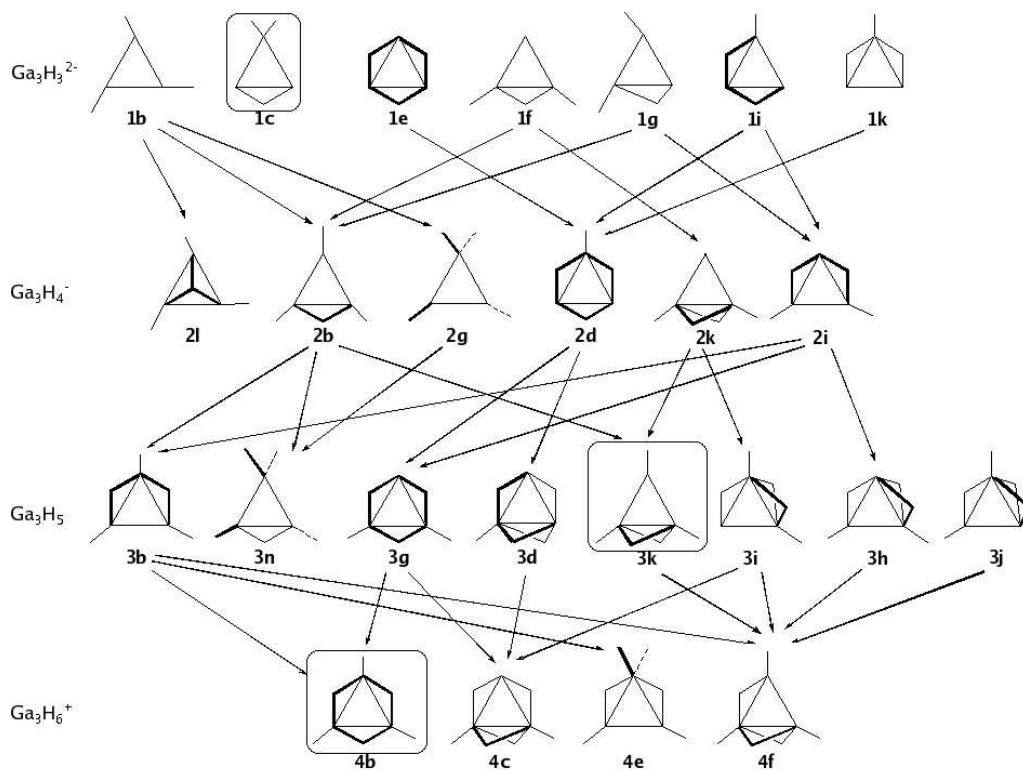
Scheme 2.8

tures to the isomers of $Al_3H_3^{2-}$. In addition to the propensity for square planar arrangements, there are several novel structural features seen in Al_3H_n, that are not seen with B_3H_n. The most dramatic one is the unsymmetric terminal Al-H bonds as seen in **1g-Al**. This is exceptional because there is only one structure in the entire Al_3 set with this feature. As explained in Scheme **2.6** above, the structure is best considered as a combination of AlH_2 and HAl-Al. The bridging hydrogen-terminal hydrogen combination is seen in the structure of Si_2H_2 as well. [14] A symmetrical C_{3h} structure with three distorted terminal Al-H bonds (**1b-Al**) was not a stationary point. Protonation of **1g-Al** led to **2b-Al** with terminal Al-H bonds which are symmetrically placed.

The next unusual structural aspect in comparison to B_3H_n is the out-

of-plane distortion of bridging hydrogens in $Al_3H_3^{2-}$, $Al_3H_4^-$ and Al_3H_5. Structures with one bridging hydrogen is in the plane of the X_3 ring in **1c**, **1f**, and **1g**; but not so in **2b**. Similarly the two bridging hydrogens are in the X_3 plane in **1k**, but out-of-the plane in **1i**. However protonation of **1i** and **1k** leads to the same triply bridged structure **2d** where all the three hydrogens are outside the X_3 plane. Three bridging hydrogens bring the same situations as has been observed in **1e** (Figure **2.5**) and remain out of the Al_3 plane.

Another difference between boron and Al structures is the propensity of doubly H-bridged structures with Al. Thus **2k**, **3k**, **3d**, **3i**, **3h**, **4c** and **4f** are all calculated to be minima. In contrast there are only two structures **3k-B** an **4h-B** with doubly H-bridged bonds amongst boron isomers. The decrease in bond energy of a regular 2c-2e X-H bond in going from X=B to X=Al perhaps explains this propensity for bridged structures.

Structures with H-capping the triangle, **2l-Al** and **3e-Al**, are also special to Al_3 series. The interaction of the 1s orbitals of the capping hydrogens with the orbitals of the Al_3 is enhanced by the tilting of the $Al-H_t$ bonds towards the side of the capping hydrogens in **2l-Al**. The second such structure, **3e-Al**, is even more remarkable with three bridging hydrogens on the opposite side, but the lone terminal Al-H bond tilted towards the capping hydrogen. These structural details are in tune with the idea of compatibility of orbitals in overlap that we have detailed elsewhere. [44, 46]

The gallium series brings in the unusual structural aspects found in Al structures in larger measure. The classical structure **1a-B** and **1a-Al** does not have a counterpart with Ga. The D_{3h} structure distorts to **1b-**

Ga (C_{3h}). The bonding model (Scheme **2.5**) which describe this structure is also suggested to explain similar C_{3h} structure of Group 4 compounds such as Pb_3R_6 and Sn_3R_6. [9, 15, 38] The C_{3h} structure **1b-Ga** leads to the C_3 structure **2l-Ga**. However similar distortion in **1g-Ga** is removed on protonation to **2b-Ga** or **2i-Ga**. Similarly the tendency for the out-of-plane distortion of the bridging hydrogens is enhanced in the structures of gallium compounds. The delicate balance between a planar bridged structure and out-of-plane tilting is also seen dramatically in the structures **2a-B**, **2b-Al** and **2b-Ga**.

Isomer **2a** obtained by protonation of a X-X bond of **1a**, is the global $B_3H_4^-$ minimum, but it is a transition structure for Al and Ga. The imaginary frequency leads to non-planar structure **2b** (C_s). An MO explanation is provided below. We note that a similar distortion from the planar C_{2v} structure has been reported for SiB_2H_4. [45] The energy difference between **2a** and **2b** is only 1.0 kcal/mol for Al and 2.4 kcal/mol for Ga. The X^2-X^3 bond distance is shortened and the X^1-X^2 distance is lengthened in **2b** as compared to **2a**. The electronic structure of **2a-B** consists of three 2c-2e X-H bonds, two 2c-2e X-X bonds and a 3c-2e X-H-X bond, and an occupied π-MO . The in-plane 3c-2e X-H-X bond is weaker for Al and Ga, (as the X-X bond gets longer) due to the less effective overlap of the bridging hydrogen with the bent Walsh orbitals. (Scheme **2.9(a)**). Instead, on moving the bridging hydrogen out of plane, better overlap with the π-orbitals on X results (Scheme **2.9(b)**). As a result, the bridging H contributes to the ring-delocalized π-orbital. The 1,2-shift in cyclic vinyl cations is another example where the bridging hydrogen is distorted from
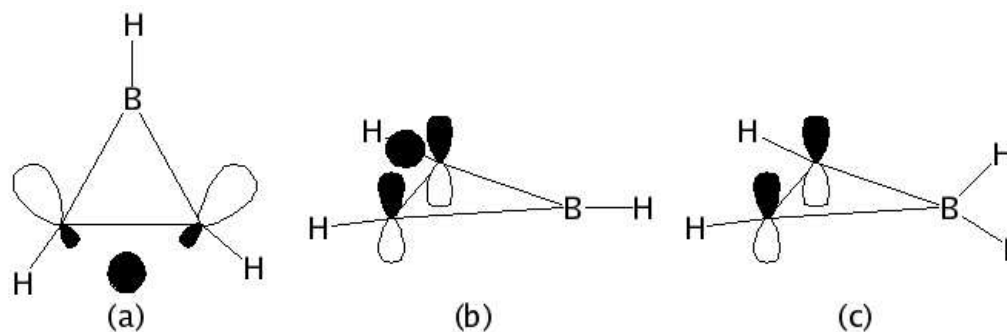
Scheme 2.9

planarity. [46]

C_{2v} structure **2e** with a *planar tetra-coordinated* boron atom is a $B_3H_4^-$ minima due to the strong π-delocalization and is only 1.6 kcal/mol less stable than **2a**. Both the van't Hoff (**2f**) and anti-van't Hoff (**2e**) structures are higher order saddle points for Al but, the twisted nonplanar form **2g-Al** (C_2) is a minimum. The experimentally known neutral Al_3R_4 $(R=Si^tBu_3)$ (**11**) radical is known to have such a nonplanar structure, [47] but that of Ga_3R_4 (**12**) reportedly has a van't Hoff structure. [48] The reduced species $Ga_3R_4^-$ (**13**) (R = tBu) has, however, a completely different geometry, in which one of the substituent's methyl groups interacts with the Ga^2 atoms leading to a very long Ga^1-Ga^2 bond distance of 2.935 Å. [48] Of the two sets of X-X bonds in **2g**, one (Al: 2.406 Å, Ga: 2.355 Å) is shorter than a normal X-X double bond and the other (Al: 2.739 Å, Ga: 2.699 Å) is longer than a regular X-X single bond. The Al^1-Al^2 bond distance in **2g-Al** is similar in length to that in **11**, but the Al^2-Al^3 distance is nearly 0.3 Å shorter. These structures are also examples of pyramidal tricoordination which along with planar tetracoordination rewrite the structural basis of the main group chemistry. The tricoordinate planar geometry of CH_3^+ and

BH_3, are taken for granted. Recently we had shown that pyramidal tricoordinate boron is a possibility. [49] Structures **2g-Al** and **2g-Ga** are the first such examples with non-planar Al and Ga atoms. The electronic structure of **2g** can be best understood by comparing it with isomer **2f**, which has an empty π- LUMO, formed from the p_z (X^2) and p_z (X^3) atomic orbitals (Scheme **2.9(c)**) and sp^2 hybridized X^2 and X^3 atoms. Due to the decreased sp^2-hybridization for the heavier elements Al and Ga, [29] their X^2-X^3 and X^2-H^6 $(X^3$-$H^7)$ bonds are weak. This is compensated by moving the H^6 and H^7 atoms out of plane to enable them to interact with the empty p_z orbital (π-MO) resulting in non-planarity of the structure and causing the XH_2 group to twist.

It is interesting to note that the imaginary frequency in **3c-Ga** led to **3d**, where as **3c-Al** led to **3e**! We also found that **3d-Al** is a minimum. However, on optimization **3e-Ga** (without any symmetry constrains) collapsed to **3d**. The singly H-bridged X^1-X^2 and X^1-X^3 bonds in **3d** are longer than those in X_2H_6 and X_2H_2. The X^3-H^8, X^3-H^6 and X^3-H^5 distances are very short compared to X^1-H^8, X^2-H^5 and X^2-H^6 respectively. For example H^5 is closer to X^3 by 0.31Å in Al_3H_5 and 0.45Å in Ga_3H_5 than to X^2. This shows that the isomer **3d** can be viewed as an adduct formed by the interaction between X_2H^+ (consists of X^1, X^2 and H^4) and XH_4^- (consists of X^3, H^5, H^6, H^7 and H^8). The NBO charges also support such an interpretation, the sum of the natural charges on Ga^3 (0.72), H^5 (-0.35), H^6 (-0.35), H^7 (-0.44) and H^8 (-0.27) is –0.7e and the sum of the charges on Ga^1 (0.70), Ga^2 (0.60) and H^4 (-0.60) is +0.7e. Similar results were found for **3d-Al**. Isomer **3e-Al** is very much close to **3d**, since the bridging hydrogen H^6 is

now interacting with both Al^1 and Al^2 in **3e** instead of only with Al^2 in **3d**. Alternatively isomer **3e** can be arrived by capping **2d** with a proton. The bond lengths in **3e** show trends similar to **3d** and the bonding features of **3e** are almost similar to that of **3d**. That is isomer **3e** can also be viewed as an adduct of AlH_4^- (Al^3, H^{5-8}) and Al_2H^+ (Al^1, Al^2 and H^4). The NBO chargers also support the interpretation (Al^1: 0.62, Al^3: 1.02, H^4: -0.59, H^5: -0.44, H^6: -0.44, H^7: -0.35). The energy difference between **3d-Al** and **3e-Al** is only 1.0 kcal/mol.

The potential energy surfaces of Al and Ga three rings contrasts dramatically with that of B three rings. The non-planarity of hydrogens with respect to X_3 ring is found to be very common for Al and Ga species. Similarly species with lone pairs on heavy atoms dominate the potential energy surfaces of Al and Ga three ring systems. The global minimum structures of B are minima for Al and Ga only in case of $X_3H_3^{2-}$ and $X_3H_6^+$. Even here $Ga_3H_3^{-2}$ has a distortion from D_{3h} to C_{3h}. On the potential energy surface of $X_3H_4^-$ and X_3H_5, the global minimum structures of B are not even minima for Al and Ga. Similarly, the influence of π-delocalization in stabilizing the structures is decreased from $X_3H_3^{2-}$ to $X_3H_6^+$. For example, the global minimum structures of $X_3H_3^{2-}$, $X_3H_4^-$ have the 2π-delocalization for both Al and Ga. However, the global minima of $X_3H_6^+$ does not have conventional 2π-electrons for both Al and Ga. In case of X_3H_5 the global minima is aromatic for Al and not aromatic for Ga. The propensity of isomers with bridging hydrogens and para Al and Ga atoms calculated here is a reflection of the nature of structure and bonding observed in heavier elements of the main group. For example the lowest energy isomer of Si_2H_2

has two bridging hydrogens. [14] The next isomer has one bridging hydrogen. In view of such experimental observations available in literature, we are confident that the novel structures that are presented here will stand experimental scrutiny.

The resonance stabilization energy (RSE) for the global minimum structures (or nearest structures to global minimum which contains π-delocalization) is computed using the isodesmic equations 1-6 (Scheme **2.1**). [4] We tried
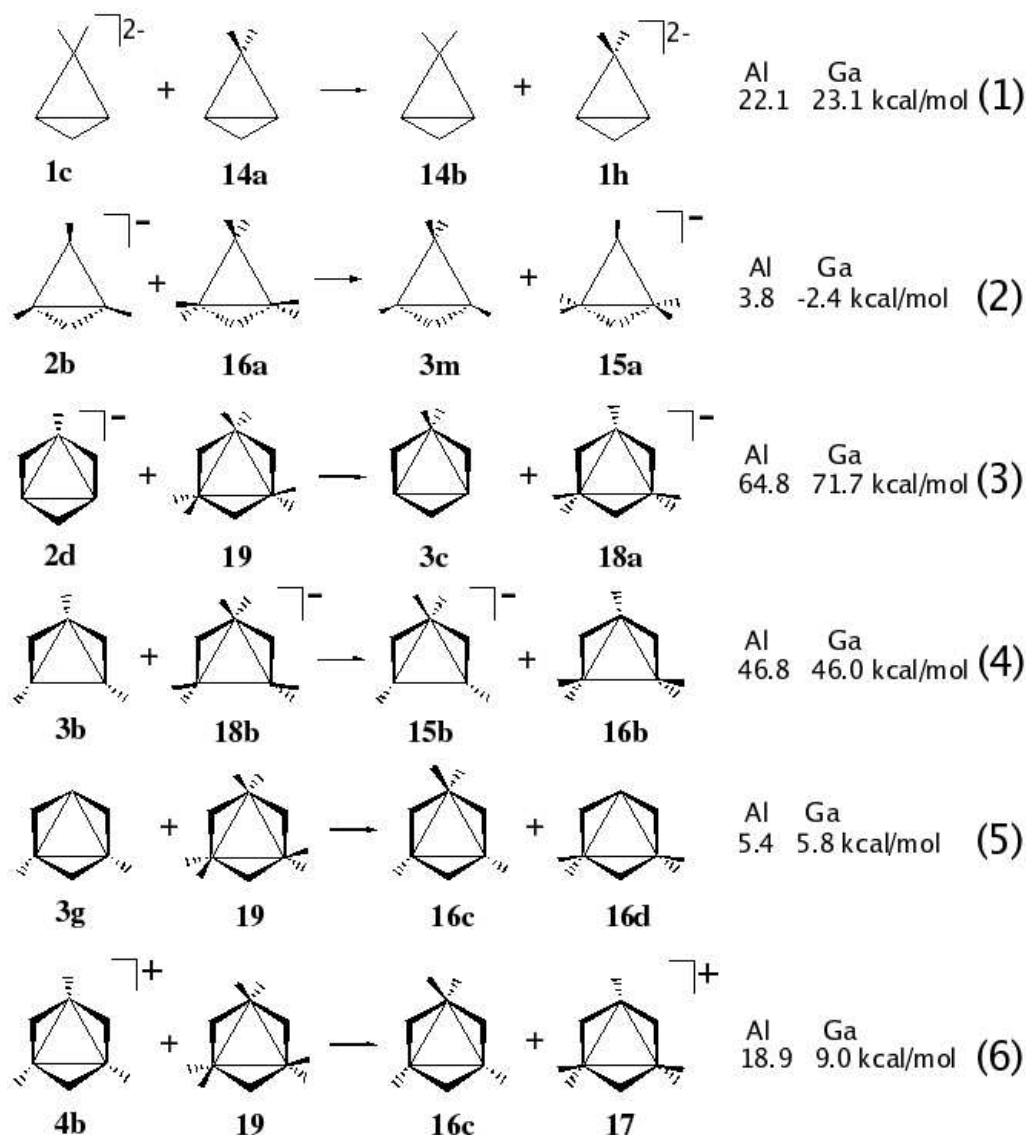
Scheme 2.10

Figure 2.6: Optimized geometries of the reference species X_3H_3(**14**), $X_3H_6^-$ (**15**), X_3H_7 (**16**), $X_3H_8^+$ (**17**), $X_3H_8^-$ (**18**) and X_3H_9 (**19**). The important bond distances for Al (in parentheses) and Ga (in brackets) are given at B3LYP/6-311G(d) level.
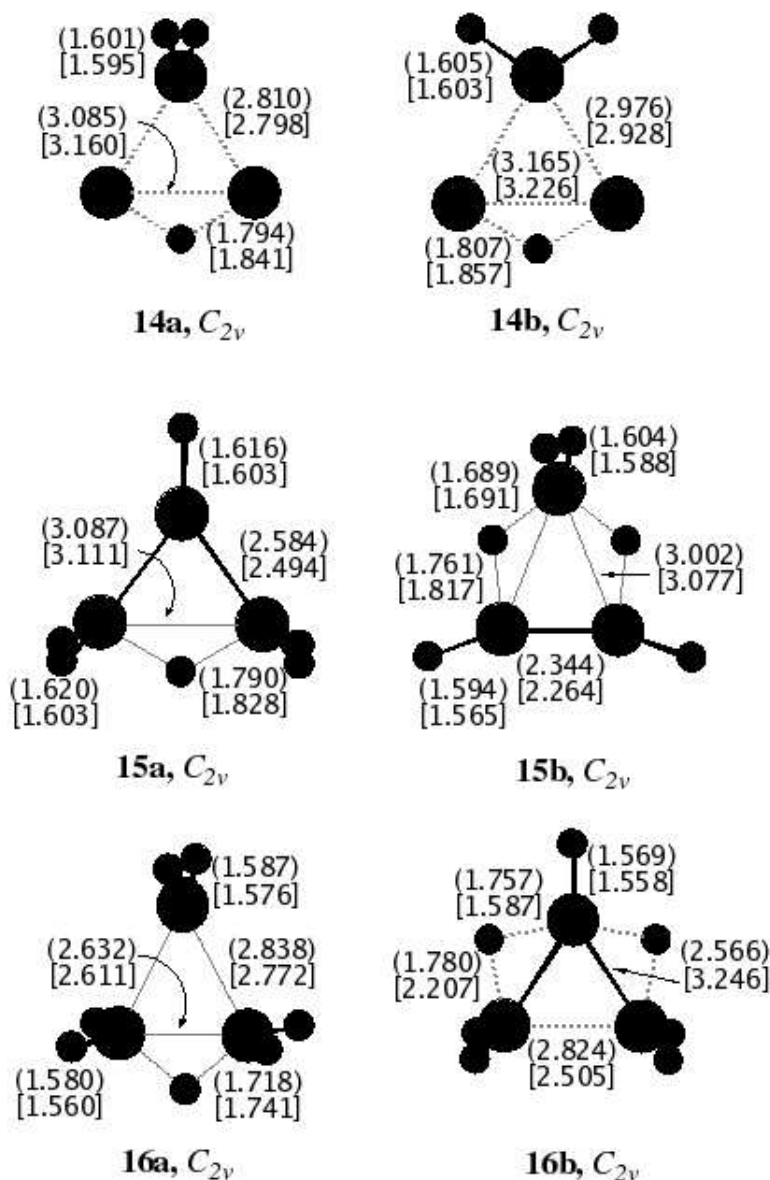
to maintain the non planarity of bridging hydrogens in the reference species (**14**-**19**) in accordance with isomers **2b**, **2d**, **3b**, **3g** and **4b**. However on optimization all the reference species **14**-**19** (except **16c**) collapsed to planar structures (Figure **2.6**). Detailed explanations for the relative energies here are difficult because the RSE differences between different compounds or

Figure 2.6: (continued)

16c, C_s **16d,** C_{2v}

17, C_{2v} **18a,** C_{2v}

18b, C_{2v} **19,** D_{3h}
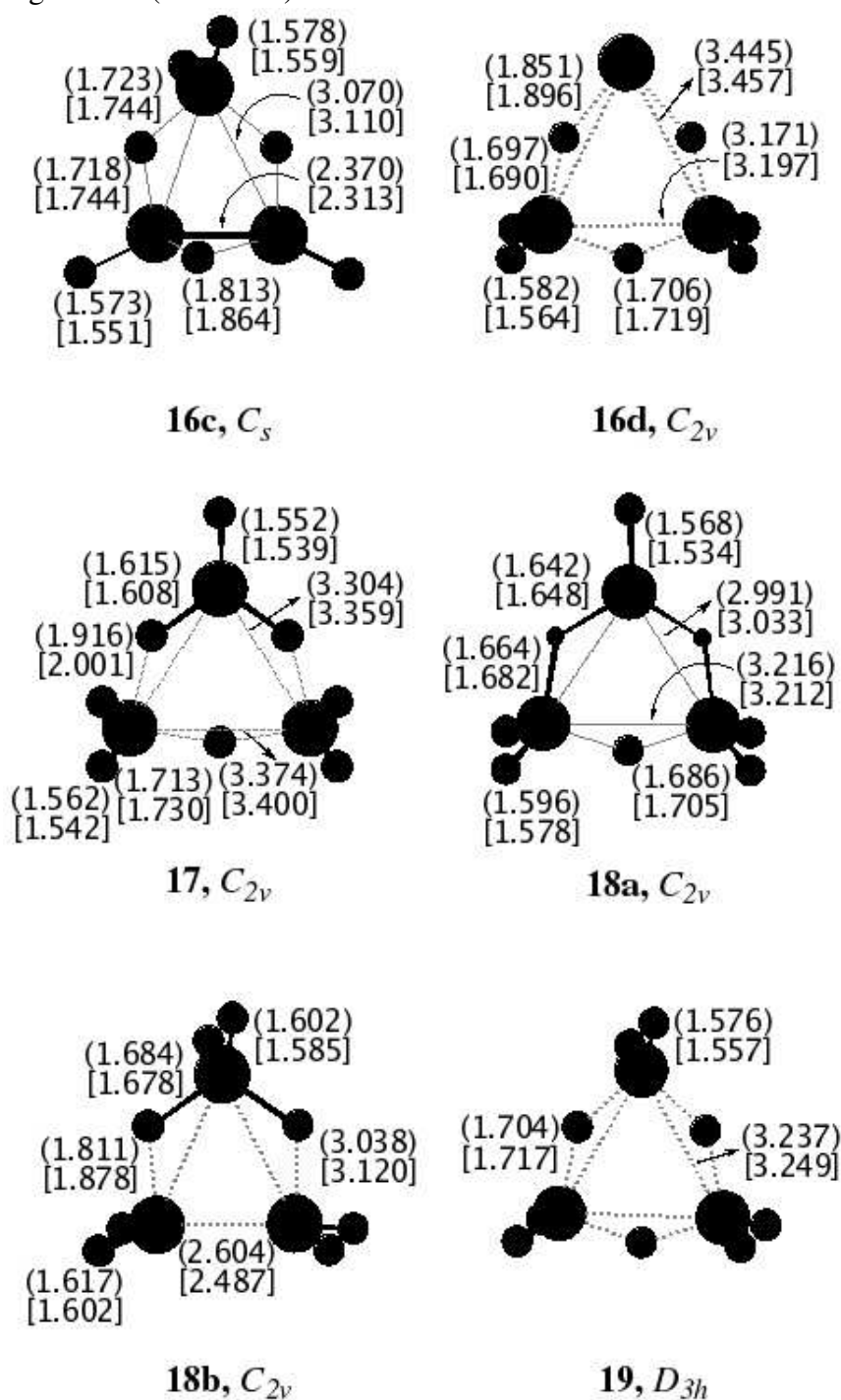
in between Al and Ga are very small. There are many uncertainties in deriving these energies. For example (a) the selection of the reference molecules is not unambiguous, (b) even if we selected some very good reference molecules, on optimization, planar or non-planar arrangement

of hydrogens may not be consistent with the molecule for which we are trying to get the RSE. For example isomer **2b** has non-planar arrangement of both terminal and bridging hydrogens where as the reference molecules **16a**, **3m** and **15a** all have planar bridging hydrogens. This will certainly have its effect on RSE since all the heavy atoms are not similar on both sides of the equation (at least in terms of hybridization). Therefore we caution the reader that the best way to know a particular molecule has π-delocalization or not is to look at its electronic structure.

2.4 Conclusions

The computational study presented in this chapter on the structures and energies of cyclic $X_3H_3^{2-}$, $X_3H_4^-$, X_3H_5 and $X_3H_6^+$ (X=B, Al and Ga) reveals several characteristics. The diversity of structures that are minima is large for Al and Ga, and differs from those of B_3 hydrides. The most salient features are: (1) $X_3H_3^{2-}$ has a total of seven minima for Al and Ga in contrast to only two cyclic minima available to B. The π-delocalized isomer with two lone pairs **1c** is the global minima for Al and Ga. (2) $X_3H_4^-$ has six minima for Al and Ga, whereas for B, there are only two cyclic minima known. Unlike $X_3H_3^{2-}$, the global minimum structure for Al and Ga are different for $X_3H_4^-$. The singly H-bridged nonplanar C_s isomer **2b** is the global minima and the triply H-bridged nonplanar C_s structure with two lone pairs **2d** is the second best structure for $Al_3H_4^-$. Contrarily, **2d** is the global minima and **2b** is the second best structure for $Ga_3H_4^-$. The energy difference between **2b** and **2d** is 5.4 kcal/mol and 1.6 kcal/mol for Al and Ga respectively. A structure with tricoordinate pyramidal arrangement at

Al and Ga is found in **2g**, contrary to the conventional wisdom of $C_3H_3^+$, B_3H_4 etc. (3) The neutral species X_3H_5 has a total of eight minima for Al and Ga, whereas B has only three cyclic minima. Similar to that of $X_3H_4^-$, the global minimum structures of Al_3H_5 and Ga_3H_5 are different. The doubly H-bridged nonplanar structure **3b** is the global minima for Al_3H_5, whereas the four H-bridged C_s isomer **3d** is the global minima for Ga_3H_5. (4) The cationic species $X_3H_6^+$ has three and four minima for Al and Ga respectively. In case of $B_3H_6^+$, there are only two cyclic structures that are minima. The four H-bridged C_{2v} isomer with a lone pair **4c** is the global minima for Al and Ga. (5) The non planarity of hydrogens with respect to X_3 ring is found to be very common for Al and Ga species. (6) Structures with lone pair on heavy atoms dominate the potential energy surfaces of Al and Ga three ring systems. (7) The influence of π-delocalization in stabilizing the structures is decreased from $X_3H_3^{2-}$ to $X_3H_6^+$. (8) The resonance stabilization energy (RSE) for the global minimum structures (or nearest structure to global minimum which contains π-delocalization) computed using the isodesmic equations give quantitative trends, but cannot be used as a test of aromaticity.

Bibliography

[1] (a) Housecroft, C.E. *Boranes and Metallobranes: Structure, Bonding and Reactivity* Ellis Horwood Limited: Chichester, England, 1990. (b) *Boron Hydride Chemistry*; Muetteries, W.L. Ed.; Academic Press: New york, 1975. (c) Adams, R.M. In *Boron, Metallo-Boron Compounds and Boranes*; Adams, R.M., Ed.; Wiley Interscience: New York, 1964; p 507. (d) Lipscomb, W.N. *Boron Hydrides*; W.A. Benjamin, Inc.: New York, 1963. (e) Stock, A.E. *Hydrides of Boron and Silicon*; Cornell University Press: Ithaca, NY, 1933.

[2] (a) Grützmacher, H. *Angew. Chem. Int. Ed. Engl.* **1992**, 31, 1329. (b) Baulder, M.; Rockstein, K.; Oelert, W. *Chem. Ber.* **1991**, 124, 1149. (c) Brellochs, B.; Binder, H. *Angew. Chem. Int. Ed. Engl.* **1988**, 27, 262. (d) Rosenstock, H.M.; Draxl, K.; Steiner, B.W.; Herron, J.T. *J. Phys. Chem. Ref. Data* **1977**, 6, Suppl. No. 1. (e) Glore, J.D.; Rathke, J.W.; Schaeffer, R. *Inorg. Chem.* **1973**, 12, 2175. (f) Halgren, T.A.; Lipscomb, W.N. *J. Chem. Phys.* **1973**, 58, 1569. (g) Paine, R.T.; Sodek, G.; Stafford, F.E. *Inorg. Chem.* **1972**, 11, 2593. (h) Fridmann, S.A.; Fehlner, T.P. *J. Am. Chem. Soc.* **1971**, 93, 2824. (i) Nordman, C.E.; Reimann, C. *J. Am. Chem. Soc.* **1959**, 91, 3538. (j) Nordman, C.E. *Acta Crystallogr.* **1957**, 10, 777.

[3] (a) Bühl, M.; Schaefer III, H.F.; Schleyer, P.v.R.; Boese, R. *Angew. Chem. Int. Ed. Engl.* **1993**, 32, 1154. (b) Berndt, A. *Angew. Chem. Int. Ed. Engl.* **1993**, 32, 985. (c) Poetzhold, P.; Géret-Baumgarten, L.; Boese, R. *Angew. Chem. Int. Ed. Engl.* **1992**, 31, 1040. (d) Eisch, J.J.; Shafii, B.; Odom, J.D.; Rheingold, A.L. *J. Am. Chem. Soc.* **1990**, 112, 1847. (e) Meyer, H.; Schmidt-Lukasch, G.; Baum, G.: Massa, W.; Berndt, A. *Z. Naturforsch.* **1988**, 43*B*, 801. (f) Wehrmann, R.; Meyer, H.; Berndt, A. *Angew. Chem. Int. Ed. Engl.* **1985**, 24, 788. (g) Pues, C.; Berndt, A. *Angew. Chem. Int. Ed. Engl.* **1984**, 23, 313. (h) Volpin, M.E.; Koreskov, Y.D.; Dulova, V.G.; Kirsanov, D.N. *Tetrahedron* **1962**, 18, 107.

[4] Korkin, A.A.; Schleyer, P.v.R.; McKee, M.L. *Inorg. Chem.* **1995**, 34, 961.

[5] (a) Schleyer, P.v.R.; Subramanian, G.; Dransfeld, A. *J. Am. Chem. Soc.* **1996**, 118, 9988. (b) McKee, M.L.; Buhl, M.; Charkin, O.P.; Schleyer, P.v.R. *Inorg. Chem.* **1993**, 32, 4549.

[6] (a) Krempp, M.; Damrauer, R.; DePuy, C.H.; Keheyan, Y. *J. Am. Chem. Soc.* **1994**, 116, 3629. (b) Glukhovtsev, M.N.; Schleyer, P.v.R.; Hommes, N.J.R.V.E.; Carn-Eiro J.W.D.M.; Koch, W. *J. Comput. Chem.* **1993**, 14, 285.

[7] 7. (a) McKee, M.L. *Inorg. Chem.* **1999**, 38, 321. (b) McKee, M.L. *J. Am. Chem. Soc.* **1995**, 117, 8001. (c) Skancke, A.; Liebman, J.F. *J. Mol. Struct. (THEOCHEM)* **1993**, 280, 75.

[8] (a) Jemmis, E.D.; Subramanian, G. *Inorg. Chem.* **1995**, 34, 6559. (b) Jemmis, E.D.; Subramanian, G.; Srinivas, G.N. *J. Am. Chem. Soc.* **1992**, 114, 7939.

[9] (a) Xie, Y.; Schreiner, P.R.; Schaefer III, H.F.; Li, X-W.; Robinson, G.H. *J. Am. Chem. Soc.* **1996**, 118, 10635. (b) Li, X-W.; Xie, Y.; Schreiner, P.R.; Gripper, K.D.; Crittendon, R.C.; Campana, C.F.; Schaefer, H.F.; Rabinson, G.H. *Organometallics*, **1996**, 15, 3798. (c) Stabenow, F.; Saak, W.; Marsmann, H.; Weidenbruch, M. *J. Am. Chem. Soc.* **2003**, 125, 10172.

[10] Li, X-W.; Penninghton, W.T.; Robinson, G.H. *J. Am. Chem. Soc.* **1995**, 117, 7578.

[11] Li, X.; Kuznetsov, A.E.; Zhang, H-F.; Boldyrev, A.I.; Wang, L-S. *Science*, **2001**, 291, 859.

[12] Kuznetsov. A.E.; Boldyrev, A.I.; Li, X.; Wang, L-S. *J. Am. Chem. Soc.* **2001**, 123, 8825.

[13] (a) Power, P.P. *Chem. Rev.* **1999**, 99, 3463. (b) Driess, M.; Grützmacher, H. *Angew. Chem. Int. Ed. Engl.* **1996**, 35, 828. (c) Kutzelnigg, W. *Angew. Chem. Int. Ed. Engl.* **1984**, 23, 272.

[14] (a) Jacobsen, H.; Ziegler, T. *J. Am. Chem. Soc.* **1994**, 116, 3667. (b) Windus, T.L.; Gordon, M.S. *J. Am. Chem. Soc.* **1992**, 114, 9559. (c) Trinquier, G. *J. Am. Chem. Soc.* **1991**, 113, 144. (d) Trinquier, G.; Malrieu, J-P. *J. Am. Chem. Soc.* **1991**, 113, 8634. (e) Curtiss, L.A.; Raghavachari, K.; Deutsch, P.W.; Pople, J.A. *J. Chem. Phys.* **1991**,

95, 2433. (f) Karni, M.; Apeloig, Y. *J. Am. Chem. Soc.* **1990**, 112, 8589. (g) Grev, R.S.; Schaefer III, H.F.; Baines, K.M. *J. Am. Chem. Soc.* **1990**, 112, 9458. (h) Schleyer, P.v.R.; Kost, D. *J. Am. Chem. Soc.* **1988**, 110, 2105. (i) Teramae, H. *J. Am. Chem. Soc.* **1987**, 109, 4140. (j) Olbrich, G. *Chem. Phys. Lett.* **1986**, 130, 115. (k) Krogh-Jespersen, K. *J. Am. Chem. Soc.* **1985**, 107, 537. (l) Krogh-Jespersen, K. *J. Phys. Chem.* **1982**, 86, 1492. (m) Bogey, M.; Bolvin, H.; Demuynck, C.; Destombes, J. L. *Phys. Rev. Lett.* **1991**, 66, 413. (n) Cordonnier, M.; Bogey, M.; Demuynck, C.; Destombes, J.-L. *J. Chem. Phys.* **1992**, 97, 7984.

[15] 15. (a) So, S.P. *Chem. Phys. Lett.* **1998**, 291, 523. (b) Srinivas, G.N.; Jemmis, E.D.; Korkin, A.A.; Schleyer, P.v.R. *J. Phys. Chem. A* **1999**, 103, 11034. (c) Jemmis, E.D.; Srinivas, G.N.; Leszczynski, J.; Kapp, J.; Korkin, A.A.; Schleyer, P.v.R. *J. Am. Chem. Soc.* **1995**, 117, 11361.

[16] Ishida, S.; Iwamoto, T.; Kabuto, C.; Kira, M. *Nature* document **2003**, 421, 725.

[17] (a) Xie, Y.; Grev, R.S.; Gu, J.; Schaefer III, H.F.; Schleyer, P.v.R.; Su, J.; Li, X-W.; Robinson, G.H. *J. Am. Chem. Soc.* **1998**, 120, 3773. (b) Su, J.; Li, X-W.; Crittendon, R.C.; Robinson, G.H. *J. Am. Chem. Soc.* **1997**, 119, 5471.

[18] 18. (a) Peric, M.; Marian, C.M.; Engels, B. *Mol. Phys.* **1999**, 97, 731. (b) Stanger, A. *J. Am. Chem. Soc.* **1998**, 120, 12034. (c) Peric, M.; Ostojic, B.; Engels, B. *J. Mol. Spectrosc.* **1997**, 182, 280. (d) Engels, B.; Suter, H.U.; Peric, M. *J. Phys. Chem.* **1996**, 100, 10121. (e) Knight,

L.B.; Kerr, K.; Miller, P.K.; Arrington, C.A. *J. Phys. Chem.* **1995**, 99, 16842. (f) Lauvergnat, D.; Hibety, P.C. *J. Mol. Struct. (THEOCHEM)* **1995**, 338, 283. (g) Tague, T.J.; Andrews, L. *J. Am. Chem. Soc.* **1994**, 116, 4970. (h) Somogyi, A.; Gomory, A. *Chem. Phys. Lett.* **1992**, 192, 221. (i) Curtiss, L.A.; Pople, J.A. *J. Chem. Phys.* **1989**, 91, 4809. (j) Sana, M.; Leroy, G.; Henriet, Ch. *J. Mol. Struct. (THEOCHEM)* **1989**, 56, 233. (k) Jouancy, C.; Barthelat, J.C.; Daudey, J.P. *Chem. Phys. Lett.* **1987**, 136, 52. (l) Scuseria, G.E.; Lee, T.J.; Schaefer III, H.F. *Chem. Phys. Lett.* **1986**, 130, 236. (m) Armstrong, D.R. *Theor. Chim. Acta* **1981**, 60, 159.

[19] (a) Jursic, B.S. *J. Mol. Struct. (THEOCHEM)* **1998**, 453, 123. (b) Stephens, J.C.; Bolton, E.E.; Schaefer III, H.F.; Andrews, L. *J. Chem. Phys.* **1997**, 107, 119. (c) Gundersen, K.; Jacobsen, K.W.; Norskov, J.K. *Surf. Sci.* **1994**, 304, 131. (d) Palagyi, Z.; Grev, R.S.; Schaefer III, H.F. *J. Am. Chem. Soc.* **1993**, 115, 1936. (e) Chertihim, G.V.; Andrews, L. *J. Phys. Chem.* **1993**, 97, 10295. (f) Baird, N.C. *Can J. Chem.* **1985**, 63, 71.

[20] (a) Klinkhammer, K.W. *Angew. Chem. Int. Ed. Engl.* **1997**, 36, 2320. (b) Palagyi, Z.; Schaefer III, H.F.; Kapuy, E. *Chem. Phys. Lett.* **1993**, 203, 195.

[21] (a) Yamaguchi, Y.; Deleeuw, B.J.; Richards, Jr. C.A.; Schaefer III, H.F.; Frenking, G. *J. Am. Chem. Soc.* **1994**, 116, 11922. (b) Treboux, G.; Barthelat, J-C. *J. Am. Chem. Soc.* **1993**, 115, 4870.

[22] (a) Curtiss, L.A.; Redfern, P.C.; Raghavachari, K.; Pople, J.A. *Chem. Phys. Lett.* **1999**, 313, 600. (b) Curtiss, L.A.; Redfern, P.C.; Raghavachari, K.; Rassolov, V.; Pople, J.A. *J. Chem. Phys.* **1999**, 110, 4703. (c) Sakaki, S.; Kikumo, T. *Inorg. Chem.* **1997**, 36, 226. (d) Lammertsma, K.; Ohwada, T. *J. Am. Chem. Soc.* **1996**, 118, 7247. (e) Mo, Y.; Lin, Z. *J. Chem. Phys.* **1996**, 105, 1046. (f) Ochterski, J.W.; Petersson, G.A.; Wiberg, K.B. *J. Am. Chem. Soc.* **1995**, 117, 11299. (g) Sorger, K.; Schleyer, P.v.R. *J. Mol. Struct. (THEOCHEM)* **1995**, 338, 317. (h) Steiner, D.; Balzereit, C.; Winkler, H-J.; Stamatis, N.; Hofmann, M.; Schleyer, P.v.R.; Massa, W.; Berndt, A. *Angew. Chem. Int. Ed. Engl.* **1994**, 33, 2303. (i) Demachy, I.; Vilatron, F. *J. Phys. Chem.* **1994**, 98, 10728. (j) Stanton, J.F.; Gauss, J.; Bartlett, R.J.; Helgaker, T.; Jorgensen, P.; Jensen, H.J.A.; Taylor, P.R. *J. Chem. Phys.* **1992**, 97, 1211. (k) Sana, M.; Leroy, G.; Wilante, C. *Organometallics* **1992**, 11, 781. (l) Curtiss, L.A.; Pople, J.A. *J. Chem. Phys.* **1989**, 90, 4314. (m) Sana, M.; Leroy, G. *J. Mol. Struct. (THEOCHEM)* **1987**, 36, 307. (n) Mohr, R.R.; Lipscomb, W.N. *Inorg. Chem.* **1986**, 25, 1053. (o) Zakzhevskii, V.G.; Charkin, O.P *Chem. Phys. Lett.* **1982**, 90, 117. (p) Vincent, M.A.; Schaefer III, H.F. *J. Am. Chem. Soc.* **1981**, 103, 5677.

[23] Lammertsma, K.; Guner, O.F.; Drewes, R.M.; Reed, A.E.; Schelyer, P.v.R. *Inorg. Chem.* **1989**, 28, 313.

[24] (a) Schailey, R.; Ray, A.K. *J. Chem. Phys.* **1999**, 111, 8628. (b) Lammertsma, K.; Leszczynski, J. *J. Phys. Chem.* **1990**, 94, 5543.

[25] (a) Kaufmann, E.; Schleyer, P.v.R. *Inorg. Chem.* **1988**, 27, 3987. (b)

Sana, M.; Leroy, G. *J. Mol. Struct. (THEOCHEM)* **1984**, 18, 251.

[26] Cotton, F.A.; Wilkinson, G.; Murillo, C.A.; Bochmann, M. *Advanced Inorganic Chemistry*, 6th Edn., Wiley-Interscience, New York 1999.

[27] (a) Willis, B.G.; Jensen, K.F. *J. Phys. Chem. A* **1998**, 102, 2613. (b) Cioslowski, J.; Liu, G.; Piskorz, P. *J. Phys. Chem. A* **1998**, 102, 9890. (c) Russell, D.K.; Claxton, T.A.; Grady, A.S.; Linney, R.E.; Mahmood, Z.; Markwell, R.D. *J. Chem. Soc., Faraday Trans.* **1995**, 91, 3015. (d) Magers, D.H.; Hood, R.B.; Leszczynski, J. *Int. J. Quantum Chem. Symp.* **1994**, 28, 579. (e) Barone, V.; Orlandini, L.; Adamo, C. *J. Phys. Chem.* **1994**, 98, 13185. (f) Shen, M.; Schaefer III, H.F. *J. Chem. Phys.* **1992**, 96, 2868. (g) Sannigrahi, A.B.; Nandi, P.K.; Behera, L.; Kar, T. *J. Mol. Struct. (THEOCHEM)* **1992**, 95, 259. (h) Bennett, F.B.; Elms, F.M.; Gardiner, M.G.; Koutsantonis, G.A.; Raston, C.L.; Roberts, N.K. *Organoemtallics* **1992**, 11, 1457. (i) Redell, A.P.; Lee, T.J.; Komornicki, A. *Chem. Phys. Lett.* **1991**, 178, 462. (j) Duke, B.J.; Liang, C.; Schaefer III, H.F. *J. Am. Chem. Soc.* **1991**, 113, 2884. (k) Van-Der-Woerd, M.J.; Lammertsma, K.; Duke, B.J.; Schaefer III, H.F. *J. Chem. Phys.* **1991**, 95, 1160. (l) Bock, C.W.; Trachtman, M.; Murphy, C.; Muschert, B.; Mains, G.J. *J. Phys. Chem.* **1991**, 95, 2339. (m) McKee, M.L. *J. Phys. Chem.* **1991**, 95, 6519. (n) Lammertsma, K.; Leszczynski, J. *J. Phys. Chem.* **1990**, 94, 2806. (o) Mains, G.J.; Bock, C.W.; Trachtman, M.; Finley, J.; McNamara, K.; Fisher, M.; Wociki, L. *J. Phys. Chem.* **1990**, 94, 6996. (p) Chey, J.; Choe, H.S.; Chook, Y.M.; Jensen, E.; Seida, P.R.; Francl, M.M. *Organometallics* **1990**, 9, 2430.

(q) Liang, C.; Davy, R.D.; Schaefer III, H.F. *Chem. Phys. Lett.* **1989**, 159, 393.

[28] (a) Dyke, J.M.; Haggerston, D.; Warschkow, O.; Andrews, L.; Downs, A.J.; Soute, R.P.F. *J. Phys. Chem.* **1996**, 100, 2998. (b) Souter, P.F.; Andrews, L.; Downs, A.J.; Greene, T.M.; Ma, B.; Schaefer III, H.F. *J. Phys. Chem.* **1994**, 98, 12824. (c) McKee, M.L. *Chem. Phys. Lett.* **1991**, 183, 510. (d) Duke, B.J. *J. Mol. Struct. (THEOCHEM)* **1990**, 67, 197.

[29] Liang, C.; Allen, L.C. *J. Am. Chem. Soc.* **1991**, 113, 1878.

[30] 30. (a) Kaltsoyannis, N. *J. Chem. Soc. Dalton Trans.* **1997**, 1. (b) Pyykkö, P. *Chem. Rev.* **1988**, 88, 563. (c) Schmidt, M.W.; Truong, P.N.; Gordon, M.S. *J. Am. Chem. Soc.* **1987**, 109, 5217. (d) Magnusson, E. *J. Am. Chem. Soc.* **1984**, 106, 1177. (e) Magnusson, E. *J. Am. Chem. Soc.* **1984**, 106, 1185. (f) Pitzer, K.S. *Acc. Chem. Res.* **1979**, 12, 271. (g) Pyykkö, P.; Desclaux, J-P. *Acc. Chem. Res.* **1979**, 12, 276. (h) Drago, R.S. *J. Phys. Chem.* **1958**, 62, 353. (i) Mulliken, R.S. *J. Am. Chem. Soc.* **1950**, 72, 4496. (j) Pitzer, K.S. *J. Am. Chem. Soc.* **1948**, 70, 2140.

[31] Hehre, W.; Radom, L.; Schleyer, P.v.R.; Pople, J.A. *Ab Initio Molecular Orbital Theory*; Wiley: New York, 1986.

[32] (a) Becke, A.D. *J. Chem. Phys.* **1993**, 98, 5648. (b) Becke, A.D. *Phys. Rev. A* **1988**, 38, 3098. (c) Lee, C.; Yang, W.; Parr, R.G. *Phys. Rev. B* **1988**, 37, 785. (d) Vosko, S.H.; Wilk, L.; Nusair, M. *Can J. Phys.* **1980**, 58, 1200.

[33] Pople, J.A.; Raghavachari, K.; Schlegel, H.B.; Binkley, J.S. *Int. J. Quantum Chem. Symp.* **1979**, 13, 255.

[34] Gaussian 98, Revision A.9, Frisch, M. J.; Trucks, G. W.; Schlegel, H. B.; Scuseria, G. E.; Robb, M. A.; Cheeseman, J. R.; Zakrzewski, V. G.; Montgomery, Jr., J. A.; Stratmann, R. E.; Burant, J. C.; Dapprich, S.; Millam, J. M.; Daniels, A. D.; Kudin, K. N.; Strain, M. C.; Farkas, O.; Tomasi, J.; Barone, V.; Cossi, M.; Cammi, R.; Mennucci, B.; Pomelli, C.; Adamo, C.; Clifford, S.; Ochterski, J.; Petersson, G. A.; Ayala, P. Y.; Cui, Q.; Morokuma, K.; Malick, D. K.; Rabuck, A. D.; Raghavachari, K.; Foresman, J. B.; Cioslowski, J.; Ortiz, J. V.; Baboul, A. G.; Stefanov, B. B.; Liu, G.; Liashenko, A.; Piskorz, P.; Komaromi, I.; Gomperts, R.; Martin, R. L.; Fox, D. J.; Keith, T.; Al-Laham, M. A.; Peng, C. Y.; Nanayakkara, A.; Challacombe, M.; Gill, P. M. W.; Johnson, B.; Chen, W.; Wong, M. W.; Andres, J. L.; Gonzalez, C.; Head-Gordon, M.; Replogle, E. S.; Pople, J. A.; Gaussian, Inc., Pittsburgh PA, 1998.

[35] (a) Fujimoto, H.; Hoffmann, R. *J. Phys. Chem.* **1974**, 78, 1167. (b) Hoffmann, R. *Angew. Chem. Int. Ed. Engl.* **1982**, 21, 711.

[36] Reed, A.E.; Curtiss, L.A.; Weinhold, F. *Chem. Rev.* **1988**, 88, 899.

[37] Subramanian, G.; Jemmis, E.D. *Chem. Phys. Lett.* **1994**, 217, 296.

[38] (a) Srinivas, G.N.; Kiran, B.; Jemmis, E.D. *J. Mol. Struct. (THEOCHEM)* **1996**, 361, 205. (b) Nagase, S. *Polyhedron* **1991**, 10, 1299.

[39] (a) Wiberg, N.; Amelunxen, K.; Blank, T.; Nöth, H.; Knizek, J. *Organometallics* **1998**, 17, 5431. (b) Uhl, W. *Z. Naturforsch.* **1988**, 43*B*, 1113. (c) Wehmschulte, R.J.; Ruhland-Senge, K.; Olmstead, M.M.; Hope, H.; Sturgeon, B.E.; Power, P.P. *Inorg. Chem.* **1993**, 32, 2983.

[40] (a) Brothers, P.J.; Power, P.P. *Adv. Organomet. Chem.* **1996**, 39, 1. (b) Uhl, W.; Layh, M.; Hildenbrand, T. *J. Organomet. Chem.* **1989**, 364, 289. (c) He, X.; Bartlett, R.A.; Olmstead, M.M.; Ruhlandt-Senge, K.; Sturgeon, B.E.; Power, P.P. *Angew. Chem. Int. Ed. Engl.* **1993**, 32, 717.

[41] a) Präsang, C.; Mlodzianowska, A.; Sahin, Y.; Hofmann, M.; Geiseler, G.; Massa, W.; Berndt, A. *Angew. Chem.* **2002**, 114, 3529; *Angew. Chem. Int. Ed.* **2002**, 41, 3380; b) Präsang, C.; Hofmann, M.; Geiseler, G.; Massa, W.; Berndt, A. *Angew. Chem.* **2002**, 114, 1597; *Angew. Chem. Int. Ed.* **2002**, 41, 1526; c) Maier, A.; Hofmann, M.; Pritzkow, H.; Siebert, W. *Angew. Chem.* **2002**, 114, 1600; *Angew. Chem. Int. Ed.* **2002**, 41, 1529.

[42] Jorgenson, W.L.; Salem, L. *The Organic Chemists Book of Orbitals*; Academic Press: New York, 1973.

[43] (a) Wang, Z-W.; Schleyer, P.v.R. *J. Am. Chem.Soc.* **2001**, 123, 994. (b) Rasmussen, D.R.; Radom, L. *Angew. Chem. Int. Ed. Engl.* **1999**, 38, 2876. (c) Siebert, W.; Gunale, A. *Chem. Rev.* **1999**, 28, 367. (d) Rottger, D.; Erker, G. *Angew. Chem. Int. Ed. Engl.* **1997**, 36, 813. (e) Collins, J.B.; Dill, J.D.; Jemmis, E.D.; Apeloig, Y.; Schleyer, P.v.R.;

Seeger, R.; Pople, J.A. *J. Am. Chem. Soc.* **1976**, 98, 5419. (f) Hoffmann, R.; Alder, R.W.; Wilcox, C.F. *J. Am. Chem. Soc.* **1970**, 92, 4992.

[44] (a) Jemmis, E. D.; Schleyer, P.v.R. *J. Am. Chem. Soc.* **1982**, 104, 4781. (b) Jemmis, E. D. *J. Am. Chem. Soc.* **1982**, 104, 7017.

[45] Subramanian, G.; Jemmis, E.D. *Chem. Phys. Lett.* **1992**, 200, 567.

[46] Jemmis, E.D.; Sarma, K.S.; Pavankumar, P.N.V. *J. Mol. Struct. (THEOCHEM)* **1985**, 121, 305.

[47] Wiberg, N.; Blank, T.; Kaim, W.; Schwederski, B.; Linti, G. *Eur. J. Inorg. Chem.* **2000**, 1475.

[48] Wiberg, N.; Blank, T.; Amelunxen, K.; Nöth, H.; Knizek, J.; Habereder, T.; Kaim, W. Wanner, M. *Eur. J. Inorg. Chem.* **2001**, 1719.

[49] Giju, K. T.; Phukan, A. K.; Jemmis, E. D. *Angew. Chem. Int. Ed. Eng.* **2003**, 42, 539.

Chapter 3

Dehydrogeno closo-Carboranes and closo-Silaboranes: A Theoretical Study of Structure and Reactivity

3.1 Introduction

Polyhedral boranes are the 3-dimensional equivalents of benzene. [1] It is natural to expect chemistry rivaling that of benzenoid aromatics to develop around polyhedral boranes. As stable, neutral polyhedral compounds, carboranes had taken the natural lead amongst boranes. After years of explorative studies, carboranes have become important reagents in many different applications. Derivatives of carboranes, which can act as carriers of ^{10}B selectively to tumor cells, have found application in Boron Neutron Capture Therapy (BCNT) of Cancer. [2] Camouflaged carboranes [3] where hydrogens are substituted by appropriate organic substituents are used as modules for the formation of specific molecular assemblies. Carborods with linearly connected 1,12-$C_2B_{10}H_{10}$ and macrocycles containing carborane cages in their peripheries find uses in Nanotechnology and

Molecular Recognition. [4] Mercuracarborands [5] resemble crown ethers with reversed coordination properties and are useful in anion complexation chemistry. Carboranes can be used as building blocks for dendrimers which can have as many as twelve primary branches. [6] Obviously, many applications with the derivatives of carboranes remain to be discovered.

Getting a handle on carboranes for further manipulation is important in any such endeavor. Chemistry of benzene provides a hint. One of the dramatic aspects of benzene chemistry has been the generation of benzyne. [7] Generation of an equivalent 'carboryne' would provide a handle to introduce substituents on the carborane skeletons. This has indeed been achieved experimentally with the icosahedral 1,2-$C_2B_{10}H_{12}$ (**1a**) [8] and should be possible with the remaining 1,2-$C_2B_nH_{n+2}$ (**2a-7a**). [9] The carboryne, $C_2B_{10}H_{10}$ (**8a**), generated from **1a** undergoes Diels-Alder and Ene reactions with dienes, acetylenes, and similar entities, which are typical of reactive multiple bonds. [10] In view of the many carboranes available with adjacent C-C bonds in the polyhedra, there should be many such candidates. The stability and reactivity of these "benzyne equivalents" (Figure 3.1, **8a-14a**) must vary considerably. We present a detailed theoretical study of the structure and reactivity of these dehydrogeno-carboranes using electronic structure theory. Dehydrogenocarboranes, 2,3-$C_2B_5H_5$ (**13a**), that may be generated from the known 2,3-$C_2B_5H_7$ (**6a**), [11] is calculated to be more favorable than $C_2B_{10}H_{10}$ (**8a**). These are compared and contrasted with those of benzynes. The carborynes also provide easy entry to heterocondensed structures such as benzo-o-carboranes [12] (Scheme 1) whose electronic requirements can be understood using the mno rule. [13]

The interactions between 2- and 3-dimensional delocalized systems and opportunities for further condensation should provide exciting new directions in chemistry.

(8a)
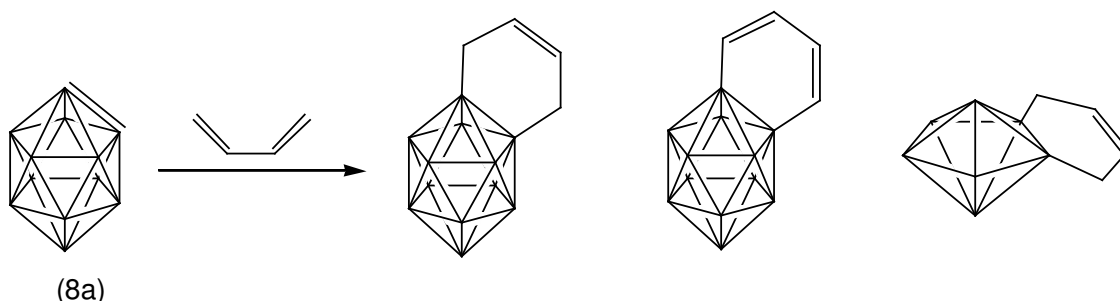
Scheme 3.1

A related question is the nature of the silaborane analogues. Silabenzene, where one carbon atom of benzene is substituted by silicon shows aromaticity. [14] There are very few experimental reports of disilaboranes. Theoretical studies show that silaboranes have structures similar to carboranes, but they differ in the relative energy of the positional isomers. [15] A Twelve-vertex dimethyldisiladodecaborane, $Si_2B_{10}H_{10}Me_2$, has been synthesized. [16] Its reactivity is substantially different from its carborane analogues. For example, nucleophilic bases attack $Me_2Si_2B_{10}H_{12}$ resulting in the loss of an MeSi vertex; [17] while in carboranes the reaction is centered on a boron adjacent to carbon. [18] The Si analogue of $C_2B_{10}H_{10}$ is not known. In view of the largely diverse nature of Si-Si multiple bonds [19] in general, $Si_2B_nH_n$ series should present examples of unusual structure and bonding. We contrast the disilaboranes, $Si_2B_nH_{n+2}$ (**1b-7b**) and their dehydrogeno derivatives, $Si_2B_nH_n$, n=4,5,8 and 10 (**8b-14b**) to the corresponding carboranes. Alternatives to multiple bonds in the dehydrogeno systems (**15**-**21**)are also analyzed.

Aromaticity of boranes and carboranes based on Nuclear Independent

Chemical Shifts (NICS), shows that the more symmetrical structures, based on octahedron and icosahedron, are more aromatic. [20] The relative stability and aromaticity of 1,2-carboranes and dehydrogeno derivatives, and their Si analogues are presented here to get further insight into the nature of these polyhedral systems when the bonding is disturbed by dehydrogenation. A preliminary communication on the icosahedral system was published previously. [21] Recent developments in the chemistry of polyhedral carboranes [5, 22] and silaboranes [23] and lack of similar attempts in smaller polyhedral structures prompted us to present the details of our study.

3.2   Methods

All the structures ($C_2B_nH_{n+2}$ (**1a-7a**), $C_2B_nH_n$ (**8a-14a**), $Si_2B_nH_{n+2}$ (**1b-8b**) and $Si_2B_nH_n$ (**15-21**) were optimized at the B3LYP/6-31G* [24, 25] level of theory. Stationary points were characterized through vibrational frequency analysis. NICS [26] values were computed at GIAO-HF/6-31+G* at B3LYP/6-31G* optimized geometries. Structures were further optimized at B3LYP/6-311+G* level and the resulting energies were used for comparison. GAUSSIAN94 package [27] of programs was used /for all calculations.

3.3   Results and discussions

The results pertaining to closo-carboranes are discussed first. This is followed by the discussion of silaboranes. Stability and aromaticity of the

Table 3.1: Total Energies (hartrees) at B3LYP/6-311+G*, X-X bond length, Wiberg Bond Index at B3LYP/6-31G*, Relative energies, NICS at GIAO-HF/6-31+G*//B3LYP/6-31G* level.

Molecule	T.E	X-X	WBI	R.E	NICS
$1,2\text{-}C_2B_{10}H_{12}(1a)$	-332.14679	1.625	0.7401	-445.32	-34.53
$1,2\text{-}C_2B_8H_{10}(2a)$	-281.15416	1.535	0.8618	-335.97	-29.69
$2,3\text{-}C_2B_{10}H_{10}(3a)$	-281.12712	1.668	0.6858	-318.71	-33.47
$2,6\text{-}C_2B_{10}H_{10}(4a)$	-281.12791	1.689	0.6866	-319.16	-34.15
$1,2\text{-}C_2B_5H_7(5a)$	-204.69702	1.642	0.7467	-191.57	-27.66
$2,3\text{-}C_2B_5H_7(6a)$	-204.73560	1.464	1.0375	-215.87	-28.05
$1,2\text{-}C_2B_4H_6(7a)$	-179.26010	1.543	0.8632	-174.35	-34.92
$1,2\text{-}C_2B_{10}H_{10}$ (8a)	-330.81240	1.356	1.6486	-483.69	-40.58
$1,2\text{-}C_2B_8H_8(9a)$	-279.80778	1.327	1.8050	-356.57	-25.82
$2,3\text{-}C_2B_8H_8(10a)$	-279.79980	1.481	1.1495	-368.49	-24.75
$2,6\text{-}C_2B_8H_8(11a)$	-279.79458	1.329	1.7809	-366.84	-26.52
$1,2\text{-}C_2B_5H_5(12a)$	-203.34109	1.453	1.3960	-241.60	-38.75
$2,3\text{-}C_2B_5H_5(13a)$	-203.43546	1.305	1.8081	-227.31	-36.94
$1,2\text{-}C_2B_4H_4(14a)$	-177.87248	1.356	1.7599	-198.01	-46.05
$1,2\text{-}Si_2B_{10}H_{12}(1b)$	-834.94761	2.316	0.4867	-483.69	-33.82
$1,2\text{-}Si_2B_8H_{10}(2b)$	-783.92692	2.216	0.7499	-356.57	-28.41
$2,3\text{-}Si_2B_8H_{10}(3b)$	-783.94610	2.375	0.3788	-368.49	-29.48
$2,6\text{-}Si_2B_8H_{10}(4b)$	-783.94292	2.348	0.5183	-366.84	-28.83
$1,2\text{-}Si_2B_5H_7(5b)$	-707.51535	2.387	0.4788	-241.60	-28.77
$2,3\text{-}Si_2B_5H_7(6b)$	-707.49207	2.173	1.0429	-227.31	-26.18
$1,2\text{-}Si_2B_4H_6(7b)$	-682.03591	2.246	0.7427	-198.01	-35.34
$1,2\text{-}Si_2B_{10}H_{10}(15)$	-833.65592	2.325	0.6109	-437.20	-34.41
$1,2\text{-}Si_2B_8H_8(16)$	-782.67509	2.269	0.3072	-335.51	-21.11
$2,3\text{-}Si_2B_8H_8(17)$	-782.65288	2.485	0.3063	-321.38	-20.18
$2,6\text{-}Si_2B_8H_8(18)$	-782.66130	2.287	0.8114	-326.51	-21.00
$1,2\text{-}Si_2B_5H_5(19)$	-706.24678	2.400	0.4627	-209.66	-44.95
$2,3\text{-}Si_2B_5H_5(20)$	-706.26933	2.338	0.7482	-224.71	-20.33
$1,2\text{-}Si_2B_4H_4(21)$	-680.78059	2.364	0.6799	-174.15	-35.57

above systems are compared at the end.

3.3.1 *Closo* –Dicarbaboranes and dedydrogenocarboranes

Closo-dicarbaboranes ($C_2B_nH_{n+2}$, n = 4,5,8,10) where carbon atoms occupy adjacent positions are all known experimentally and several theoretical studies are available. [9] Geometry of these polyhedral structures

Figure 3.1: Schematic drawings of closo-dicarbaboranes 1a-7a ($C_2B_nH_{n+2}$ and closo-disilaboranes 1b-7b ($Si_2B_nH_{n+2}$. The two black spheres indicate the position of the CH or SiH groups. Relative energies of the isomers are given in parenthesis (kcal/mol) wherever more than one isomer is considered.
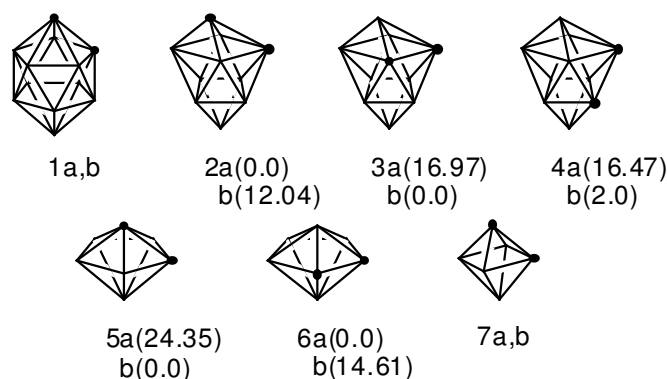

with carbon atoms in the adjacent positions (**1a-7a**) and their dehydrogeno derivatives (**8a-14a**) are optimized and are found to be minima. The only dehydrogenoderivative synthesized as a transient species, $C_2B_{10}H_{10}$ (**8a**) [8] shows interesting reactivity, comparable to benzyne. The calculated C-C bond lengths are in tune with the high reactivity of $C_2B_{10}H_{10}$. The C-C bond length in **1a** of 1.625 Å is reduced to 1.356 Å in **8a**. Wiberg bond index (1.648) indicates double bonding—WBI for **1a** is 0.740. This C-C bond length is still considerably longer than that calculated for benzyne (1.245 Å). The skeletal requirement of rigid icosahedral borane cage does not allow further decrease in the C-C distance.

Just as the rigid icosahedral skeleton demands a rather long C-C distance in **1a**, varying C-C distances are demanded by the peculiar structures in the nonicosahedral analogues. For example, isomers of the ten vertex polyhedra $C_2B_8H_8$ has relatively long C-C distances (e.g., 1.668 Å in **3a** and 1.481Å in **10a**). On the other hand, the structures based on the pentagonal bipyramid have short distances, (1.464 Å in **6a** and 1.305Å in

13a). The structural variation can be explained based on the ring-cap or-
bital overlap matching. [28] Four membered rings have poor overlap with
BH caps as the caps have relatively more diffused orbitals. The ring-cap
overlap can be enhanced by stretching the bonds involved in the four mem-
bered rings explaining the longer C-C distances in **3a** and **10a**. On the other
hand, the five membered ring in **5a, 6a**, **12a** and **13a** are too large in rela-
tion to the caps. The ring-cap overlap can be improved by decreasing the
bond lengths of the five membered rings, leading to short C-C distance of
1.464Å in **6a** and 1.305Å in **13a**. Thus C-C distance in $C_2B_nH_{n+2}$ spans
a large range of 1.464 Å in 2,3-$C_2B_5H_7$ (**6a**), 1.535 Å in 1,2-$C_2B_8H_{10}$
(**2a**), 1.543 Å in $C_2B_4H_6$ (**7a**), 1.625 Å in $C_2B_{10}H_{12}$ (**1a**) and 1.642 Å in
1,2-$C_2B_5H_7$ (**5a**). This is indeed a large range for structures with similar
polyhedral bonding. Dehydrogenation shifts this range to 1.304 Å to 1.481
Å.

In contrast to the large number of experimental studies involving $C_2B_{10}H_{10}$,
the dehydrogenation of lower vertex dicarbaboranes is not reported so far.
We compare here the stability of 1,2-closo-dicarbaboranes, $C_2B_nH_{n+2}$ (n
= 4,5,8 and 10) (**1a-7a**) and their dehydrogenodervatives using theoretical
methods. π-bonding is inherently destabilizing for any system in compar-
ison to σ-bonding. The extent of this destabilization of the dehydrogeno-
carboranes in relation to the destabilization of the π-bond in ethylene is
computed using equation 3.1.

$$C_2B_nH_{n+2} + C_2H_4 \rightarrow C_2H_6 + C_2B_nH_n \tag{3.1}$$
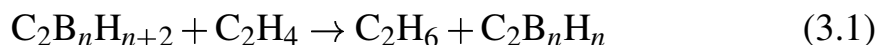
where n=4,5,8 and 10.

Figure 3.2: Dehydrogenocarboranes and the extent of π-bond destabilization from equation 1(in kcal/mol).
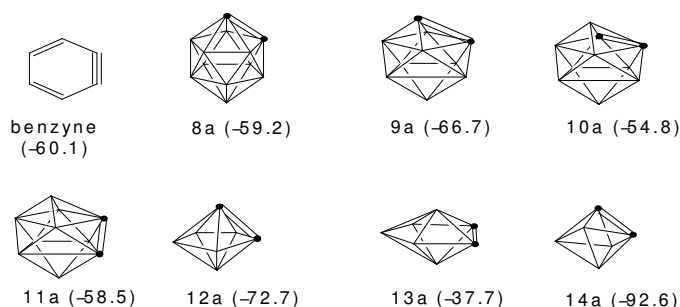
The reaction energy (ΔH) for **8a** is 59.2 kcal/mol whereas for benzyne it is 60.1 kcal/mol (Figure 3.1). Among the isomers of ten vertex dehydrogenocarboranes, the π-bond in 1,2-$C_2B_8H_8$ (**9a**) is slightly less stable than benzyne whereas 2,3- and 2,6-$C_2B_8H_8$ (**10a** and **11a**) have more favorable π-bond. The external π-bond in the seven vertex 2,3-$C_2B_5H_5$ (**13a**) is more favorable than that in benzyne by 22.4 kcal/mol. This is best explained by the ring-cap matching. [28] The pentagonalbipyramidal $B_7H_7^{2-}$ is highly reactive because the B_5H_5 ring is too large to interact optimally with the BH caps (Scheme 2a). Replacements of two BH groups of the five membered rings by two CH groups decreases the ring size so that 2,3-$C_2B_5H_7$ is considerably more favorable than $B_7H_7^{2-}$ (Scheme 2b). The orbital matching can be even better if the ring size could be further reduced as is possible in the dehydrogeno structure 2,3-$C_2B_5H_5$ (**13a**). The natural requirement of a smaller ring size to enhance the ring-cap overlap coincided here with the enhanced C-C π-interactions (Scheme 2). The π-bond stabilization in $C_2B_4H_4$ (**14a**) is much less, probably due to the decreased overlap of splayed out exohedral orbitals.

An estimate of the reactivity of dehydrogenocarboranes towards Diels-
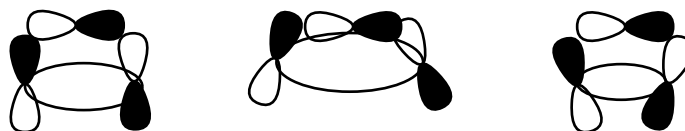
Scheme 3.2

Alder reactions can be made using Frontier Molecular Orbital theory. The relative reactivity of a diene-dienophile system is reflected in the stabilization energy of the transition state which in turn is known to depend on the interaction of the Highest Occupied Molecular Orbitals (HOMO) and Lowest Unoccupied Molecular Orbitals (LUMO) of the reacting species. The smaller the difference in energy between the interacting orbitals, the higher is the reactivity. For the systems studied here, the relevant orbital pairs are the HOMO of butadiene and the LUMO of the ene $(C_2B_nH_n)$. The $E(HOMO_{butadiene}\text{-}LUMO_{ene})$ for all carboranes studied here, is lower than that for ethylene and benzyne (Figure 3.3). In view of the easy Diels-Alder reactions of ethylene, benzyne and **8a** with butadiene, other dehydrogenocarboranes should also show similar reactivity. While the reactivity with butadiene based on HOMO-LUMO difference puts $2,3\text{-}C_2B_5H_5$ in the same group as other $C_2B_nH_n$ systems, the short C-C distance of 1.301Å and the largeπ-π* energy difference indicate a strong bond. This should therefore be an example of relatively stable ethyleneic double bond, still more reactive than benzyne to towards butadiene. Derivatives of **6a** is already known. [11]. Attempts to synthesize **13a** equivalent should be rewarding.

Figure 3.3: The energy difference between HOMO of butadiene and LUMO of the 8a-14a, ethylene and benzyne, shown as dark squares. The dark spheres indicate the $\pi - \pi^*$ energy difference for the pi-bond in 8a-14a ethylene and benzyne.
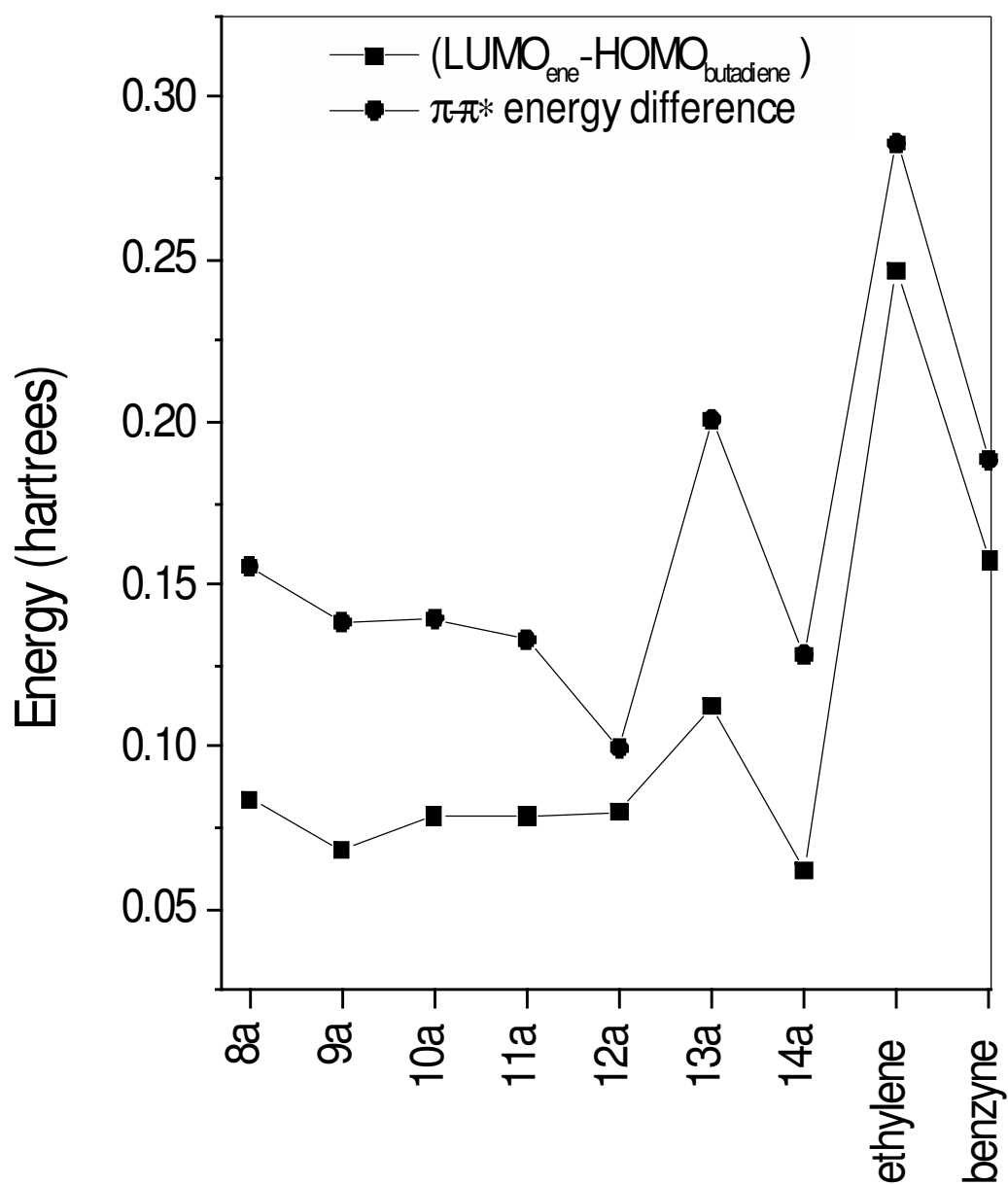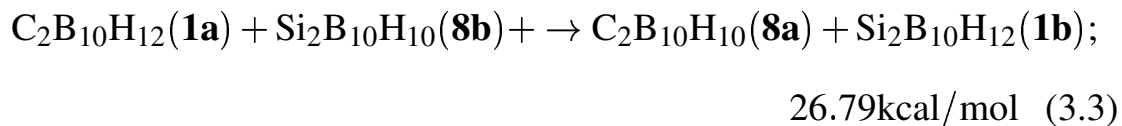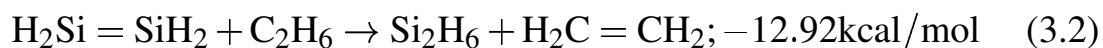
3.3.2 *Closo-o*-Disilaboranes and *closo-o*-dehydrogenodisilaboranes

In contrast to the well-developed chemistry of carboranes, silaboranes are a novelty. The icosahedral $1,2\text{-}Si_2B_{10}H_{10}Me_2$ was synthesized recently. [29] The calculated structure of $1,2\text{-}Si_2B_{10}H_{12}$ (**1b**), compares well with the salient features of the experimental structure. The topological features of $Si_2B_nH_{n+2}$ are very similar to those of the corresponding $C_2B_nH_{n+2}$ skeletons. However, the inherently longer Si-Si distance, in relation to the C-C distance, has dramatic energetic and structural consequences. For example, in $1,2\text{-}C_2B_{10}H_{12}$ (**1a**) the standard C-C distance of 1.54 Å is lengthened to 1.625Å to accommodate the rigid polyhedral skeleton with average B-B distance of 1.70Å. On the other hand, in $Si_2B_{10}H_{12}$ (**1b**) the standard Si-Si distance of 2.34Å of Si_2H_6 is compressed to 2.316Å to accommodate the shorter B-B distance of the polyhedral skeleton.

Replacement of carbon by silicon in *closo*-boranes substantially changes the energetics. This is reflected in the relative energies of various isomers (**2b-4b, 5b-6b**, Figure 3.2) as well as in other aspects. The relative energies of the position isomers of *closo*-disilaboranes, $Si_2B_nH_{n+2}$, are in different order compared to the corresponding carboranes. The reversal of the isomer stability is better understood by the ring-cap matching rule. [15, 28] Since valence orbitals of SiH are more diffused compared to those of CH, SiH prefers to cap large rings. Thus, SiH is better suited to cap five-membered rings, CH is the better choice while for four-membered ring. Among the three isomers of eight vertex systems, 1,2 isomer in which SiH caps a four-membered ring, is higher in energy than the others. In seven-vertex system, the 2,3-isomer has a Si_2B_3 ring for which even the BH cap

is not large enough. Therefore the 1,2-isomer where one of the ring Si atoms replaced by B is calculated to be lower in energy.

The dehydrogeno structure, $Si_2B_{10}H_{10}$ (**15**) has a shorter Si-Si distance than $Si_2B_{10}H_{12}$ (**1b**) but the decrease is not very large. The icosahedral skeleton is highly strained to accommodate the long Si-Si distance in **1b**. Any decrease in the Si-Si distance is stabilizing for the icosahedron. The requirement of the relatively long distances for icosahedral structures is also seen in the contrasting energetics of the equation 3.2 and 3.3.

$$H_2Si = SiH_2 + C_2H_6 \rightarrow Si_2H_6 + H_2C = CH_2; -12.92 \text{kcal/mol} \quad (3.2)$$

$$C_2B_{10}H_{12}(\textbf{1a}) + Si_2B_{10}H_{10}(\textbf{8b}) + \rightarrow C_2B_{10}H_{10}(\textbf{8a}) + Si_2B_{10}H_{12}(\textbf{1b});$$
$$26.79 \text{kcal/mol} \quad (3.3)$$

The exothermicity of equation 3.2 is attributed among other factors to the strong C-C π-bonds. However, equation 3.3 is endothermic. A probable explanation for the reversal could be obtained from the structural details of the icosahedral skeletons. The B-B distance in $B_{12}H_{12}^{2-}$ is 1.800 Å. To accommodate this skeletal distance, the C-C bond in **1a** is stretched to 1.625 Å. The strain goes up further in **8a** (Figure 3.2) because the C-C double bond is energetically more expensive to stretch. The calculated distance of 1.356 Å in **8a** is only marginally longer than that in ethylene (1.329 Å). The structure is distorted considerably from an ideal skeleton.

Figure 3.4: $Si_2B_{10}H_{10}$ (**8b** is transition state and **15** is minima). Important orbitals are shown. Orbitals of trans (V) and monobridged(VI) Si_2H_2, trans (VII) and cis-Si_2H_4(VIII).
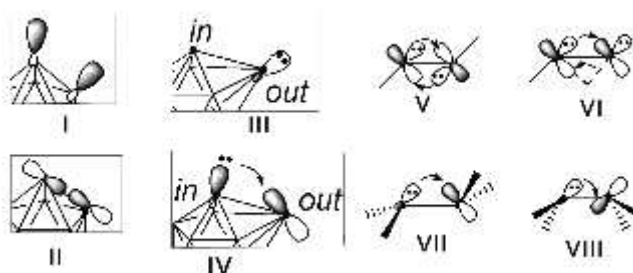
Another source of strain is the pyramidalization of the carbons in **8a**. A contraction, instead of elongation, is in order in **8b**; the Si-Si distance decreases to 2.228 Å. This is still far from the standard icosahedral value of 1.800Å in $B_{12}H_{12}^{2-}$. Further reduction of strain is achieved in the silicon system by the introduction of the double bond. In addition, the pyramidalization at Si is less demanding energetically. Thus, the combination of **1a** and **8b** is better compared to **8a** and **1b**. Despite this, **8b** is calculated to be a transition state. Following the imaginary frequency led to an unusual structure **15** with C_s symmetry.

The surface of **15** is kinky. One Si atom has moved out of the icosahedral surface (Si_{out}, Figure 3.4) and the other has moved slightly in (Si_{in}). The average Si-B bond distance of 2.121 Å in **15** has gone to 2.360 Å for the Si_{out} and 2.043 Å for the Si_{in}. The Si-Si distances and WBI values in **1b** (2.316 Å. 0.57) and **8b** (2.325Å, 0.67) are comparable. However, the Si-Si bond in **8b** is very different from that in **1b**. The results indicate that a good approximation to bonding can be obtained starting with the interaction of two sp^2 hybrid Si groups. In a symmetrical arrangement as in **8b**, there is a σ orbital and a π orbital (**I** and **II**, Figure 3.4). In **15** one

of the Si atoms goes up and the other goes down, resulting in two different MO's. The σ MO arises from the interaction of the p orbital on Si_{out} with the sp^n hybrid on Si_{in} (**IV**). A lone pair formed on Si_{out} is the HOMO (**III**). There are a few examples in literature where the p-orbital of one Si accepts electrons from the hybrid orbital of the adjacent Si. The *trans* and the monobridged Si_2H_2 (**V** and **VI**, Figure 3.4) present the closest comparison. Although the environment around Si is very different in Si_2H_2 and **15**, the Si_2H_2 structures present such an interaction. The Si_2 unit in **15** can also be compared to that in Si_2H_4. The *trans* structure (**VII**) is calculated to be more favorable than the *cis* (**VIII**) structure; the latter is not even a stationary point. However, the constraints of the B_{10} template force a *cis*-arrangement with the unusual bonding pattern (**III** and **IV**).

Similarly other $Si_2B_nH_n$ (**9b-11b**) also distorts to give (**16-18**). 1,2-$Si_2B_5H_5$ (**19**) has a pentagonal bipyramidal structure. The Si that is part of the five membered ring has a lone pair of electrons. Structure **19** completes the n+1 skeleton electron pair count by accepting formal lone pair of electrons from the capping Si atom to the skeletal bonding. The 2,3-$Si_2B_5H_5$ (**13b**) distorts to a qualitatively different structure (**20**) and can be visualized as an octahedron with the silicon capping one of the faces. Similarly, $Si_2B_4H_4$ (**21**) also distorts to a trigonal bipyramid structure with silicon capping one face. These structures with reduced cage size (**20** and **21**) satisfy the (n+1) electron count by accepting two electrons from the bridging atom. In this respect these structures are equivalent to the BH bridging structures such as $B_{13}H_{13}$ (a $B_{12}H_{12}$ with one of the triangular faces bridged by a BH group) and smaller analogues described earlier. [30]

Figure 3.5: Structure of Dedhydrogenosilaboranes ($Si_2B_nH_n$) optimized at the B3LYP/6-31+G*.
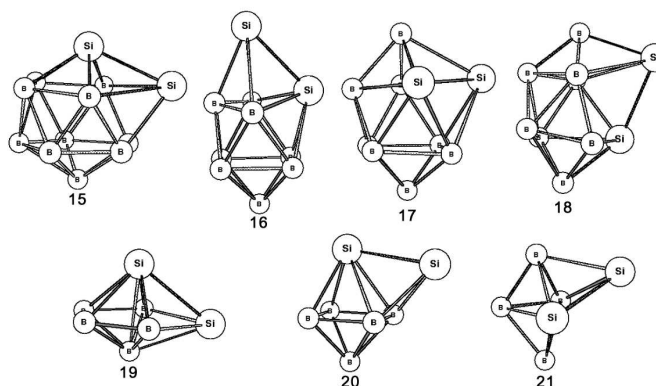
The BH–Si isolobal analogy anticipates this equivalence.

3.3.3 Relative Stabilities and Aromaticity of Carboranes and Silaboranes

Several methods have been used for calculating the stability of borane clusters. [31] In the following equations 3.3-3.6, in which n BH fragments combine with a heteroatom unit giving $X_2B_nH_{n+2}$, or $X_2B_nH_n$, the quantity, heat of reaction divided by n ($\Delta H/n$), is taken as the relative stability of the cluster with n+2 vertex where n=4,5,8 and 10. BH_{inc} is the difference energy between B_3H_5 (C_{2v} planar) and B_2H_4(ethylene-like, D_{2h}). The species used for calculating BH_{inc} is chosen such that hyperconjugation or delocalization is avoided.

The extend of exothermicity of the equations (3.3-3.6) is a measure of the relative stability of the cluster formed. It is evident form Figure 3.6 that six and twelve vertex clusters are most stable for the carboranes and silaboranes while for dehydrospecies, 7 vertex structure stands out. The 2,3-$Si_2B_5H_5$ (**20**) is actually an octahedron with one Si capped to a face

Table 3.2: Relative energy of formation of the carboranes, silaboranes and their dehydrogenoderivaties from the BH units obtained by dividing the reaction energies (equation 3.3-3.6) by n, where n+2 is corresponds to the number of vertexes.

Equation	eq.#	10	8	5	4
$C_2H_2 + nBH_{inc} \rightarrow C_2B_nH_{n+2}$	3.4)	-51.4(**1a**)	-49.5(**2a**)	-49.2(**5a**)	-52.0(**7a**)
			-49.0(**3a**)	-61.1 (**6a**)	
			48.4(**4a**)		
$Si_2H_2 + nBH_{inc} \rightarrow Si_2B_nH_{n+2}$	(3.5)	-48.4(**1b**)	-44.6(**2b**)	-48.3 (**5b**)	-49.5(**7b**)
			-46.1(**3b**)	-45.4(**6b**)	
			-45.9(**4b**)		
$C_2 + nBH_{inc} \rightarrow C_2B_nH_n$	(3.6)	-44.5(**8a**)	-41.9(**9a**)	-38.3(**12a**)	-43.5(**14a**)
			-39.8(**10a**)	-43.1 (**13a**)	
			-39.9(**11a**)		
$Si_2 + nBH_{inc} \rightarrow Si_2B_nH_n$	(3.7)	-43.7(**15**)	-41.9(**16**)	-41.9(**19**)	-43.5(**21**)
			-40.2(**17**)	-44.9 (**20**)	
			-40.8(**18**)		

and is represented at n=6 in the Figure 3.6. The stabilization energy of **19** is used at n=7. Similarly 1,2-$Si_2B_4H_4$ (**21**) is a pentagonal bipyramid with an Si capping to one of the faces. It should be noted that though cross comparison among, carboranes, silaboranes and its dehydrogeno derivatives, is not possible based on equation 3.3-3.6 since the heteroatom fragments are not isoelectronic, i.e., C_2 and C_2H_2, or Si_2 and Si_2H_2, the exothermicity of 2,3-$C_2B_5H_7$ (**6a**) is clearly seen.

The aromatic character of the species considered here can be estimated from the magnitudes of Nucleus Independent Chemical Shift (NICS). Absolute chemical shieldings (with the sign reversed) calculated at the cage center of the molecule indicates the ring current; positive values indicate antiaromatic and negative values aromatic nature. All the compounds have large, negative NICS values. This reflects that multiple bonds on carborane or silaborane surfaces, or reduction from higher vertex to lower vertex systems has very little effect on the three-dimensional aromatic nature of boranes in general. The plots of NICS values (Figure 3.7) show that the

Figure 3.6: Plots of relative stabilities (kcal/mol) of most stable position isomers of $C_2B_nH_{n+2}$, $C_2B_nH_n$, $Si_2B_nH_{n+2}$ and $Si_2B_nH_n$ using the equations 3.3-3.6 (relative energy values divided by n).
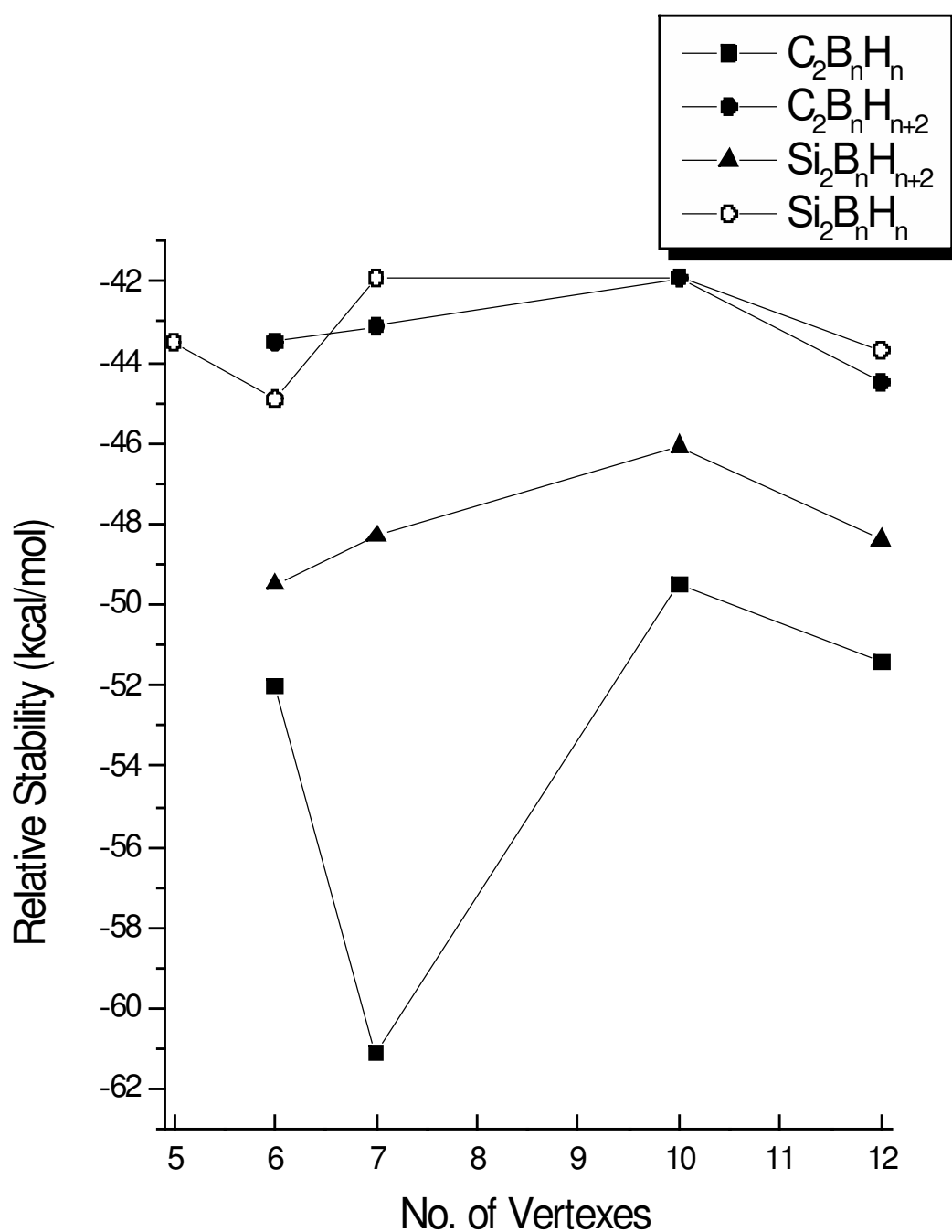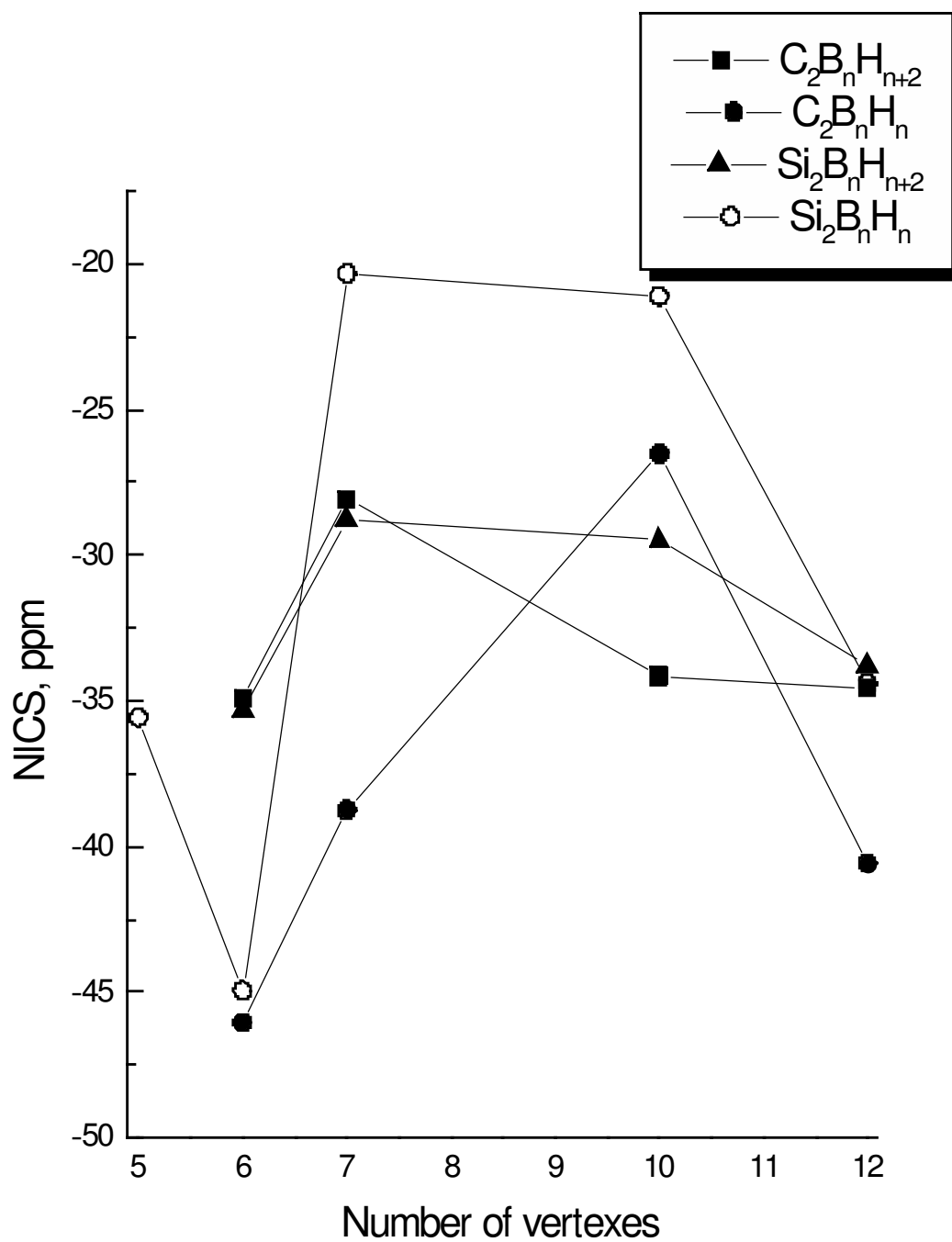
Figure 3.7: Plots of NICS (ppm) of most stable position isomers of $C_2B_nH_{n+2}$, $C_2B_nH_n$, $Si_2B_nH_{n+2}$ and $Si_2B_nH_n$

magnetic criterion of aromaticity is affected more by the symmetry of the cage. The delocalization is more for the most symmetrical cages. Six vertex octahedral and twelve vertex icosahedral compounds of all these four family of compounds are more aromatic than the others. The dehydrogenodisilaboranes brings in an additional complication. The 6-vertex $Si_2B_4H_4$ has a pentagonal bipyramidal structure, **21**, with an Si bridging a face and is represented as a five vertex structure in Figure 3.5. Similarly the more favorable 2,3-$Si_2B_5H_5$ structure is based on the octahedron (**20**). Thus the relative energies are strictly plotted according to the shapes in Figure 3.5. The general reactivity and stability follow the same trends as found for aromaticity.

3.4   Conclusions

Structural details of individual polyhedra determine the ease of dehydrogenation of carboranes and silaboranes. The effect of dehydrogenation is different in o-carboranes and o-silaboranes. Carboranes gives a double bonded system while Silaborane gives face-bridged system. Stability considerations show that double bonded dehydrogenocarboranes other than the experimentally found one (1,2-$C_2B_{10}H_{10}$), are synthetic possibility and Frontier Molecular Orbital Energy considerations show that they could be more reactive. Dehydrogeno silaborane, on the other hand, adopts a different structure in which one Si atom is off the cluster surface. In six vertex and seven vertex clusters, one of the Si atoms moves out and bridge to the triangular face of the skeleton, which is a polyhedra with vertex size reduced by one. Relative stabilities of carboranes and silaboranes show that

the more symmetrical structures are more stable. The dehydrogeno species follow the same pattern of relative stability except for the seven vertex systems. NICS calculations show that aromaticity also follow the trends in stability, that is, the most symmetrical structures are more aromatic. The multiple bonding in the surface and the reduction of the cage do not affect aromaticity, which in turn shows that bonding inside the cage is least affected by the transformation on the surface.

Bibliography

[1] King, R. B; *Chem. Rev.* **2001**, *101*, 5.

[2] Kane, R. R.; Drechsel, K.; Hawthorne, M. F. *J. Am. Chem. Soc.*, **1993**, 115, *19*, 8853. Nemoto, H.; Cai, J.; Yamamoto, Y. *J.Organomet. Chem.* **1999**, 581, *1/2*, 170. Miura, M.; Micca, P.L.; Slatkin, D.N. *Br. J.Radiol.* **1998**, 71, *847*, 773. Kim, Y. S.; Kane, R. R.; Hawthorne, M. F. *Tett. lett.*, **1995**, 36, *29*, 5147. Kane, R. R.; Drechsel, K.; Hawthorne, M. F. *J. Am. Chem. Soc.*, **1993**, 115, *19*, 8853.

[3] Jiang, W.; Knobler, C.B.; Hawthorne, M.F. *Angew. Chem. Int. Ed. Engl.* **1995**, 34, *12*, 1332.

[4] Hawthorne, M. F.; Jiang, W.; Harwell, D. E. *Inorg. Chem.* **1996**, 35, *15*, 4355. Hawthorne M. F.; Zheng Z. *Acc. Chem. Res.* **1997**, 267, *30*,. Jiang. W; Chizhevsky, I. T.;. Mortimer, M. D.; Chen, W.; Knobler, C. B.; Johnson, S. E.; Gomez, F. A.; Hawthorne, M. F. *Inorg. Chem.,* **1996**, *35*, 5417.

[5] Lee, H.; Knobler, C. B.; Hawthorne, M. F., *Angew.Chem.*, **2001**, 113, *11*, 2182-2184. Lee, H.; Knobler, C. B.; Hawthorne, M. F. *Angew. Chem. Int. Ed. Engl.* **2001**, 40, *11*, 2124-2126. Badr, I. H.A.; Johnson, D.; Bachas, L. G. *Anal. Chem.*, **2001**, 73, *1*, 134. Badr, I. H. A.; John-

son, R. D.; Bachas, L. G. *Anal. Chem.*, **2000**, 72, *18*, 4249. Lee, H.; Diaz, M.; Hawthorne, M. F. *Tet. Lett.*, **1999**, 40, *43*, 7651. Zinn, A. A.; Knobler, C. B.; Hawthorne, M. F. *Inorg. Chem.* **1999**, 38, *9*, 2227. Badr, I. H. A.; Diaz, M.; Bachas, L. G. *Anal. Chem.,* **1999**, 71, *7*, 1371. Hawthorne, M. F.; Zheng, Z.. *Acc. Chem. Res.* **1997**, 30, *7*, 267.

[6] Housecroft, C. E. *Angew. Chem. Int. Ed*. **1999**, 38, *18*, 2717.

[7] Hoffmann, R. W., *Dehydrobenzene and Cycloalkynes*, Academic Press, New York, 1967.

[8] H. L. Gingrich, T. Ghosh, Q. Huang, M. Jones Jr., *J. Am. Chem. Soc*. **1990**, *112*, 4082.

[9] Grimes, *Carboranes*, Academic Press, New York, 1970. Bregadze, V. I. *Chem. Rev.* **1992**, *92*, 202-223. Stibr, B. *Chem. Rev.* **1992**, *92*, 225-250.

[10] Jackson, J. E. *Inorg. Chem.* **1996**; *35*(25); 7311-7315. Atkins, J.H.; Ho, D.M.; Jones, Jr., M. *Tet. Lett.* **1996**, 37, *40*, 7217. Ho, D. M., Cunningham, R. J., Brewer, J.; Judson, A.; Bian, N.; Jones, M., Jr. *Inorg. Chem.* **1995**, *344*, 5274-5278. Cunningham, R. J.; Bian, N.; Jones, M., Jr., *Inorg. Chem*. **1994**, *33*, 4811-481Ghosh, T.; Gingrich, H. L.; Kam, C. K.; Mobraaten, E. C.; Jones, M., Jr. *J. Am. Chem. Soc.* **1991**, *113*, 1313-1318. Huang, Q.; Gingrich, H. L.; Jones ,M., Jr. *Inorg. Chem.* **1991**, *30*, 3254-48122.

[11] Bausch, J. W.; Caroll, P. J.; Sneddon, L. G., *Current Topics in the Chemistry of Boron,* ed. Kabalka, G. W., Royal Society of Chemistry, Cambridge, 1994, 224-227. Rietz, R. R.; Schaeffer, R. *J. Am.*

Chem. Soc. **1971**, *93*, 1263. Rietz, R. R.; Schaeffer, R. *J. Am. Chem. Soc.* **1973**, *95*, 6254. Beck, J. S.; Kahn, A. P.; Sneddon, L. G. *Organometallics*, **1986**,*5*, 2552. Beck, J. S.; Sneddon, L. G. *Inorg. Chem.* **1990**, *29*, 295. Fox, M. A.; Greatrex, R. *J. Chem. Soc. Dalton Trans.* **1994**, 3137.

[12] Bradley, A. Z.; Cohen, A. D., Jones, A. C.; Ho, D. M., Jones, M. *Tet. Lett.* **2000**, *41*, 8695-8698. Bradley, A. Z.; Cohen, A. D.; Jones, A. C.; Ho, D. M.; Jones Jr., M. *Tet. Lett.*, **2000**, 41, *45*, *8695*-8698. Barnett-Thamattoor, L.; Zheng, G.; Ho, D. M., Jones Jr., M. *Inorg. Chem.* **1996**, *35*, 7311-7315. . Hota, N. K.; Matterson, D. S. *J. Am. Chem. Soc.* **1971**, *93*, 2893. Hota, N. K.; Matterson, D. S. *J. Am. Chem. Soc.* **1968**, *90*, 3570.

[13] Jemmis, E. D.; Balakrishnarajan, M. M.; Pancharatna, P. D. *J. Am. Chem. Soc*. **2001** *123*, 4313-4323. Balakrishnarajan, M. M.; Jemmis, E. D. *J. Am. Chem. Soc*. **2000** *122*, 4516-4517.

[14] Dysard, J. M.; Tilley, T. D.; Woo, T. K. *Organometallics*, **2001**, 20, *6*, 1195-1203. Priyakumar, U. D.; Sastry, G. N. *J. Am. Chem. Soc.* **2000,** *122,* 11173-11181. Baldridge, K. K.; Uzan, O.; Martin, M. L. *Organometallics*, **2000**, *19*, 1477-1487. Wakita, K.; Tokitoh, N.; Nagase, S. *J. Am. Chem. Soc*. **2000**, 122, *23*, 5648. Brown, E. C.; Borden, W. T. *Organometallics*, **2000**, 19, *11*, 2208. Jutzi, P.; Meyer, M.; Dias, H. V. R *J. Am. Chem. Soc*, **1990**, 112, *12*, 4841. Mal'tsev, A.K.; Kagramanov, N.D.; Bragilevskii, I.O. Bulletin of the Academy of Sciences

of the USSR, **1989**, 38, *5*, 950. Jutzi, P.; Meyer, M.; Reisenauer, H. P. *Chemische Berichte*, **1989**, 122, *7*, 1227.

[15] (a) McKee, M. L. *J. Phys. Chem.* **1992**, *96*, 1679-1683. (b) Jemmis, E. D.; Subramanian, G.; Radom, L. *J. Am. Chem. Soc.* **1992**, *114*, 1481-1483. Jemmis, E. D.; Subramanian, G. *Indian J. Chem.* **1992**, *31A*, 645.

[16] Wesemann, L.; Ramjoie, Y.; Trinkaus, M.; Ganter, B.; Muller, J. *Angew. Chem. Int. Ed. Engl.* **1998**, *37*, 10, 1412-1415. Wesemann, L.; Ganter, B. *Organometallics*, **1996**, 15, *10*, 2569. Wesemann, L.; Englert, U.; Seyferth, D. *Angew. Chem. Int. Ed. Engl.* **1995**, 34, *20*, 2236. Olliges, J.; Lotz, A.; Wesemann, L. *J. Chem. Phys.* **1995**, 103, *22*, 9568. Wesemann, L.; Englert, U.; Seyferth, D. *Angew. Chem. Int. Ed. Engl.* **1991**, *30*,902. Wesemann, L.; Englert, U. *Angew. Chem. Int. Ed. Engl.* **1988**, *27*, 1201.

[17] Wesemann, L.; Englert, U.; Seyferth, D. *Angew. Chem. Int. Ed. Engl.* **1995**, 34, *20*, 2236.

[18] Hawthorne, M. F.; Young, D. C.; Garnett, P. M.; Owen, D. A.; Schwerin, S. G.; Tebbe,F. N.; Wegner, P. A.; *J. Am. Chem. Soc.* **1968**, *90*, 862-868.

[19] Srinivas, G. N.; Jemmis, E. D.; Korkin, A. A.; Schleyer, P. V R. *J. Phys. Chem. A* **1999**, *103,* 11034-11039.

[20] Schleyer, P. v. R.; Najafian, K *Inorg. Chem.* **1998**, *37*, 3454-3470.

[21] Jemmis, E. D.; Kiran, B. *J. Am. Chem. Soc.***1997**, *119*, 4076-4077.

[22] Vyakaranam, K.; Li, S.; Zheng, C.; Hosmane, N. S. *Inorg. Chem. Comm.* **2001**, *4*, 180-182. Ol shevskaya, V. A.; Evstigneeva, R. P.; Luzgina, V. N.; Gyul malieva, M. A.; Petrovskii, P. V.; Morris, J. H.; Zakharkin, L. I. *Mendeleev Commun.* **2001**, *1*, 14. Weller, A. S.; Mahon, M. F.; Steed, J. W. *J. Organomet. Chem.* **2000**, *614-615*, 113 - 119. Chui, K.; Li, H.-W.; Xie, Z. *Organometallics*, **2000**, *19*, 25, 5447-5453. Songkram, C.; Tanatani, A.; Endo, Y. *Tet. Lett.*, **2000**, *41*, 36, 7065.

[23] Wesemann, L.; Trinkaus, M.; Muller, J. *Eur. J. Inorg. Chem.* **2000**, 4, 735. Wesemann, L.; Ramjoie, Y.; Trinkaus, M.; Ganter, B.; Muller, J. *Angew. Chem. Int. Ed. Engl.* **1998**, *37*, 10, 1412-1415. Wesemann, L.; Ramjoie, Y.; Wrackmeyer, B. *Angew. Chem. Int. Ed. Engl.* **1997**, 36, *8*, 888. Wesemann, L.; Ganter, B. *Organometallics*, **1996**, 15, *10*, 2569. Wesemann, L.; Englert, U.; Seyferth, D. *Angew. Chem. Int. Ed. Engl.* **1995**, 34, *20*, 2236. Olliges, J.; Lotz, A.; Wesemann, L. *J. Chem. Phys.* **1995**, 103, *22*, 9568. Wesemann, L.; Englert, U.; Seyferth, D. *Angew. Chem. Int. Ed. Engl.* **1991**, *30*,902. Wesemann, L.; Englert, U. *Angew. Chem. Int. Ed. Engl.* **1988**, *27*, 1201.

[24] B3LYP is Becke's three parameter hybrid method with LYP correlation functional: Becke, A. D. *J.Chem.Phys.*, **1993**, *98*, 5648. Lee, C.; Yang, W.; Parr, R.G. *Phys. Rev. B*, **1988**, *37*, 785; Vosko, S. H.; Wilk, L.; Nusair, M. *Can. J. Phys.*, **1980**, *58*, 1200.; Stephens, P.J.; Delvin, F.J.; Chabalowski, C.F.; Frisch, M.J. *J. Phys. Chem.*, **1994**, *98*, 11623.

[25] Hehre, W. J.; Radom, L.; Schleyer, P. v. R.; Pople, J. A.; *Ab initio*

Molecular Orbital Theory, Wiley, New York, 1986

[26] Schleyer, P. v. R.; Maerker, C.; Dransfeld, A.; Giao, H.; Hommes, N. J. v. E. *J. Am. Chem. Soc.* **1996**, *118*, 6317.

[27] Frisch, M. J.; Trucks, G. W.; Schelegel, H. B.; Gill, P. M. W.; Johnson, B. G.; Robb, M. A.; Cheeseman, J. R.; Keith, T.; Peterson, G. A.; Montgomery, J. A.; Raghavachari, K.; Al-Laham, M. A.; Zakrzewski, V. G.; Ortiz, J. V.; Foresman, J. B.; Cioslowsky, J.; Stefenov, B. B.; Nanayakkara, A.; Challacombe, M.; Peng, C. Y.; Ayala, P. Y.; Chen, W.; Wong, M. W.; Andres, J. L.; Replogle, E. S.; Gomberts, R.; Martin, R. L.; Fox, D. J.; Binkley, J. S.; Defrees, D. J.; Baker, J.; Stewart, J. P.; Head-Gordon, M.; Gonzalez, C. Pople, J. A.; Gaussian 94, Revision D.1, Gaussian Inc., Pittsburg PA, 1995.

[28] (a) Jemmis. E. D. *J. Am. Chem. Soc.* **1982**, *104*, 7017-7020. (b) Jemmis. E. D; Pavankumar, P. N. V.(c) *Proc. Indian Acad. Sci.(Chem. Sci.)*, **1984**, *93*, 479-489. (d) Jemmis, E. D.; Subramanian, G.; Radom, L. *J. Am. Chem. Soc.* **1992**, *114*, 1481-1483.

[29] (a) Seyferth, D.; Buchner, K.; Rees, W. S.; Davis, W. M *Angew. Chem. Int. Ed. Engl.* **1990**, *29*, 918-920. (b) Seyferth, D.; Buchner, K. D.; Rees, W. S.; Wesemann, L.; Davis, W. M.; Bukalov, S. S.; Leites, L. A.; Bock, H.; Sloloki, B. *J. Am. Chem. Soc.* **1993**, *115*, 3586-3594.

[30] McKee M. L.; Wang Z.X.; Schleyer P.v.R. *J.Am.Chem.Soc.*,**2000**, *122*, 4781-4793.

[31] Schleyer, P. v. R.; Najafian, K; Mebel, A. M. *Inorg. Chem.* **1998**, *37*, 6765-6772.

Chapter 4

Theoretical Study on the Double Insertion of Acetylene to the Nickel Complexes of Benzyne and Carborynes.

4.1 Introduction

Carboranes stand out among the polyhedral boranes as stable, neutral, aromatic compounds. [1] Many carborane derivatives have become important reagents in many different applications. Derivatives of carboranes, which can act as carriers of ^{10}B selectively to tumor cells, have found application in the Boron Neutron Capture Therapy (BNCT) of cancer. [2] Macromolecules such as camouflaged carboranes, [4] carborods, [4] dendrimers, [5] find applications in many areas. Fine tuning of the carborane's functionality requires newer methods of synthesis and functionalization of carborane derivatives. An approach in this context is to compare and adopt the reactions of the two dimensionally aromatic systems, benzene and benzyne. Carborynes (dehydrogenocarboranes) are shown to behave similar to benzynes in cycloaddition reactions. [6, 7]

Reactions of benzynes can be modified by coordination with metals. Benzynes form complexes with, early and late transition metals. Benzyne metal complexes undergo reductive coupling with various species such as, alkene, alkyne, CO. [8, 9] Among the various insertion reaction of benzyne metal complexes, the double insertion of substituted acetylenes to the benzyne nickel complex is particularly interesting, as it gives substituted naphthalenes as the final product. As the formation of naphthalenes and benzocarboranes through the pericyclic pathway is known, it would be interesting to study their formation in the catalytic way.

$Ni(\eta^2-C_6H_4)L_2$ (2L=dcpe, 2P-i-Pr$_3$, 2PEt$_3$) has been made by reduction of the corresponding (2-bromophenyl)nickel(II) chloro complexes with 0.5-1.0 % sodium amalgam. $Ni(\eta^2-C_6H_4)L_2$ inserts successively 2 equiv. of alkynes to give substituted naphthalenes, after reductive elimination of the $Ni(PEt_3)_2$ moiety, with fair to good regioselectivity. [10] The similarity of
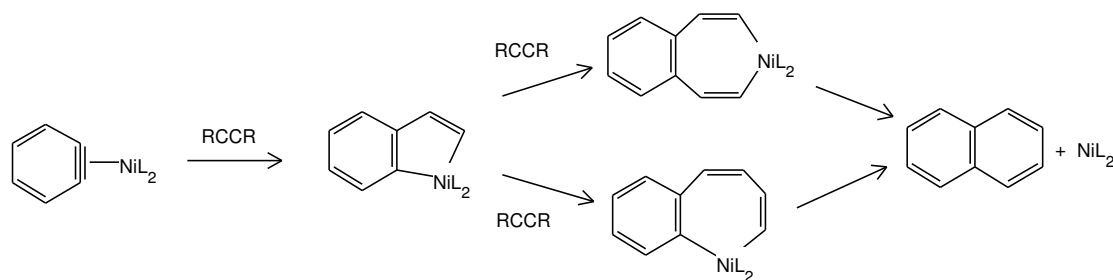
Scheme 4.1

benzyne with carboryne prompts us to compare the metal complexes of benzyne with carborynes. A study of the stability and reactivity of metal complexes of carborynes is important in this regard.

Here we present a computational study of the double insertion of acetylene to carboryne-nickel complex with a proposed reaction mechanism, comparing the energetics of the reaction in each step with experimentally

known reaction of benzyne. Carborynes considered here are $C_2B_{10}H_{10}$ and $C_2B_5H_5$. The selection was based on the theoretical study which showed that they are the best among the carborynes with vertex sizes 6,7,10 and 12. [12] Phosphines are used as the ligands instead of the experimental ligands to reduce the computational cost.

4.2 Methods

All structures were optimized at B3LYP/LANL2DZ [6, 8, 24]using Gaussian 03 program package [9] at Maui High Performance Computing Center. In view of the large number of structures involved we selected this method which is economical and reproduces the trends well. [27] Total energies are corrected with Zero-Point vibrational Energy. The stationary points were characterized as minima or transition state using the vibrational frequency analyzes. The stationary points in the reaction are labeled with the numbers **1**-**15** appended with the letters represent the 'ynes' (benzyne or carboryne): **a** for acetylene; **b** for benzyne; **c** for $C_2B_{10}H_{10}$ and **d** for $C_2B_5H_5$. For example, **1b** represent (benzyne)(bisphosphine)nickel complex. Total energy, Zero-poing energy and number of imaginary frequencies are given in Tables 4.1-4.4

4.3 Results and Discussions

The discussion is organized in the following lines. The geometry of the metal phosphine complexes of acetylene, benzyne and carborynes are discussed in relation to the experimentally found benzyne nickel complexes.

Table 4.1: Total Energy (T.E., au), Zero-point Vibrational Energy (Z.P.E, kcal/mol) and Number of imaginary frequecies for the structures **1a-16a**) calculated at B3LYP/LANL2DZ level.

Molecule	T.E.(au)	Z.P.E. (kcal/mol)	T.E.+Z.P.E. (au)	NImag
1a	-263.21732	51.12	-263.13585	0
2a	-340.52922	67.49	-340.42167	0
3a	-332.26885	53.00	-332.18439	0
4a	-254.91463	34.22	-254.86010	0
5a	-332.24489	54.83	-332.15752	0
6a	-332.29507	55.84	-332.20609	0
7a	-340.59201	73.00	-340.47568	0
8a	-409.63083	74.00	-409.51290	0
9a	-409.71237	77.31	-409.58918	0
10a	-409.63083	74.00	-409.51290	0
11a	-409.71237	77.31	-409.58918	0
12a	-417.90786	90.49	-417.76367	0
13a	-418.07586	95.78	-417.92323	0
14a	-417.90787	90.49	-417.76366	0
15a	-418.07586	95.78	-417.92323	0
16a	-232.21333	63.55	-232.11205	0
TSa3-5	-332.24302	53.93	-332.15707	1
TSa8-9	-409.62288	74.92	-409.50349	1
TSa10-11	-409.62288	74.92	-409.50349	1
TSa12-13	-417.89795	90.86	-417.75316	1
TSa14-15	-417.89795	90.86	-417.75316	1

The bonding energy and relative stability of these compounds are presented next. This is followed by the details of the reaction mechanism of the double insertion of acetylenes.
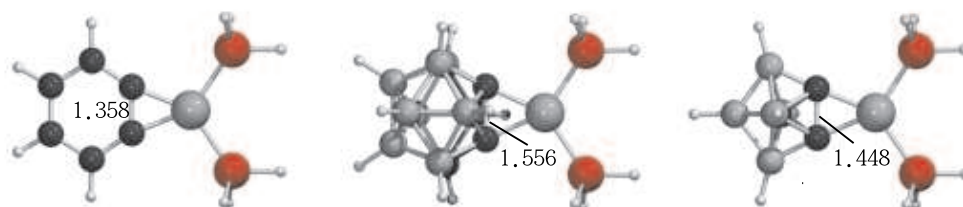
Scheme 4.2

Important geometric parameters of the benzyne and carboryne com-

Table 4.2: Total Energy (T.E., au), Zero-point Vibrational Energy (Z.P.E, kcal/mol) and Number of imaginary frequecies for the structures **1b-16**b) calculated at B3LYP/LANL2DZ level

Molecule	T.E. (au)	Z.P.E.(kcal/mol)	T.E.+Z.P.E. (au)	NImag
1b	-416.83235	82.28	-416.70123	0
2b	-494.14090	83.70	-494.00752	0
3b	-485.87742	84.15	-485.74332	0
4b	-408.52588	65.41	-408.42164	0
5b	-485.88559	85.93	-485.74865	0
6b	-485.93982	86.48	-485.80201	0
7b	-494.23383	103.63	-494.06869	0
8b	-563.27375	104.64	-563.10699	0
9b	-563.34035	107.37	-563.16925	0
10b	-563.27415	104.65	-563.10738	0
11b	-563.34152	107.84	-563.16967	0
12b	-571.54687	120.78	-571.35439	0
13b	-571.62118	125.67	-571.42090	0
14b	-571.54865	120.68	-571.35632	0
15b	-571.62376	125.61	-571.42359	0
16b	-385.83316	93.43	-385.68426	0
TSb3-5	-485.87114	84.51	-485.73647	1
TSb8-9	-563.26487	104.71	-563.09800	1
TSb10-11	-563.26139	105.40	-563.09343	1
TSb12-13	-571.53393	121.15	-571.34086	1
TSb14-15	-571.53182	121.11	-571.33882	1

plexes are given in Scheme 2. $(C_6H_4)Ni(PH_3)_2$ used as the model compound, is compared with X-ray structure of $(C_6H_4)Ni(dcpe)$. Calculated and experimental values of bond lengths are: C-C=1.358 Å,1.331 Å; Ni-C=1.897 Å; 1.870 Å; Ni-P=2.278 Å, 2.153 Å. Considering that the ligands used in the calculation are simplified form of the actual ligands, the geometric parameters are in reasonable agreement with the experimental values. The C-C bond length in benzyne and carborynes are elongated on complexation. The C1-C2 bond length in free benzyne is 1.266Å which is stretched to 1.358Å. Similarly, in $(C_2B_{10}H_{10})Ni$ complex, C-C bond length is 1.556 Å which is longer compared to that in $C_2B_{10}H_{10}$, 1.368

Table 4.3: Total Energy (T.E., au), Zero-point Vibrational Energy (Z.P.E, kcal/mol) and Number of imaginary frequecies for the structures **1c-16c**) calculated at B3LYP/LANL2DZ level.

Molecule	T.E. (au)	Z.P.E. (kcal/mol)	T.E.+Z.P.E. (au)	NImag
1c	-516.59588	128.17	-516.39163	0
3c	-585.63573	129.73	-585.42899	0
4c	-508.28177	111.04	-508.10482	0
5c	-585.65276	131.21	-585.44366	0
6c	-585.70395	132.74	-585.49242	0
7c	-594.00605	150.01	-593.76700	0
8c	-663.04277	151.06	-662.80204	0
9c	-663.08583	153.39	-662.84140	0
10c	-663.04154	150.95	-662.80100	0
11c	-663.09896	153.85	-662.85379	0
12c	-671.31702	167.10	-671.05073	0
13c	-671.38139	171.34	-671.10834	0
14c	-671.31758	166.54	-671.05218	0
15c	-671.38450	170.18	-671.11330	0
16c	-485.54283	138.77	-485.32168	0
TSc3-5	-585.62802	130.01	-585.42083	1
TSc8-9	-663.03169	151.54	-662.79019	1
TSc10-11	-663.00516	151.33	-662.76400	1
TSc12-13	-671.30054	167.44	-671.03371	1
TSc14-15	-671.27791	167.67	-671.01072	1

Å. The C-C bond length in $C_2B_5H_5$ is elongated from 1.327 Å to 1.448 Å on complexation. The corresponding distances in acetylene and its complex are 1.222 and 1.297 Å. The increase in bond length are 0.092, 0.188, 0.121 and 0.075 Å for benzyne, $C_2B_{10}H_{10}$, $C_2B_5H_5$ and acetylene. The larger increase in carboryne compared to that of acetylene and benzyne are due to the release of strain. C-C bond in carborynes are highly strained because they are stretched from the normal C=C distance to accommodate the skeletal requirement. In $C_2B_{10}H_{10}$, C-C bond length is 1.556 Å, compared to the regular icosahedral dodecacarborane vertex size 1.787 Å and the C=C bond in benzyne, 1.347 Å. On complexation C-C bond length

Table 4.4: Total Energy (T.E., au), Zero-point Vibrational Energy (Z.P.E, kcal/mol) and Number of imaginary frequecies for the structures **1a-16a**) calculated at B3LYP/LANL2DZ level.
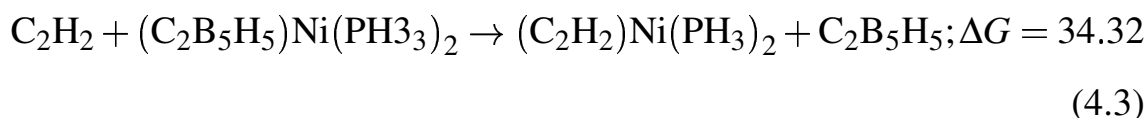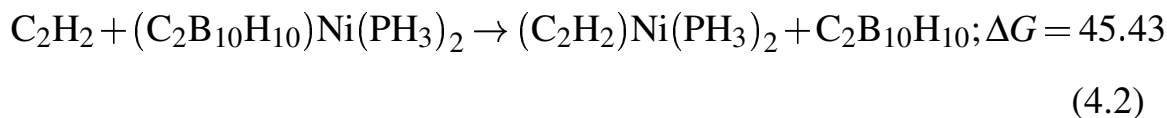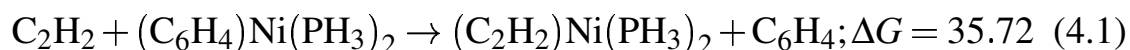
Molecule	T.E. (au)	Z.P.E. (kcal/mol)	T.E.+Z.P.E. (au)	NImag
1d	-389.26963	82.12	-389.13876	0
2d	-466.58043	98.96	-466.42272	0
3d	-458.31359	83.97	-458.17978	0
4d	-380.96029	65.20	-380.85639	0
5d	-458.31128	85.41	-458.17517	0
6d	-458.36833	86.31	-458.23079	0
7d	-466.66634	103.60	-466.50124	0
8d	-535.70327	104.52	-535.53671	0
9d	-535.75493	106.90	-535.58457	0
10d	-535.70146	104.37	-535.53513	0
11d	-535.76757	107.58	-535.59614	0
12d	-543.97816	120.76	-543.78572	0
13d	-544.05598	124.53	-543.85753	0
14d	-543.97439	120.14	-543.78294	0
15d	-544.04960	123.79	-543.85234	0
16d	-358.22589	92.46	-358.07855	0
TSd3-5	-458.30105	84.22	-458.16683	1
TSd8-9	-535.69496	104.97	-535.52768	1
TSd10-11	-535.67458	105.18	-535.50696	1
TSd12-13	-543.96131	121.06	-543.76840	1
TSd14-15	-543.94454	120.81	-543.75203	1

increases by 0.188 Å which reduces the strain of the cage. The strain release is less in $C_2B_5H_5$ because pentagonal bipyramid with BH caps would prefer smaller rings and thus increase on complexation is 0.121 Å. [12]

π-bonds in alkene and alkyne coordinates with metals. Both the π orbitals in acetylene can form bonds with metals, compared to one in ethylene. Deviation from linearity helps in increasing the overlap of the in-plane orbitals with the metal orbitals. The bent C-C-C bond in benzynes, forced by the geometry of the six membered ring, helps in better overlap with the metal. Similar should be the case with carborynes. Among the carborynes, heptacarboryne has more splayed out orbitals. These trends can be qual-

itatively tested with the geometric parameters, and with the complexation energies of ML_n fragments with alkynes or carborynes. The stronger the interaction, the more it behaves like metallacycle.

The relative stability of the complexes of carborynes compared to that of acetylenes and benzynes are calculated using the equations 4.1-4.3. These equations show that all the three compounds make better complexes than acetylene, the relative stability being $C_2B_{10}H_{10}>$ benzyne $> C_2B_5H_5$. To a large extend, the instability of the -yne is reflected in these isodesmic equations.

$$C_2H_2 + (C_6H_4)Ni(PH_3)_2 \rightarrow (C_2H_2)Ni(PH_3)_2 + C_6H_4; \Delta G = 35.72 \quad (4.1)$$

$$C_2H_2 + (C_2B_{10}H_{10})Ni(PH_3)_2 \rightarrow (C_2H_2)Ni(PH_3)_2 + C_2B_{10}H_{10}; \Delta G = 45.43$$
$$(4.2)$$

$$C_2H_2 + (C_2B_5H_5)Ni(PH3_3)_2 \rightarrow (C_2H_2)Ni(PH_3)_2 + C_2B_5H_5; \Delta G = 34.32$$
$$(4.3)$$

The relative preference between the carboranes for complexation is estimated using the following reactions.

$$(C_2B_{10}H_{10})Ni(PH_3)_2 + C_2B_5H_5 \rightarrow (C_2B_5H_5)Ni(PH_3)_2 + C_2B_{10}H_{10}; \Delta G = 11.1$$
$$(4.4)$$
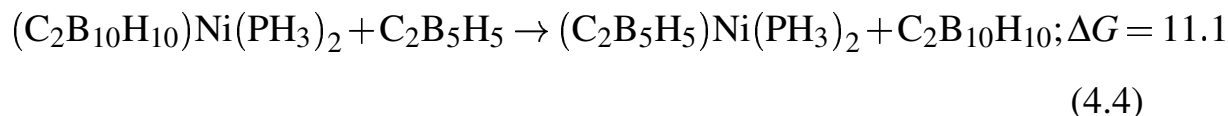
Another comparison of relative stability can be obtained as the complexation energy of benzynes and carborynes with NiL_2 fragment. The energy released on the formation of the corresponding metal complex from two

fragments as is calculated from the following equation (equation 4.5).

$$Ni(PH_3)_2 + X \rightarrow Ni(PH_3)_2(X) \tag{4.5}$$
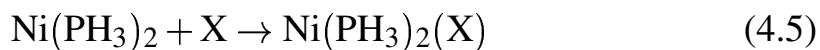
where X=acetylene, benzyne, $C_2B_{10}H_{10}$, $C_2B_5H_5$. The complexation energy of benzyne is 60.38 kcal/mol. Complexation energies are 70.09 kcal/mol for $C_2B_{10}H_{10}$ and 58.99 kcal/mol for $C_2B_5H_5$ and 24.66 for acetylene. The low value calculated for acetylene is a consequence of the geometric distortion required in the complex from a linear geometry. The benzynes and the carborynes are already in a geometry appropriate for complexation.

4.3.1 Acetylene insertion to $(C_6H_4)Ni(PH_3)_2$(**1b**)

The sequential insertion of two acetylene molecules to the benzyne complex is analyzed next. The proposed reaction mechanism is shown in Figure 4.1. Insertion of acetylene to benzyne nickel complex can be associative or dissociative. In the associative pathway acetylene coordinates with the benzyne-nickel complex. Release of PH_3 from this geometry gives (benzyne)(acetylene)nickel complex. In the dissociative way the release of PH_3 occurs first providing a vacant site, followed by the addition of acetylene. Insertion of acetylene to Ni-C bond occurs with the rearrangement of (benzyne)(acetylene)nickel complex to give the five membered nickelacycle.

Experiments to study the regioselectivity of the insertion of unsymmetrical acetylenes to **1b** showed that the first insertion occurs under steric control and forms a nickelaindane in which the substituted carbon atom is bound to nickel, and second insertion occurs in the nickel-vinyl bond of

Figure 4.1: Insertion of acetylene to benzyne nickel complex
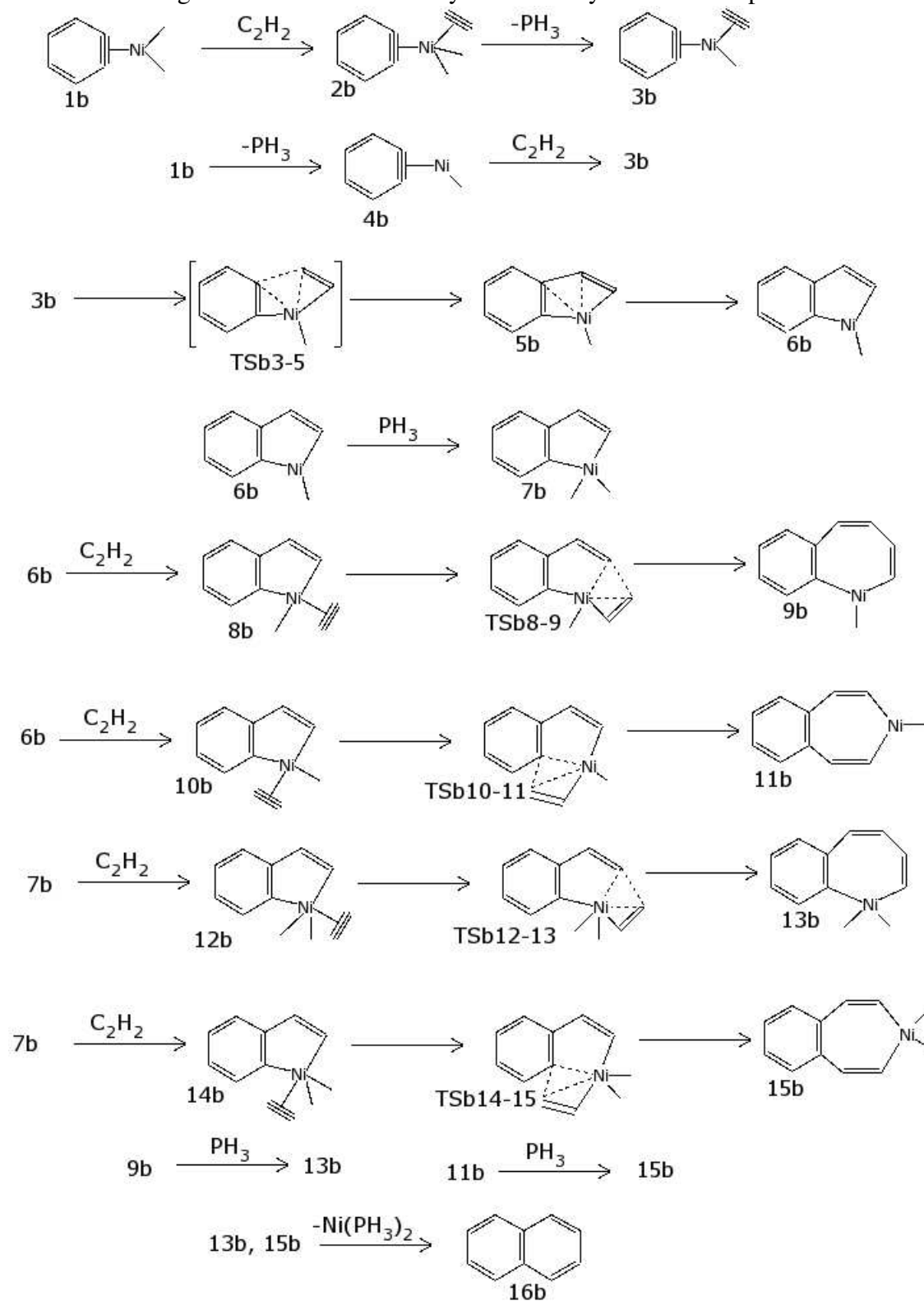
this species, not nickel-aryl bond, also under steric control. [11]

First stationary point in the associative pathway is (acetylene)(benzyne)-

Figure 4.2: Reaction profile for the insertion of acetylene to benzyne nickel complex (1b)
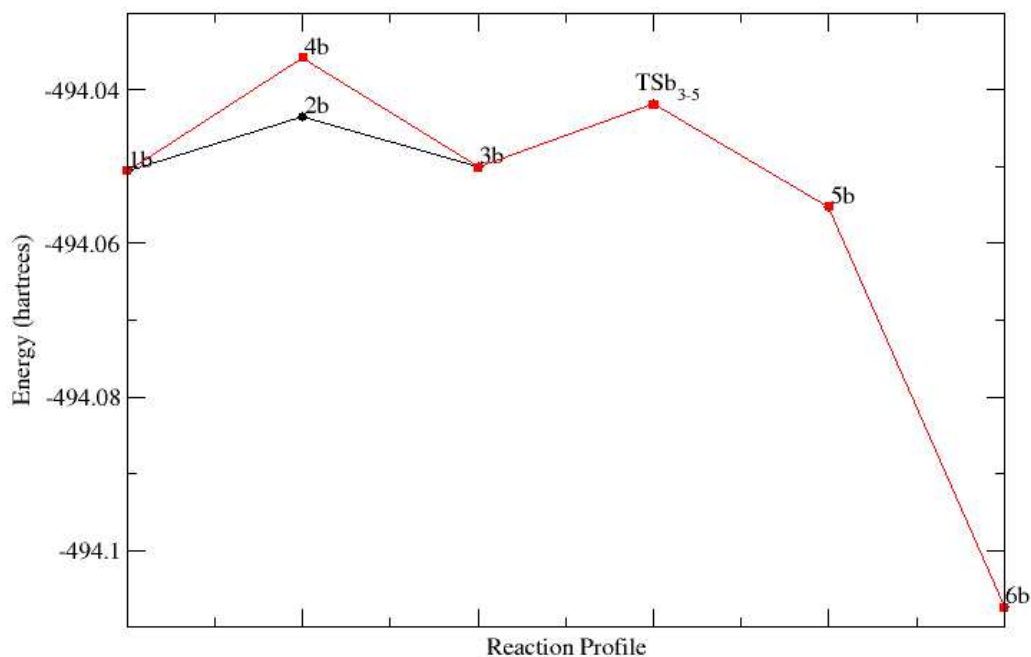
bis(phosphine) nickel (**2b**). This process is calculated to be endothermic by 4.37 kcal/mol. Release of PH_3 from **2b** to give **3b** is exothermic by 4.12 kcal/mol. In the dissociative pathway the release of PH_3 to give **4b** occurs first. This step is endothermic 9.25 kcal/mol. The next step is the exothermic addition of acetylene to **4b** giving **3b** with the release of energy 9.00 kcal/mol. Comparison of energetics involved in the associative and dissociative paths shows that, associative substitution is more favorable. The substitution of PH_3 in **1b** by acetylene to form **3b**, is exothermic (0.25 kcal/mol). The complex, **3b**, rearranges to **5b**. Acetylene in **3b** is inserted to the benzyne triple bond through a transition state TSb_{3-5} with an activation energy 5.18 kcal/mol. **5b** is an intermediate structure where four carbon atoms are coordinated to the Ni in η^4-fashion. **5b** rearranges to

the nickelacycle, **6b**. Association of one more PH_3 gives **7b** with exothermicity 1.88 kcal/mol.

In the case of second insertion of acetylene to the nickelacycle there are two bonds to which acetylene can be inserted: Ni-vinyl and Ni-aryl. For each of this, there are associative and dissociative pathways. In the dissociative pathway, acetylene coordinates to the two possible sites of **6b** to give **8b** and **10b**. In **8b**, acetylene is nearer to the vinyl group, whereas in **10b** acetylene is nearer to the aryl group. **8b** lead to **9b** through the transition state, TS_{8-9} with an activation energy of 6.47 kcal/mol; **10b** lead to **11b** through the transition state, TS_{10-11}, with an activation energy of 10.54 kcal/mol. Th structure **9b** is lower in energy than **11b** by 0.25 kcal/mol. **9b** and **11b** coordinates with a molecule of PH_3 to form the nickelacycles **13b** and **15b** respectively with endothermicity 12.13 and 9.42 kcal/mol.

First step in the associative path is the association of acetylene to **7b**. Acetylene can be coordinated to the site nearer to the benzene ring or farther. The former (**14b**) is more stable than the latter (**12b**) by 1.21 kcal/mol. The insertion of acetylene in **14b** to Ni-aryl bond leads to **15b**, through TS_{14-15} with an activation energy of 12.0 kcal/mol. Similarly, acetylene in **12b** inserts to the Ni-vinyl bond to form **13b** through the transition state, TS_{12-13}, with the activation energy of 9.07 kcal/mol.

Reductive elimination of $Ni(PH_3)_2$ from the nickelacycles **13b** an **15b** gives naphthalene.

Figure 4.3: Reaction profile for the dissociative insertion of acetylene to 6b
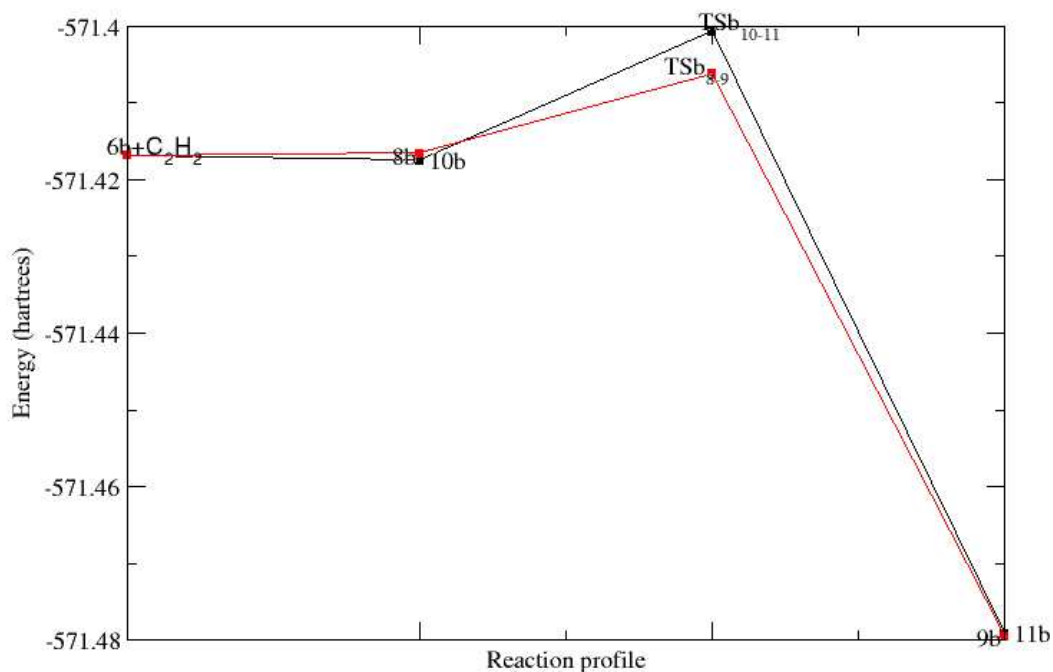
4.3.2 Acetylene insertion to $C_2B_{10}H_{10}$ and $C_2B_5H_5$ nickel bisphosphine

We considered the same mechanism as benzyne for the carborynes. The coordination of PH_3 to **1d** to form **2d** is endothermic by 12.40 kcal/mol, whereas The complex **2c** is not a local minima at this level. The steric crowding of $C_2B_{10}H_{10}$ makes the unfavorable situation around Ni. The endothermicity of the formation of 2d is 8.03 kcal/mol higher than that of **2b**. In the dissociative pathway, the release of PH_3 is endothermic with 13.94 and 11.21 kcal/mol from **1c** and **1d** respectively compared to 9.25 for **1b**. The resulting complexes **4c** and **4d** are then coordinated with acetylene to form **3c** and **3d** respectively which are exothermic steps with energy

Figure 4.4: Reaction profile for the associative insertion of acetylene to 7b
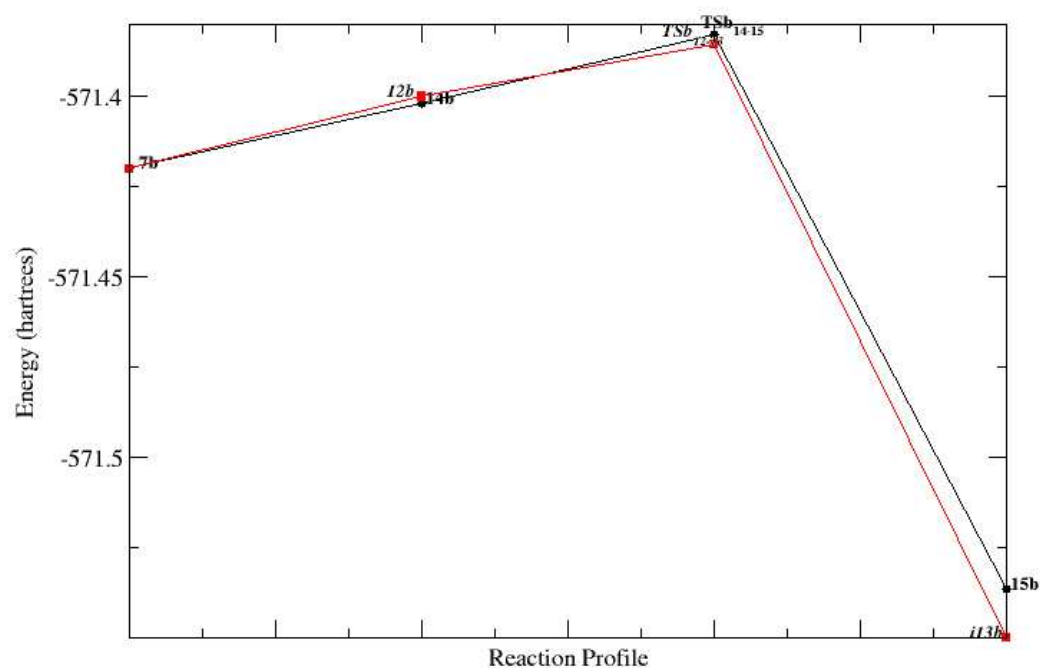
11.05 and 10.23 kcal/mol. The overall reaction, the substitution of PH_3 by acetylene is endothermic (2.89 and 0.98 kcal/mol). **3c,d** has acetylene and carboryne coordinated to Ni in η^2-fashion in addition to the phosphine ligand. The five membered nickelacycle is formed by the insertion of the acetylene to the C-Ni bond of **3c,d**. The transition states for this conversion is calculated ($TS(c,d)_{3-5}$) and activation barriers are computed as 6.23 kcal/mol for **3c** to **5c** and 8.74 kcal/mol for **3d** to **5d**. The complexes **5c,d** with η^4-coordination, rearranges to **6c,d**. The addition of one more phosphine gives the nickelacycles **7c,d**.

The coordination of acetylene to the nickelacycles **7c,d** is the first step in the associative insertion reaction. Among the possible coordination sites, one is cis to the Ni-vinyl bond and the other cis to the Ni-aryl bond.

Figure 4.5: Reaction profile for the insertion of acetylene to $(C_{10}B_{10}H_{10})Ni$
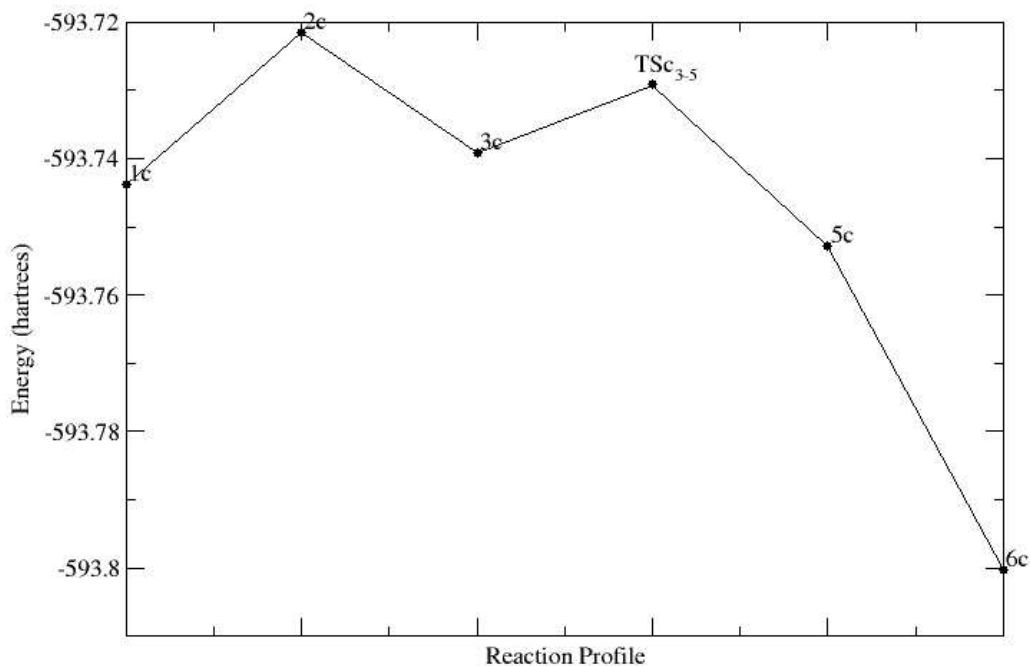
The former structure **12c** is less stable than the latter **14c**. On the other hand, **12d** and **14d** are nearly isoenergetic. The activation energy for the insertion to the Ni-aryl bond is very high, 30.25 kcal/mol for **14c** and 21.50 kcal/mol for **14d**, compared to the barrier for insertion to the Ni-vinyl bond, 11.75 and 11.33 kcal/mol respectively for **12c** and **12d**. Insertion to the Ni-vinyl bond gives the nickelacycle **13c,d** and to the Ni-aryl bond gives **15c,d**.

The substitution of phosphine by acetylene of **7c,d** for the dissociative insertion pathway is endothermic by 4.24 kcal/mol for **7c** to **8c** and 3.38 kcal/mol for **7c** to **8d**. The acetylene in **8c,d** is cis to the Ni-vinyl bond. The isomer, **10c,d**, also have similar reaction energies for the substitution of phosphine trans to the Ni-vinyl bond by acetylene; 4.41 kcal/mol for

Figure 4.6: Reaction profile for the insertion of acetylene to $(C_2B_5H_5)Ni$ complex
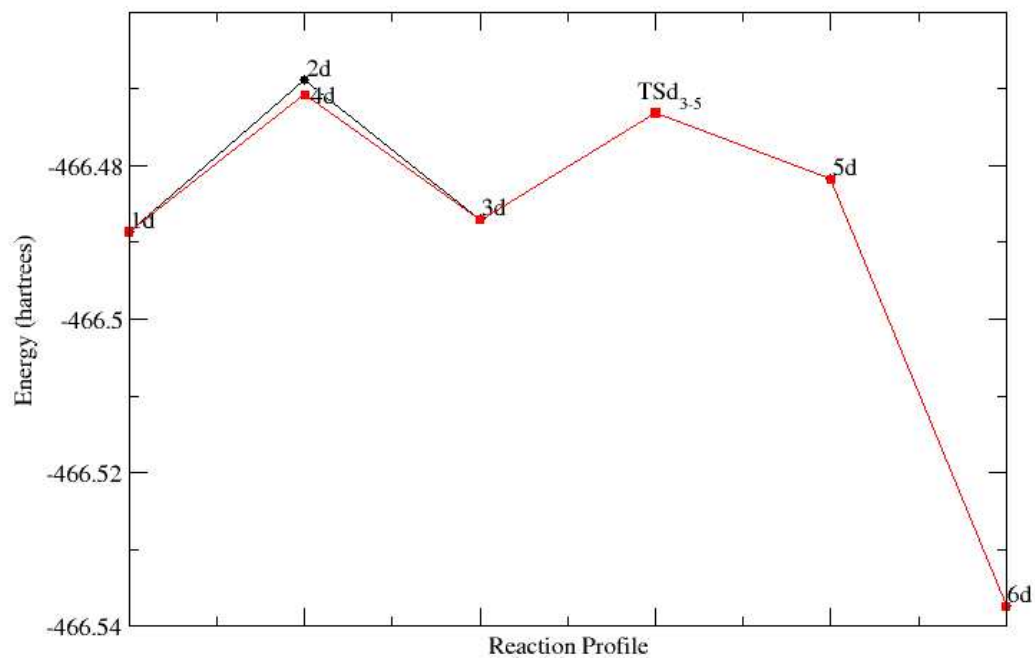
Figure 4.7: Reaction profile for the associative insertion of acetylene to 7c
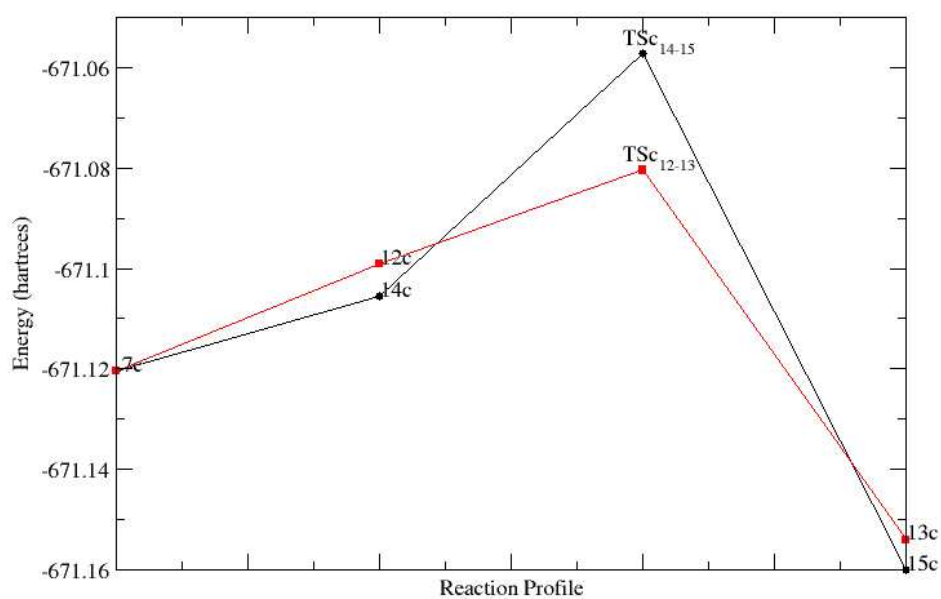
Figure 4.8: Reaction profile for the associative insertion of acetylene to 7d
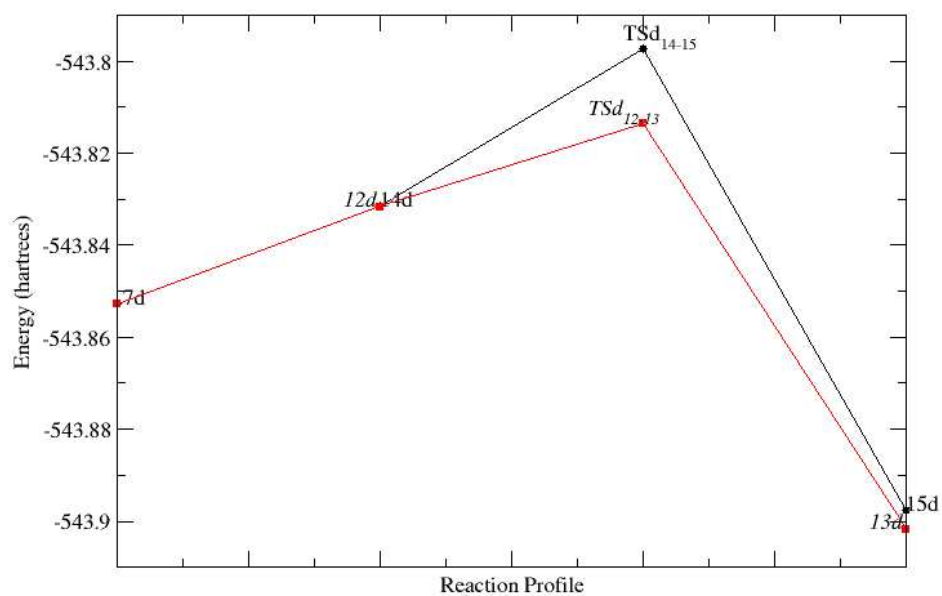
Figure 4.9: Reaction profile for the dissociative insertion of acetylene to 6c

Figure 4.10: Reaction profile for the dissociative insertion of acetylene to 6d

10c and 3.80 kcal/mol for **10d**. The acetylene in **8c,d** insert to the Ni-vinyl bond through the transition state TSc,d_{8-9} with the activation energies 8.46 and 7.09 kcal/mol. The insertion to the Ni-aryl bond in **10c,d** has much higher activation energy 24.41, 19.77 kcal/mol.

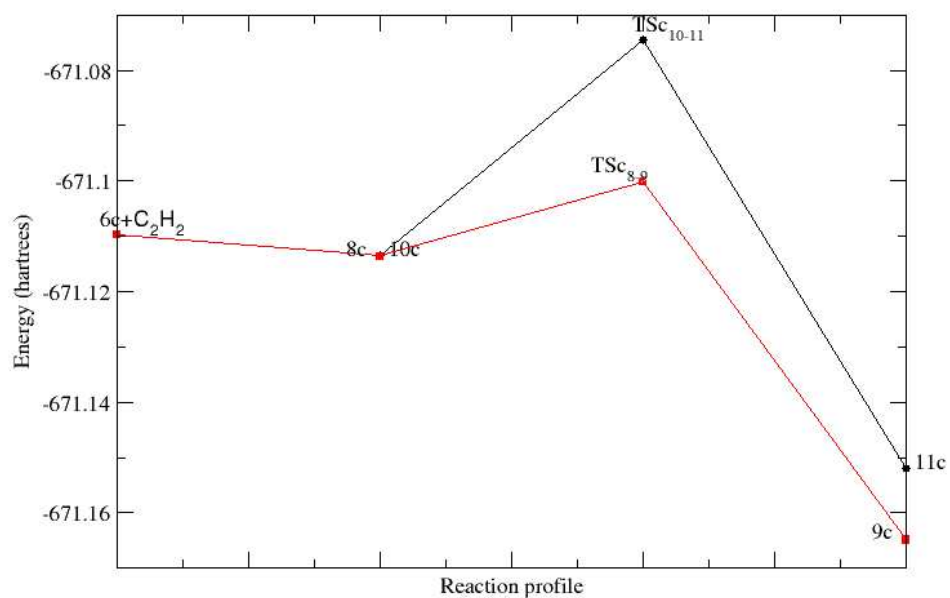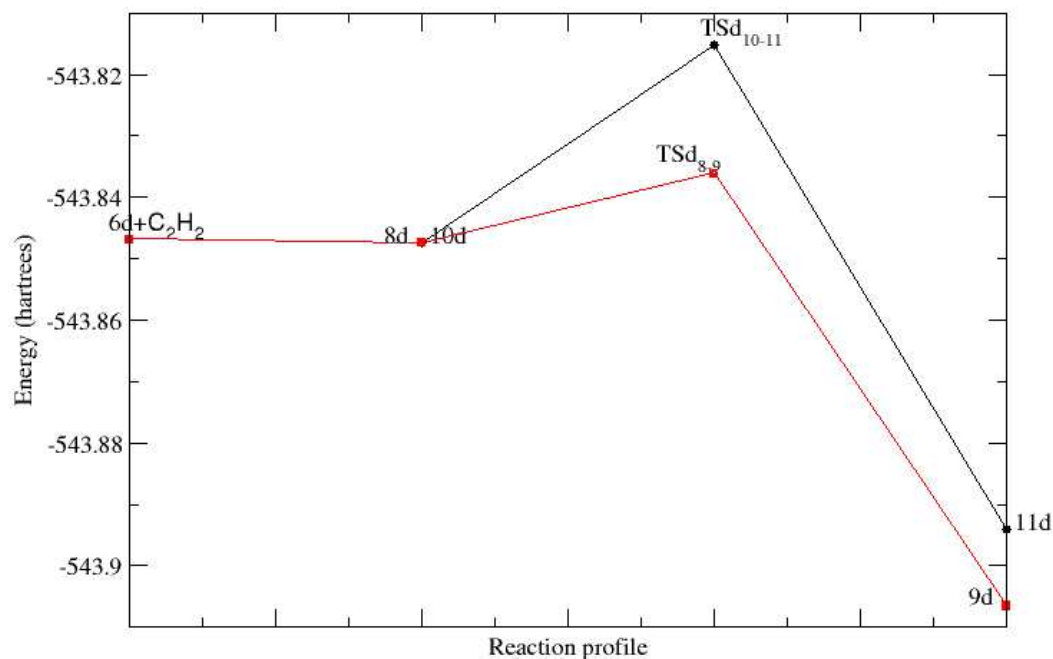Table 4.5: Free energy of reaction (ΔG, kcal/mol) for the steps shown in Figure 4.1 calculated at B3LYP/LANL2DZ.

Step	a	b	c	d
$1+C_2H_2\rightarrow2$	11.14	4.37	–	12.40
$2\rightarrow3+PH_3$	-14.62	-4.12	–	-11.42
$1\rightarrow4+PH_3$	8.15	9.25	13.94	11.21
$4+C_2H_2\rightarrow3$	-11.63	-9.00	-11.05	-10.23
$1+C_2H_2\rightarrow3+PH_3$	-3.48	0.25	2.89	0.98
$3\rightarrow TS3\text{-}5$	16.91	5.18	6.23	8.74
$3\rightarrow5$	17.17	-3.18	-8.58	3.32
$5\rightarrow6$	-29.71	-32.77	-29.76	-34.92
$6+PH_3\rightarrow7$	-3.26	-1.88	-6.70	-3.70
$1+C_2H_2\rightarrow7$	-19.29	-37.58	-42.16	-34.32
$6+C_2H_2\rightarrow8$	-1.07	0.19	-2.46	-0.32
$8\rightarrow TS8\text{-}9$	7.27	6.47	8.46	7.09
$8\rightarrow9$	-48.25	-39.26	-24.10	-29.42
$6+C_2H_2\rightarrow10$	-1.07	-0.37	-2.30	0.10
$10\rightarrow TS10\text{-}11$	7.27	10.54	24.41	19.77
$10\rightarrow11$	-48.25	-38.70	-24.27	-29.83
$7+C_2H_2\rightarrow12$	10.88	12.47	13.34	13.24
$12\rightarrow TS12\text{-}13$	7.17	9.07	11.75	11.33
$12\rightarrow13$	-100.21	-37.53	-34.40	-43.96
$7+C_2H_2\rightarrow14$	10.89	11.19	9.32	13.25
$14\rightarrow TS14\text{-}15$	7.17	12.00	30.25	21.50
$14\rightarrow15$	-100.22	-39.20	-34.12	-41.50
$9+PH_3\rightarrow13$	-43.28	12.13	-1.20	-4.68
$11+PH_3\rightarrow15$	-43.28	9.18	-4.95	-2.21
$7+C_2H_2\rightarrow13$	-89.33	-25.06	-21.06	-30.72
$7+C_2H_2\rightarrow15$	-89.33	-28.01	-24.81	-28.24
$13\rightarrow16$	1.53	-49.34	-16.18	-20.76
$15\rightarrow16$	1.53	-46.39	-12.43	-23.23

4.4   Conclusion

The coordination of acetylene to **1a,b,d** is endothermic with lowest value
for **1b**. (Table 4.5) The dissociation of PH_3 is also endothermic for **a-d**.
For **1a,d** associative pathway for the substition of PH_3 by acetyelene is
the lowest energy pathway whereas for **1b** dissociative pathway is more
favorable. The activation energy for the insertion step is 5.18 kcal/mol
for **3b**. **3a,c** and **3d** has higher activation barriers, 16.91, 6.23 and 8.74
kcal/mol respectively. The activation energy for the insertion to the vinyl
C-C bond in the second insertion step is more favorable than to the aryl C-
C bond. Similarly for the dissociative pathway also insertion to the vinyl
bond is more favorable than to the aryl bond. The dissociative insertion is
more favorable than the associative insertion.

Bibliography

[1] (a)Grimes, R. N. *Carboranes*; Academic Press: New York, **1970**, and references therein. (b) Onak, T. *Comprehensive Organometallic Chemistry*; Wilkinson, G., Stone, F. G. A., Abel, E., Eds.; Pergamon: Oxford, **1982**; Vol I, Chapter 5 and references therein. *Comprehesive Organomettalic Chemistry II*; Abel, W., Stone, F. G. A., Wilkinson, G., Eds.; Pergamon Press: Oxford, **1995**; Vol. I, Chapter 6.

[2] Kane, R. R.; Drechsel, K.; Hawthorne, M. F. *J. Am. Chem. Soc.*, **1993**, *115*, 8853. Nemoto, H.; Cai, J.; Nakamura, H.; Fujiwara, M.; Yamamoto, Y. *J. Organomet. Chem.* **1999**, *581*, 170. Miura, M.; Micca, P. L.; Slatkin, D. N. Br. *J. Radiol.* **1998**, *71*, 773. Kim, Y. S.; Kane, R. R.; Beno, C. L.; Romano, S.; Mendez, G.; Hawthorne, M. F. *Terahedron Lett.* **1995**, *36*, 5147.

[3] Maderna, A.; Herzog, A.; Knobler, C. B.; Hawthorne, M. F. *J. Am. Chem. Soc.* **2001**, *123*, 10423. Rockwell, J. J.; Herzog, A.; Peymann, T.; Knobler, C. B.; Hawthorne, M. F. *Curr. Sci.* **2000**, *78*, 405. Herzog, A.; Knobler, C. B.; Hawthorne, M. F.; Maderna, A.; Siebert, W. *J. Org. Chem.* **1999**, 64, 1045. Jiang, W.; Knobler, C. B.; Mortimer, M. D.; Hawthorne, M. F. *Angew. Chem., Int. Ed. Engl.* **1995**, *34*, 1332.

[4] Jiang, W.; Harwell, D. E.; Mortimer, M. D.; Knobler, C. B.; Hawthorne, M. F. *Inorg. Chem.* **1996**, *35*, 4355. Hawthorne, M. F.; Zheng, Z. *Acc. Chem. Res.* **1997**, *30*, 267. Jiang, W.; Chizhevsky, I. T.; Mortimer, M. D.; Chen, W.; Knobler, C. B.; Johnson, S. E.; Gomez, F. A.; Hawthorne, M. F. *Inorg. Chem.* **1996**, *35*, 5417.

[5] Housecroft, C. E. *Angew. Chem., Int. Ed.* **1999**, *38*, 2717.

[6] Gingrich, H. L.; Ghosh, T.; Huang, Q.; Jones Jr., M., *J. Am. Chem. Soc*. **1990**, *112*, 4082.

[7] Jemmis, E. D.; Kiran, B. *J. Am. Chem. Soc.***1997**, *119*, 4076-4077.

[8] Buchwald, S. L.; Nielsen, R. B. *Chem. Rev.* **1988**, *88*, 1047-1058.

[9] Retboll, M.; Edwards, A. J.; Rae, A. D.; Willis, A. C.; Bennett, M. A.; Wenger, E. *J. Am. Chem. Soc.* **2002**, *124*, 8348-8360.

[10] Bennett, M. A.; Hambley, T. W.; Roberts, N. K.; Rotertson, G. B. *Organometallics*, **1985**, *4*, 1992. Bennett, M. A.; Wenger, E. *Organometallics*, **1995**, *14*, 1267. Bennett, M. A.; Hockless, D. C. R.; Wenger, E. *Organometallics* **1995**, *14*, 2091.

[11] Bennett, M. A.; Wenger, E. *Organometallics,* **1996**, *15, 5356.*

[12] Kiran, B.; Anoop, A; Jemmis, E. D. *J. Am. Chem. Soc.* **2002**, *124*, 4402.

[13] Erker G. *J. Organomet. Chem.* 134, 189. Erker, G; Kropp, K., *J. Am. Chem. Soc.* **1979**, *101*, 3659.

[14] Massi, H; Sonogashira, K; Hagihara, H. *Bull. Chem. Soc. Jpn.* **1968**, *41*, 750., Kolomnikov, I. S.; Lobeeva, T. S.; Gorbachevskaya, V. V.; Aleksandrov, G. G.; Struckhov, Yu. T.; Vol'pin, M. E. *J. Chem. Soc. Chem. Commun.* **1971**, 972. Boekel, C. P.; Teuben, J. H.; de Leifde Meijer, H. J. *J. Organomet. Chem.* **1974**, *81*, 371. Boekel, C. P. Teuben, J. H. de Liede Meijer H. J. *J. Orgmet. Chem.* **1975**, *102*, 161.

[15] Houseknecht, K. L.; Stockman, K. E.; Sabat, M.; Finn. M. G.; Grimes, R. N. *J. Am. Chem. Soc.* **1995**, *117*, 1163.

[16] McLain, S. J.; Schrock, R. R.; Sharp, P. R.; Churchill, M. R.; Youngs, W. J. *J. Am. Chem. Soc.* **1979**, *101*, 263. Churchill, M. R.; Youngs, W. J. *Inorg. Chem.*, **1979**, *18*, 1697.

[17] Gibson, J. K. *J. Phys. Chem.* **1996**, *100*, 15688.

[18] Thorn, D. L.; Hoffmann, R. *J. Am. Chem. Soc.*, **1978**, *100*, 2079.

[19] Niu, S.; Hall, M. B. *Chem. Rev.* **2000**, *100*, 353.

[20] Sodupe, M.; Bauschlicher, C. W. *J. Phys. Chem.* **1991**, *95*, 8640.

[21] Kitaura, K.; Sakaki, S.; Morokuma, K. *Inorg. Chem.* **1981**, *20*, 2292. Ziegler, T. *Inorg. Chem.* **1985**, *24*, 1547. Li, J.; Schreckenbach, G.; Ziegler, T. *Inorg. Chem.* **1995**, *34*, 3245.

[22] Frenking, G.; Frohlich, N. *Chem. Rev.*, **2000**, *100*, 717.

[23] Hehre, W.; Radom, L.; Schleyer, P.v.R.; Pople, J. A. *Ab Initio Molecular Orbital Theory*; Wiley: New York, 1986.

[24] (a) Becke, A. D. *J. Chem. Phys.* **1993**, *98*, 5648. (b) Becke, A. D. *Phys. Rev. A.* **1988**, *38*, 3098. (c) Lee, C.; Yang, W.; Parr, R.G. *Phys. Rev. B.* **1988**, *37*, 785. (d) Vosko, S.H.; Wilk, L.; Nusair, M. *Can J. Phys.* **1980**, *58*, 1200.

[25] Hay, P. J.; Wadt, W. R. *J. Chem. Phys.* **1985**, *82*, 270.

[26] Gaussian 03, Revision B.03, Frisch, M. J.; Trucks, G. W.; Schlegel, H. B.; Scuseria, G. E.; Robb, M. A.; Cheeseman, J. R.; Montgomery, Jr., J. A.; Vreven, T; Kudin, K. N.; Burant, J. C.; Millam, J. M.; Iyengar, S. S.; Tomasi, J. Barone, V.; Mennucci, B.; Cossi, M.; Scalmani, G.; Rega, N.; Petersson, G. A.; Nakatsuji, H.; Hada, M.; Ehara, M.; Toyota, K.; Fukuda, R.; Hasegawa, J.; Ishida, M.; Nakajima, T.; Honda, Y.; Kitao, O.; Nakai, H.; Klene, M.; Li, X.; Knox, J. E.; Hratchian, H. P.; Cross, J. B.; Adamo, C.; Jaramillo, J.; Gomperts, R.; Stratmann, R. E.; Yazyev, O.; Austin, A. J.; Cammi, R.; Pomelli, C.; Ochterski, J. W.; Ayala, P. Y.; Morokuma, K.; Voth, G. A.; Salvador, P. Dannenberg, J. J.; Zakrzewski, V. G.; Dapprich, S.; Daniels, A. D.; Strain, M. C.; Farkas, O.; Malick, D. K.; Rabuck, A. D.; Raghavachari, K.; Foresman, J. B.; Ortiz, J. V.; Cui, Q.; Baboul, A. G.; Clifford, S.; Cioslowski, J.; Stefanov, B. B.; Liu, G.; Liashenko, A.; Piskorz, P.; Komaromi, I.; Martin, R. L.; Fox, D. J.; Keith, T.; Al-Laham, M. A.; Peng,C. Y.; Nanayakkara, A.; Challacombe, M.; Gill, P. M. W.; Johnson, B.; Chen, W.; Wong, M. W.; Gonzalez, C.; Pople, J. A. Gaussian, Inc., Pittsburgh PA, 2003.

[27] Frenking, G.; Frohlich, N.; *Chem. Rev.*; **2000**; *100*, 717.

Chapter 5

# Transition Metal Catalyzed Activation of β-C-H Bond

5.1 Introduction

Many useful chemicals are derivatives of saturated hydrocarbons. Since alkanes are the main constituent of petroleum and natural gas, efficient reactions which convert alkanes into desired products are highly sought after. However the CH bond is well-known for its inertness under normal reaction conditions, and under drastic conditions, reactions are uncontrollable. Thus selectively activating the CH bonds is necessary for the synthesis of the hydrocarbon derivatives. In many such high barrier reactions, catalysis by transition metals are helpful. In the activation of CH bonds transition metal catalysis is found to be especially effective. Binding a transition metal to the CH bond is found to leverage its breaking. [1]

The formation of the agostic complex is first step in the CH bond activation reactions. Agostic interaction, a term first introduced by Brookhart and Green, is described as an attractive interaction between metal atom and

the CH fragment of an appended ligand. [2] The term agostic is "used to discuss the various manifestations of covalent interactions between carbon-hydrogen groups and transition metal centers in organometallic compounds, in which a hydrogen atom is covalently bonded simultaneously to both a carbon and to a transition metal atom". All the CH activation reactions proceed from the initially formed agostic complex in various directions leading to the different products.

Among the vast variety of reactions involving agostic complexes, the β-hydride elimination reaction is chosen for the current study. Activation of β-C-H bond is unique because addition does not involve a formal oxidation at the metal since the product is an ethylene-hydride complex; there is only an increase of 2 in the electron count around the metal. This is a com-
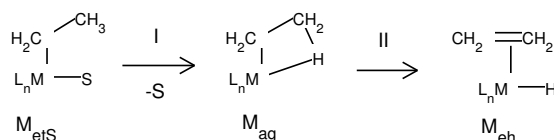
Scheme 5.1

mon intermediate step in many important processes. This step involves the transformation of metal ethyl complex to β-agostic complex which go on to form an ethylene hydride complex, from which many other process can continue. For example, in the polymerization reaction, agostic complex is the resting state, from where propagation, termination or hydride exchange can occur.

Even though the agostic complexes are widely talked about, there are very few experimentally characterized structures. β-agostic complexes reported in CCSD are: $TiCl_3(dmpe)$, [3] $CoCp^*(PPh_3)$, [4] $C_{19}H_{25}Os^+$ ((η^6-

Mesitylene)-(2,3,5-η^4-3a,4,6,7,7a-pentahydro-4,7-methano-1H-inden-5- yl)-osmium(ii) hexafluorophosphate), [5] (norbornyl)PtL, [10] Ni$^+$(dmpe). [11] Though not large in number, the available examples point to the occurrence of β-agostic interactions across the periodic table. The energy of a C-H bond at the β-position is not expected to vary considerably with changes in other parts of the molecule. On the other hand metals across the periodic table (for example with metals from Ti-Ni with Valance State Ionization Potentials (eV) for the d-orbitals: Ti=-10.81, V=-11.00, Cr= -11.22, Mn= -12.53, Fe= -12.70, Co= -13.18, Ni= -13.40) are involved in the agostic interaction and β-CH bond activation. The differing ligand combinations on different metals must lead to appropriate frontier orbitals that stabilize the agostic interactions. Our objective is to study the agostic complexes across the first row transition metals and to decipher the ways in which ligands enable every metal to support agostic interactions. As the experimental structures are not available for all of them, we have tried some preliminary calculations to find the agostic structures, which also lead to structures for the metal ethyl complex and metal ethylene hydride complex. With these model compounds, we have studied the CH addition step. The model structures are neutral or cationic metal complexes, with a combination of phosphine and cyclopentadienyl ligands which gives a VE count of 12 for early and 16 for late TM's. Among the many possible combinations of ligands, we have chosen the ones which gave local minima for all the three species involved in the step.

5.2   Methods

The molecules considered are, $TiCpEt(PH_3)_2$, $V^+CpEt(PH_3)_2$, Cr^+Cp_2Et, $MnEt(PH_3)_4$, $Fe^+Et(PH_3)_4$, $Co^+CpEt(PH_3)$, $NiCpEt$. We use the following labels for the structures: M_{etS} for the metal ethyl complex with a co-ordinated solvent (PH_3); M_{frag} for the metal fragment without the solvent molecule; M_{et} for non-agostic metal ethyl complex; M_{ag} for the agostic intermediate; and M_{eh} for metal ethylene hydride complex. All geometries are optimized and characterized by frequency analysis at B3LYP/LANL2DZ [6–8] level using Gaussian 03 program package. [9] Total Energies and Relative energies of the optimized geometries are given in Table 5.1 and the geometric parameters are given in Table 5.2.

5.3   Results and discussions

The formation of agostic complex in β-elimination reaction is preceded by the detaching of a solvent molecule or a labile ligand attached to the metal. (Scheme 5.1, Step I) The stability of agostic structure is decided by factors such as the electrophilicity around the metal center, spatial orientation of the ligands, electron density of the CH bond etc. In this study the metals and the ligand combinations are varied in order to stabilize the agostic complex. Agostic complexes can go on to form the metal(ethylene)(hydride) complex under favorable conditions. (Scheme 5.1, Step II) The reaction profile is shown in the Figure 5.1.

Table 5.1: Total energy (in au), Zero point energy (ZPE, in kcal/mol) Total Energy with Zero Point correction (in au) and Relative Energy (RE, in kcal/mol) at B3LYP level using 6-31G* basis.

Molecule	T.E.	Z.P.E.	T.E.+Z.P.E.	R.E.
Ti_{etS}	-355.58967	141.52	-355.36414	–
Ti_{et}	-347.33754	124.24	-347.13955	0.44
Ti_{ag}	-347.33825	124.90	-347.13921	0.00
Ti_{eh}	-347.32536	123.07	-347.12923	8.09
V_{etS}	-368.62585	143.68	-368.39688	–
V_{et}	-360.36134	126.00	-360.16055	7.75
V_{ag}	-360.37369	127.10	-360.17114	0.00
V_{eh}	-360.33648	125.55	-360.13641	23.35
Cr_{etS}	-560.50816	165.37	-560.24462	–
Cr_{et}	-552.19775	148.19	-551.96159	18.55
Cr_{ag}	-552.22731	148.52	-551.99064	0.00
Cr_{eh}	-552.21002	146.74	-551.97617	10.85
Mn_{etS}	-224.44479	123.67	-224.24770	–
Mn_{et}	-216.15559	105.87	-215.98688	5.16
Mn_{ag}	-216.16382	106.36	-215.99433	0.00
Mn_{eh}	-216.16141	105.60	-215.99312	1.51
Fe_{etS}	-243.82108	125.53	-243.62104	–
Fe_{et}	-235.52144	107.82	-235.34962	9.09
Fe_{ag}	-235.53592	108.37	-235.36323	0.00
Fe_{eh}	-235.52312	107.15	-235.35237	8.03
Co_{etS}	-434.11580	128.65	-433.91078	–
Co_{et}	-425.79714	110.28	-425.62139	10.50
Co_{ag}	-425.81387	110.99	-425.63700	0.00
Co_{eh}	-425.79957	109.49	-425.62508	8.98
Ni_{etS}	-450.27669	109.60	-450.10204	–
Ni_{et}	-441.96714	92.12	-441.82033	7.92
Ni_{ag}	-441.97977	92.34	-441.83261	0.00
Ni_{eh}	-441.97272	90.71	-441.82817	4.42

5.3.1 Dissociation of solvent

The dissociation of the solvent, i.e., $M_{etS} \rightarrow M_{frag} + S$, is endothermic for all the metal complexes, because the removal of the solvent leaves a coordinatively unsaturated species, M_{frag}. The optimization of the M_{frag} species lead to M_{et}. The formation of M_{et} is endothermic for all the metals, except for Ti and V. The close examination of the structures Ti_{et} and V_{et}

Figure 5.1: Reaction profile for the reaction $M_{etS} \rightarrow M_{et} + S \rightarrow M_{ag} + S \rightarrow M_{eh} + S$ calculated at B3LYP/LANL2DZ.
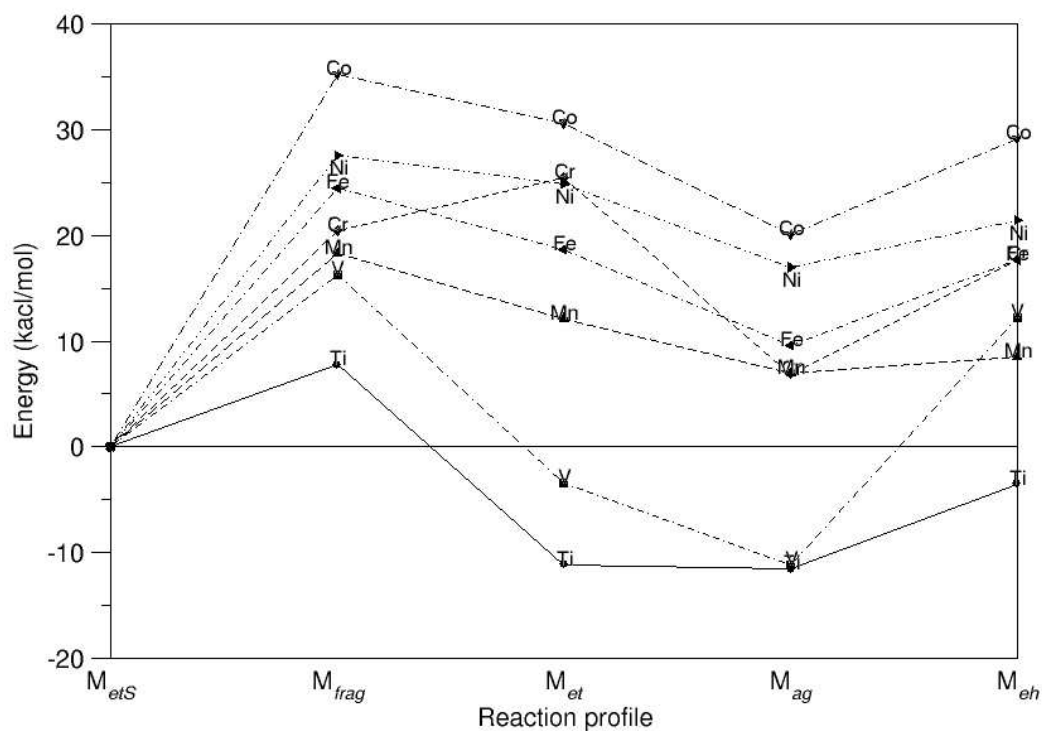
shows that their α-CH is involved in an agostic interaction with the metals which is characterized by the C-H bond length and MCH bond angle. One of the α-CH distance, in Ti_{et} (1.114 Å) is longer than the other, 1.101 Å. The MCH angle is small 97.97°for agostic CH than the other, 122.63°. V_{ag} is more stable by 3.98 kcal/mol than V_{et} even though there are two α-CH interactions in the V_{et}. This is seen in the C_α-H distance of 1.125Å and $MC_\alpha H$ bond angle of 83.5°. (Table 5.2) The geometry of Ti_{et} and V_{et} is shown in the Figure 5.2.

Table 5.2: Selected geometric parameters of the structures optimized at B3LYP/LANL2DZ

Bond(A)	compound	Ti	V	Cr	Mn	Fe	Co	Ni
	Agostic	1.122	1.128	1.143	1.172	1.170	1.173	1.171
C_β-H	Ethyl	1.101	1.098	1.096	1.102	1.098	1.096	1.098
	Hydride							
	Agostic	1.549	1.534	1.526	1.524	1.520	1.512	1.516
C_α-C_β	Ethyl	1.555	1.552	1.530	1.563	1.544	1.521	1.534
	Hydride	1.457	1.420	1.395	1.424	1.401	1.398	1.409
	Agostic	2.264	2.131	2.015	1.845	1.842	1.785	1.763
M-H	Ethyl							
	Hydride	1.733	1.590	1.540	1.596	1.526	1.473	1.465
	Agostic	2.110	1.999	2.086	2.070	2.001	1.956	1.901
M-C_α	Ethyl	2.107	2.144	2.260	2.093	2.005	1.907	1.887
	Hydride	2.108	2.249	2.351	2.133	2.184	2.155	2.047
	Agostic	2.623	2.480	2.440	2.320	2.297	2.219	2.195
M-C_β	Ethyl	2.968	3.083	3.178	2.905	3.166	3.091	2.930
	Hydride	2.201	2.264	2.362	2.173	2.199	2.175	2.048
	Agostic	1.097	1.093	1.093	1.097	1.094	1.091	1.094
C_β-H'	Ethyl	1.101	1.098	1.096	1.102	1.098	1.096	1.098
	Hydride							
	Agostic	90.23	88.121	83.451	78.809	80.182	78.409	79.073
M-C_α-C_β	Ethyl	107.20	112.094	112.543	104.314	125.774	128.460	117.450
	Hydride	73.734	71.105	73.204	69.191	71.943	71.950	69.879
	Agostic	112.77	112.696	113.033	112.991	111.889	112.649	111.412
C_α-C_β-H	Ethyl							
	Hydride							

Figure 5.2: α-agostic complexes of Ti and V.

5.3.2 β-agostic complex

The formation of agostic complex, M_{ag}, from the M_{etS} species is endothermic for the metals other than Ti and V. The energy involved in the forma-

Figure 5.3: Agostic stabilization, the energy difference between the agostic and nonagostic structure ($\Delta E_{agostic} = E_{ag} - E_{et}$), and the energy difference between the M-C-CH orbitals on agostic and nonagostic geometry, calculated at B3LYP/LANL2DZ level of theory for the first row transition metal complexes.
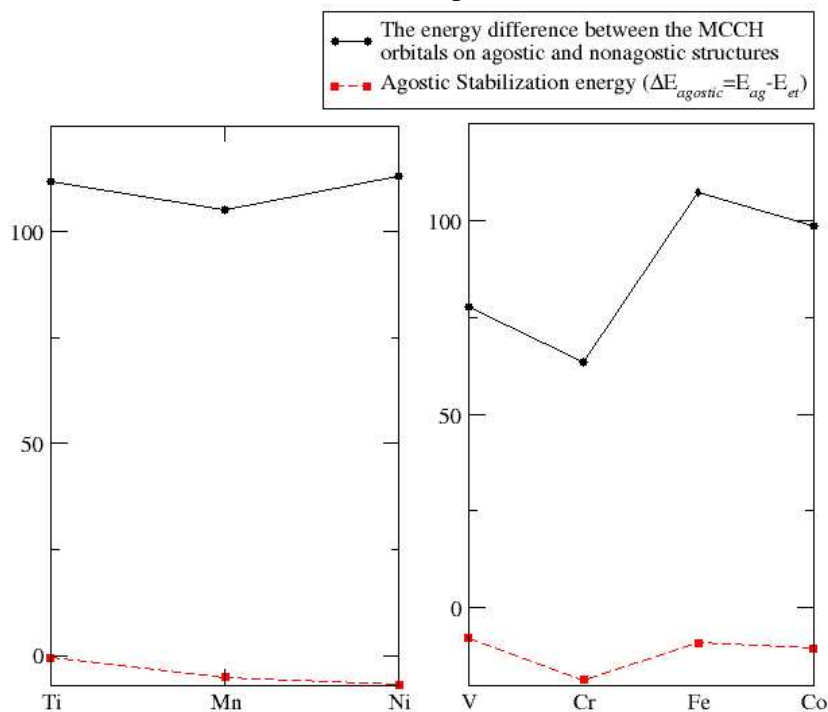
tion of agostic complex is the sum of the dissociation energy of the solvent and the agostic stabilization. In other words, it gives the magnitude of stabilization offered by the formation of agostic interaction compared to that given by the coordination of solvent molecule. Th metal ethyl complex, M_{et}, which is non-β-agostic structure, rearranges to the β-agostic structure, M_{ag} and the energy involved in this rearrangement is agostic stabilization.

The agostic stabilization is calculated as the energy difference between the agostic structure and the nonagostic structure ($\Delta E_{agostic} = E_{ag} - E_{et}$). The agostic stabilization is presented in the Figure 5.3. The plot also shows the energy difference between the σ-CH bonding MO and the vacant metal MO. The variation of the energies of corresponding orbitals across the pe-

Figure 5.4: The energies of the vacant metal orbital and σ-CH orbital for the metal ethyl complexes
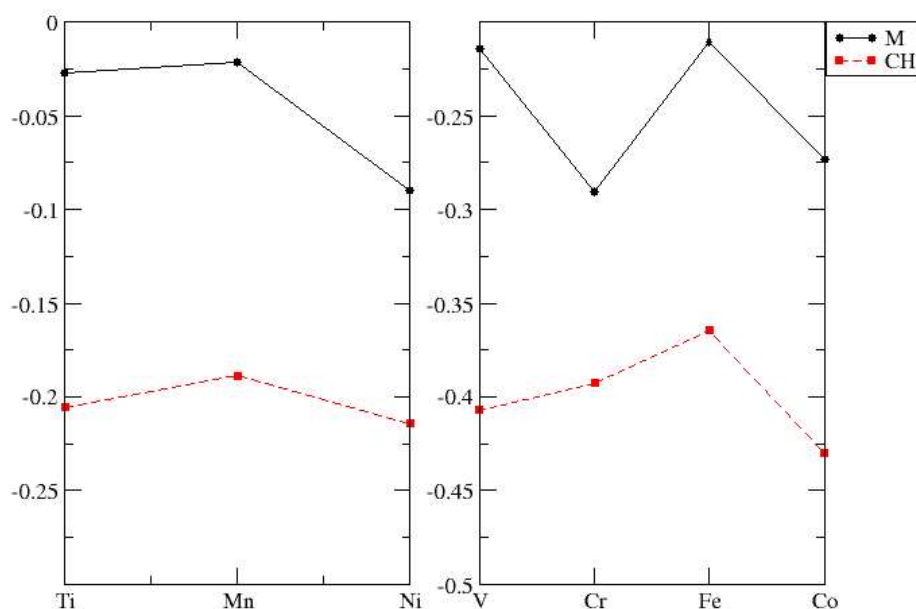
riodic table is shown in the Figure 5.4. The complexes of Ti, Mn and Ni are separated from those of V, Cr, Fe and Co as as the latter all positively charged. The MO energy differ largely in these systems and hence analysis is more meaningful this way. The interaction between CH donor and the metal acceptor orbitals results in the delocalized MO in M_{ag} shown in Figure 5.5. The torus of the M d_{z^2} orbital interacts with the pseudo-π^*-orbital of the ethyl group which give a delocalization over M-H-C_α-C_β.

All the M_{ag} structures show β-agostic stabilization. For Ti_{ag} which has a β-agostic interaction is only 0.44 kcal/mol more stable than the Ti_{et} structure which has an α-agostic interaction. For vanadium, the β-agostic structure is 7.75 kcal/mol more stable than the α-agostic structure.

Highest magnitude of agostic stabilization among the complexes under

Figure 5.5: The delocalized orbitals of M_{ag}.

Ti (HOMO-1)   V (HOMO-1)   Cr (HOMO-1)

Mn (HOMO-3)   Fe (HOMO-2)   Co (HOMO)

Ni (HOMO-2)
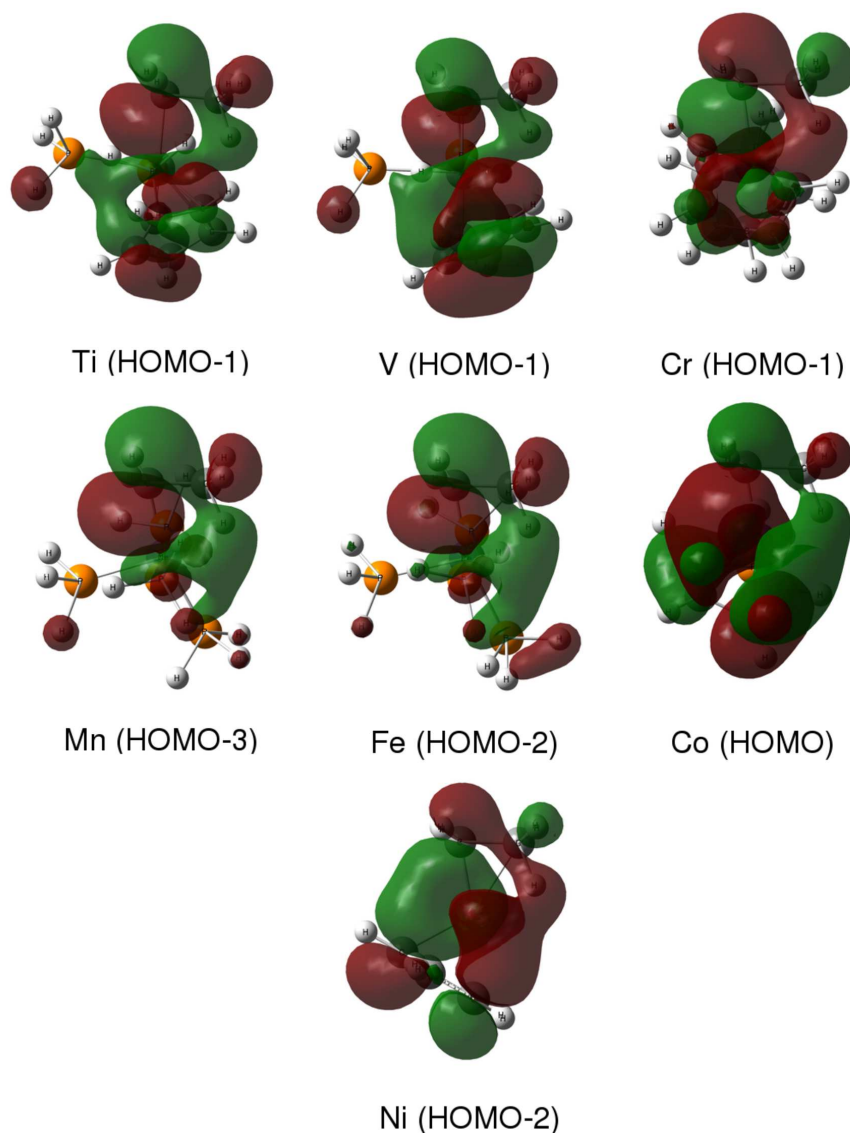
study are seen in Cr_{ag}. The changes in geometrical parameters on going from Cr_{et} to Cr_{ag} are: C_β-H increased by 0.047 Å; C_α-C_β distance decreased by 0.004 Å; M-C_α distance decreased by 0.176 Å; M-C_β decreased by 0.738 Å; $MC_\alpha C_\beta$ angle reduced from 112.5°to 83.5°. Similar trends in geometric parameters are seen in Mn, Fe, Co and Ni complexes. The optimized geometries of the agostic structures M_{ag} is given in the Figure 5.6.

Figure 5.6: Optimized geometries of M_{ag} at B3LYP/Lanl2DZ

Ti   V   Cr

Mn   Fe   Co

Ni
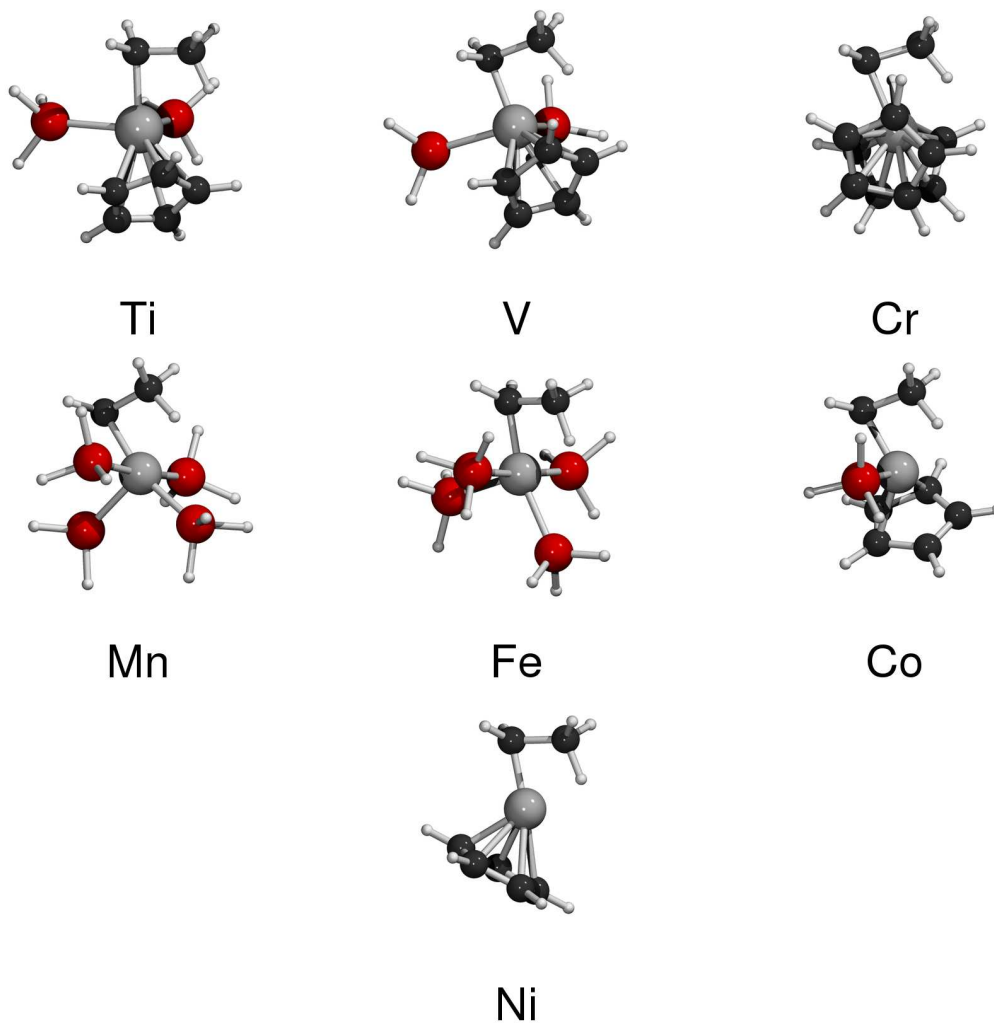
5.3.3   Ethylene hydride complex

The formation of ethylene hydride metal complex is endothermic for all the complex, highest for V and lowest for Mn. (See Figure 5.1) In Ti_{eh}, V_{eh} and Ni_{eh} complexes, MH is orthogonal to the ethylene plane, while in others MH is coplanar to the ethylene group. The optimization of Ti_{eh}, V_{eh} and Ni_{eh} structures with coplanar ethylene and hydride falls back to agostic structure.

5.4   Conclusion

In this model study of β-hydride elimination reaction, we have engineered the complex in such a way to get the optimized structure for all the three species, metal ethyl, agostic metal, and metal ethylene hydride complex. We have analyzed the stability and geometric characteristics of the structures. Further study is needed to fine-tune the ligands so that the agostic structures are only stabilized to the extend needed to trigger the reaction, but not to be very stable structure. For the β-elimination reaction to proceed from the agostic complex, ethylene hydride complex should be thermodynamically more stable than the agostic complex. In all the structures under study, it was observed that agostic complexes are more stable. Further tuning of the ligands around the metal and the ethyl carbons are required to attain synthetically feasible reactions. However this study demonstrates that given a specific metal it is possible to do so. It is clear from these studies that any metal can be taken and the ligands can be fine-tuned to stabilize an agostic interaction. Further, changes can be brought in to make the agostic systems more or less stable that the addition is quick.

Bibliography

[1] Labinger J. A., Bercaw J. E., Nature 2002, 417, 507.

[2] a) Brookhart, M.; Green, M. L. H. *J. Organomet. Chem.* **1983**, *250*, 395. b) Brookhart, M.; Green, M. L. H.; Wong, L.-L. *Prog. Inorg. Chem.* **1988**, *36*, 1-124.

[3] a) Dawoodi, Z.; Green, M. L. H.; Mtetwa, V. S. B.; Prout, K. *Chem.Commun.* **1982**, 802. b) Cotton, F. A.; Petrukhina, M. A. *Inorg.Chem.Commun.*, **1998**, *1*, 195. c) Scherer, W.; Priermeier, T.; Haaland, A.; Volden, H. V.; McGrady, G. S.; Downs, A. J.; Boese, R.; Blaser, D. *Organometallics*, **1998**, *17*, 4406. d) Scherer, W.; Hieringer, W.; Spiegler, M.; Sirsch, P.; McGrady, G.S.; Downs, A.J.; Haaland, A.; Pedersen, B. *Chem.Commun.*, **1998**, 2471. e) Dawoodi, Z.; Green, M. L. H.; Mtetwa, V. S. B.; Prout, K.; Schultz, A. J.; Williams, J. M.; Koetzle, T. F. *J.Chem.Soc.,Dalton Trans.*, **1986**, 1629.

[4] Cracknell, R. B.; Orpen, A. G.; Spencer, J. L. *Chem.Commun.* **1984**, 326.

[5] Bennett, M. A.; McMahon, I. J.; Pelling, S.; Robertson, G. B.; Wickramasinghe, W. A. *Organometallics*, **1985**, *4*, 754. Cracknell, R. B.; Orpen, A. G.; Spencer, J. L. *Chem.Commun.*, **1984**, 326.

[6] Hehre, W.; Radom, L.; Schleyer, P.v.R.; Pople, J.A. *Ab Initio Molecular Orbital Theory*; Wiley: New York, 1986.

[7] (a) Becke, A. D. *J. Chem. Phys.* **1993**, 98, 5648. (b) Becke, A. D. *Phys. Rev. A* **1988**, 38, 3098. (c) Lee, C.; Yang, W.; Parr, R.G. *Phys. Rev. B* **1988**, 37, 785. (d) Vosko, S.H.; Wilk, L.; Nusair, M. *Can J. Phys.* **1980**, 58, 1200.

[8] Hay, P. J.; Wadt, W. R. *J. Chem. Phys.* **1985**, *82*, 270.

[9] Gaussian 03, Revision B.03, Frisch, M. J.; Trucks, G. W.; Schlegel, H. B.; Scuseria, G. E.; Robb, M. A.; Cheeseman, J. R.; Montgomery, Jr., J. A.; Vreven, T; Kudin, K. N.; Burant, J. C.; Millam, J. M.; Iyengar, S. S.; Tomasi, J. Barone, V.; Mennucci, B.; Cossi, M.; Scalmani, G.; Rega, N.; Petersson, G. A.; Nakatsuji, H.; Hada, M.; Ehara, M.; Toyota, K.; Fukuda, R.; Hasegawa, J.; Ishida, M.; Nakajima, T.; Honda, Y.; Kitao, O.; Nakai, H.; Klene, M.; Li, X.; Knox, J. E.; Hratchian, H. P.; Cross, J. B.; Adamo, C.; Jaramillo, J.; Gomperts, R.; Stratmann, R. E.; Yazyev, O.; Austin, A. J.; Cammi, R.; Pomelli, C.; Ochterski, J. W.; Ayala, P. Y.; Morokuma, K.; Voth, G. A.; Salvador, P. Dannenberg, J. J.; Zakrzewski, V. G.; Dapprich, S.; Daniels, A. D.; Strain, M. C.; Farkas, O.; Malick, D. K.; Rabuck, A. D.; Raghavachari, K.; Foresman, J. B.; Ortiz, J. V.; Cui, Q.; Baboul, A. G.; Clifford, S.; Cioslowski, J.; Stefanov, B. B.; Liu, G.; Liashenko, A.; Piskorz, P.; Komaromi, I.; Martin, R. L.; Fox, D. J.; Keith, T.; Al-Laham, M. A.; Peng,C. Y.; Nanayakkara, A.; Challacombe, M.; Gill, P. M. W.; John-

son, B.; Chen, W.; Wong, M. W.; Gonzalez, C.; Pople, J. A. Gaussian, Inc., Pittsburgh PA, 2003.

[10] a) Carr, N.; Dunne, B. J.; Orpen, A. G.; Spencer, J. L. *Chem. Commun.*, **1988**, 926. b) Carr, N.; Dunne, B. J.; Mole, L.; Orpen, A. G.; Spencer, J. L. *J.Chem.Soc.,Dalton Trans.* **1991**, 863.

[11] Conroy-Lewis, F. M.; Mole, L.; Redhouse, A. D.; Litster, S. A. Spencer, J. L. *Chem.Commun.*, **1991**, 1601.

[12] Koga N.; Obara S.; Kitaura K.; Morokuma K. *J. Am. Chem. Soc.* **1985**, *107*, 7109.

[13] Pavankumar, P. N. V.; Ashok B.; Jemmis E. D. *J. Organomet. Chem.* **1986**, *315*, 361.

[14] Crabtree R. H. *Chem. Rev.* **1995**, *95*, 987.

[15] Shilov A. E.; Shulâpin G. B. *Chem. Rev.* **1997**, *97*, 2879.

List of Publications

1. Control of Stability through Overlap Matching: closo-Carboranes and closo-Silaboranes, B. Kiran, A. Anoop, E. D. Jemmis, *Journal of the American Chemical Society*, **2002**, *124*, 4402 - 4407.

2. Face-selectivity in [4+2]-cycloadditions to novel polycyclic benzo-quinones. Remarkable stereodirecting effects of a remote cyclopropane ring and an olefinic bond, G. Mehta, C. L. Droumaguet, K. Islam, A. Anoop and E. D. Jemmis, *Tetrahedron Letters*, **2003**, *44*, 15, 3109 - 3113

3. Effect of metal complexation on ring opening of bowl-shaped hydrocarbons: Theoretical study, E. D. Jemmis, P. Parameswaran, A. Anoop, *International Journal of Quantum Chemistry*, **2003**, *95*, 810 - 815.

4. Non-planarity at Tri-coordinated Aluminum and Gallium: Cyclic Structures for $X_3H_n^m$, G. N. Srinivas, A. Anoop, E. D. Jemmis, T. P. Hamilton, K. Lammertsma, J. Leszczynski, H. F. Scheafer III, *J. Am. Chem. Soc.* **2003** *125*, 16397 - 16407.

5. Hyperconjugation and Torsional Strain in $B_{12}H_{11}$, $B_{12}H_{10}$ and Related Species, A. Anoop, E. G. Jayasree, P. K. Sharma, M. M. Balakr-

ishnarajan, E. D. Jemmis, to be submitted.

6. Theoretical Study on the Double Insertion of Acetylene to the Nickel Complexes of Benzyne and Carborynes. A. Anoop, E. D. Jemmis, manuscript under preparation.

7. Transition Metal Catalyzed Activation of β-C-H Bond, E. D. Jemmis, A. Anoop, B. Pathak, manuscript under preparation.